INFORMATION TO USERS

This manuscript has been reproduced from the microfilm master. UMI films the text directly from the original or copy submitted. Thus, some thesis and dissertation copies are in typewriter face, while others may be from any type of computer printer.

The quality of this reproduction is dependent upon the quality of the copy submitted. Broken or indistinct print, colored or poor quality illustrations and photographs, print bleedthrough, substandard margins, and improper alignment can adversely affect reproduction.

In the unlikely event that the author did not send UMI a complete manuscript and there are missing pages, these will be noted. Also, if unauthorized copyright material had to be removed, a note will indicate the deletion.

Oversize materials (e.g., maps, drawings, charts) are reproduced by sectioning the original, beginning at the upper left-hand corner and continuing from left to right in equal sections with small overlaps.

Photographs included in the original manuscript have been reproduced xerographically in this copy. Higher quality 6" x 9" black and white photographic prints are available for any photographs or illustrations appearing in this copy for an additional charge. Contact UMI directly to order.

UMI®

University of Alberta

Applications of Capillary Electrophoresis

in Biological and Clinical Research

by

Nan Li   ©

A thesis submitted to the Faculty of Graduate Studies and Research in partial fulfillment

of the requirements for the degree of Doctor of Philosophy

Department of Chemistry

Edmonton, Alberta

Fall, 2001

The author has granted a non-exclusive licence allowing the National Library of Canada to reproduce, loan, distribute or sell copies of this thesis in microform, paper or electronic formats.

The author retains ownership of the copyright in this thesis. Neither the thesis nor substantial extracts from it may be printed or otherwise reproduced without the author's permission.

L'auteur a accordé une licence non exclusive permettant à la Bibliothèque nationale du Canada de reproduire, prêter, distribuer ou vendre des copies de cette thèse sous la forme de microfiche/film, de reproduction sur papier ou sur format électronique.

L'auteur conserve la propriété du droit d'auteur qui protège cette thèse. Ni la thèse ni des extraits substantiels de celle-ci ne doivent être imprimés ou autrement reproduits sans son autorisation.

0-612-68963-8

Canada

University of Alberta

Library Release Form

Author of Thesis: **Nan Li**

Title of Thesis: **Applications of Capillary Electrophoresis in Biological and Clinical Research**

Degree: **Doctor of Philosophy**

Year this Degree Granted: **2001**

Permission is hereby granted to the University of Alberta Library to reproduce single copies of this thesis and to lend or sell such copies for private. scholarly. or scientific research purposes only.

The author reserves all other publication and other rights in association with the copyright in the thesis. and except as herein before provided. neither the thesis nor any substantial portion thereof may be printed or otherwise reproduced in any material form whatever without the author's prior written permission.
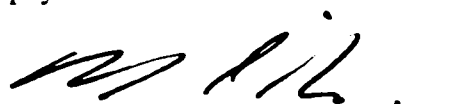
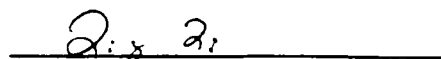#6. 10720-85 Ave.

Edmonton. Alberta

Canada. T6E 2K8

Oct. 1 . 2001

University of Alberta

Faculty of Graduate Studies and Research

The undersigned certify that they have read, and recommend to the Faculty of Graduate Studies and Research for acceptance, a thesis entitled **Applications of Capillary Electrophoresis in Biological and Clinical Research** by Nan Li in partial fulfillment of the requirements for the degree of Doctor of Philosophy.
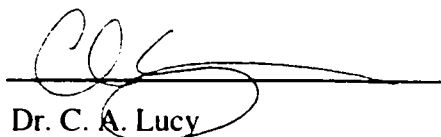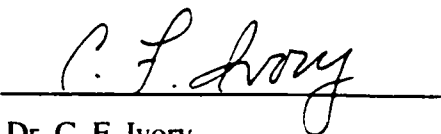
Dr. N. J. Dovichi

Dr. L. Li

Dr. M. M. Palcic

Dr. C. A. Lucy

Dr. J. R. Mackey

Dr. C. E. Cass

Dr. C. F. Ivory

Date ___Sept. 28___ , 2001

To my Father and in memory of my Mother

ABSTRACT

High sensitivity and high efficiency analysis of biomolecules has become increasingly important in biological and clinical research. In this thesis, development and application of techniques such as capillary electrophoresis with laser-induced fluorescence detection (CE-LIF), polymerase chain reaction (PCR), cell synchronization and slab gel electrophoresis are presented in an effort to address a few of the challenging goals in this field.

A CE-LIF based method for accurate and reliable PCR quantification was developed. Using duck hepatitis B virus (DHBV) as a model, the developed technique was validated by evaluating its linearity, sensitivity, accuracy and precision. The method is more convenient and is applicable to a wider variety of PCR amplifications than other popular assays.

Understanding nucleoside anti-cancer drug resistance mechanisms at the single-cell level is crucial in improving clinical treatment. The human equilibrative nucleoside transporter 1 (hENT1) and deoxycytidine kinase (dCK) are two of the molecular determinants of nucleoside drug resistance. The first use of CE-LIF in hENT1 quantification in the plasma membrane is presented and applied successfully to five cultured human cell lines. Theoretical sensitivity of this method suggests that single cell hENT1 quantification is possible. The potential of measuring dCK activity using a fluorescent substrate was studied as the initial step in developing a single cell enzyme assay. Aspects of separation, substrate preparation, enzyme kinetics, substrate uptake and substrate distribution were studied. Preliminary results indicated a more suitable substrate is required to ensure successful future development. In parallel, studies such as assisting the substrate uptake,

optimizing the enzyme assay conditions and localizing the substrate in the cytoplasm are also required.

Until analysis at the single-cell level becomes routine, cell synchronization is necessary in understanding cell cycle-dependent biological events. Two examples are presented in this thesis using HeLa cells. The first study combined cell synchronization techniques with my hENT1-CE-LIF assay. Results showed that hENT1 expression levels changed during the cell cycle and may be correlated with cell proliferation. In the second study, slab gel electrophoresis and capillary gel electrophoresis (CGE) were applied to probe the general protein expression differences at different cycle phases.

ACKNOWLEDGUOEMENTS

I would like to extend my sincere gratitude to my supervisor. Dr. Norman J. Dovichi, for giving me the opportunity to work in his group, investing enormous amounts of time and effort in me and providing endless encouragement.

I would like to thank Dr. Monica Palcic for her great supervision, friendship and advice during my last year. Thank you to Drs. Carol Cass and John Mackey for their vast knowledge and help with the nucleoside drug resistance projects. I would also like to express my heartfelt appreciation to Dr. Liang Li for giving me an opportunity to work in his group after my graduation, and Dr. Charles Lucy for always being there whenever I need help.

I would like to thank the Alberta Heritage Foundation for Medical Research for granting me a full-time scholarship and research allowance for the second half of my PhD study.

There are so many group members who supported my work and myself over my years as a graduate student. Drs. Woei Tan, Charles Liu, and Jianzhong Zhang are not only great friends but also teachers and idols of mine. Thanks to Dr. Dawn Richards for helping me with SDS-PAGE and 2-D work, proofreading my thesis and encouraging me through my lonely days here in my last year. I would like to thank Lillian Cook for her tissue culture expertise and her great companionship. Her contribution was crucial to almost all of the work in this thesis. I sincerely thank Eric Carpenter for his incredible resource and editing my thesis. Many thanks to Roger Tsang, Laura Horlick and Dr. Shen Hu for their work in helping me fulfill the projects in Chapters 2, 5 and 6. I very much appreciated the friendship and advice of many great friends in this department: Julia Fang, Rob

Polakowski, Rob Bujalski, Weijie Wang, Zhengping Wang, Rui Chen, and many more. Thanks are extended to Cheryl Santos, Geraldine Barron, Juanita Wizniak, Drs. Marilyn Clarke, Charlotte Spencer and Rajam Mani and many more in the Cross Cancer Institute.

I am deeply indebted to my mother Chunrong Zhang and my father Guangzu Li, for sacrificing their careers for my education, for providing unconditional love and support during my studies and for teaching me the important things in life. From the bottom of my heart, I want to acknowledge my dear husband, Han Zhu, who completely and tirelessly supported me throughout my Ph.D. study and believed in me and my abilities. I would also like to thank my mother-in-law, Guo Fu, and my lovely sister, Jing Zhang who provided much inspiration and motivation.

TABLE OF CONTENTS

CHAPTER 1

Introduction

CHAPTER 3

Study of Nucleoside Anti-cancer Drug Uptake and Metabolism Using Capillary Electrophoresis with Laser-induced Fluorescence Detection: (I) Quantification of Human Equilibrative Nucleoside Transporter 1 (hENT1) Protein

CHAPTER 4

Study of Nucleoside Anti-cancer Drug Uptake and Metabolism Using

Capillary Electrophoresis with Laser-Induced Fluorescence Detection:

(II) The Possibility of Using [TAMRA]dCyd As A Substrate for

LIST OF TABLES

CHAPTER 6

LIST OF FIGURES

CHAPTER 4

CHAPTER 5

CHAPTER 6

LIST OF ABBREVIATIONS AND SYMBOLS

180/1	human cervical carcinoma cell line
435S	human breast carcinoma cell line
5-Sx8f	5-SAENTA-x8-fluorescein
A2780	human ovarian carcinoma cell line
AG6000	a highly nucleoside drug resistant variant of A2780
AP	alkaline phosphatase
ATP	adenosine triphosphate
APS	ammonium persulfate
bp	base pairs
BSA	bovine serum albumin
CaCo-2	human colon carcinoma cell line
CE	capillary electrophoresis
CGE	capillary gel electrophoresis
CHES	2-(cyclohexylamino)-ethanesulfonic acid
CIAP	calf intestinal alkaline phosphatase
CIEF	capillary isoelectric focusing
cladribine	2-chloro-2'-deoxyadenosine
cytarabine	1-β-D-arabinofuranosyl cytosine
CZE	capillary zone electrophoresis
dAdo	deoxyadenosine
dCyd	deoxycytidine
dCK	deoxycytidine kinase
dGuo	deoxyguanosine
DHBV	duck hepatitis B virus

DMEM	Dulbecco's Minimal Essential Medium
DNA	deoxyribonucleic acid
DTT	dithiothreitol
E	electric field
ε	dielectric constant
ζ	zeta potential
EDTA	ethylenediaminetetra-acetic acid
EOF	electroosmotic flow
FACS	fluorescence-activated cell sorting
FBS	fetal bovine serum
fludarabine	9-β-D-arabinosyl-2-fluoroadenine
[Fluorescein]dCyd	
	Fluorescein labeled dCyd
FQ	3-(2-furoyl)quinoline-2-carboxaldehyde
gemcitabine	2',2'-difluorodeoxycytidine
HBV	hepatitis B virus
HEC	hydroxyethylcellulose
HeLa	human cervical carcinoma cell line
hENT1	human equilibrative nucleoside transporter protein 1
HEPES	4-(2-hydroxyethyl)-1-piperazineethanesulfonic acid
HMC	hydroxymethylcellulose
I.D.	inner diameter
IEF	isoelectric focusing
IPG	immobilized pH gradient
L_c	length of the capillary
L_d	length of the capillary from the injection end to the detector

LIF	laser-induced fluorescence
LOD	limit of detection
LPA	linear polyacrylamide
MAPS	γ-methacryloxy-propyltrimethoxysilane
MCF-7	human breast carcinoma cell line
MECC	micellar electrokinetic capillary chromatography
MESF	molecules of equivalent soluble fluorescein
MI	mitotic index
mRNA	messenger ribonucleic acid
MS	mass spectrometry
η	viscosity
NBMPR	nitrobenzylthioinosine
nocodazole	methyl[5-(2-thienylcarbonyl)-1H-benzimidazole-1-yl]carbamate
NT	nucleoside transport
O.D.	outer diameter
PA	polyacrylamide
PBS	phosphate buffered saline
PCR	polymerase chain reaction
PEG	poly(ethylene glycol)
PEO	poly(ethylene oxide)
PI	propidium iodide
pI	isoelectric point
PMT	photomultiplier tube
PVA	poly(vinyl alcohol)
QC-PCR	quantitative competitive PCR
R6G	rhodamine 6G

[R6G]dCyd	rhodamine 6G labeled dCyd
RPMI	Roswell Park Memorial Institute
RSD	relative standard deviation
RT-PCR	reverse transcriptase PCR
SAENTA	5'-S-(2-Aminoethyl)-N^6-(4-nitrobenzyl)-5'-thioadenosine
SD	standard deviation
SDS	sodium dodecylsulfate
SDS-PAGE	sodium dodecylsulfate polyacrylamide gel electrophoresis
TAMRA	carboxytetramethylrhodamine

[TAMRA]dCyd

    TAMRA labeled dCyd

[TAMRA]dCydMP

    TAMRA labeled deoxycytidine monophosphate

[TAMRA]dCydDP

    TAMRA labeled deoxycytidine diphosphate

[TAMRA]dCydTP

    TAMRA labeled deoxycytidine triphosphate

TAPS	N-tris[Hydroxymethyl]methyl-3-aminopropanesulfonic acid
TEMED	N,N,N',N'-tetramethylethylenediamine
TGS	Tris-glycine-SDS-buffer
TMR	tetramethylrhodamine
t_r	migration time
Tris	tris[hydroxymethyl]aminomethane
TrisHCl	Tris-hydrochloric acid
Triton X-100	t-octylphenoxypolyethoxyethanol
μ_{eo}	electroosmotic mobility

μ_{ep}	electrophoretic mobility
UV	ultraviolet
V	voltage applied across the capillary
v_{eo}	electroosmotic velocity
v_{ep}	electrophoretic velocity

CHAPTER 1

Introduction

1

1.1 Capillary electrophoresis

1.1.1 General background

Capillary electrophoresis (CE) has been developed rapidly during the past two decades with the contributions of many researchers. As a powerful separation technique. CE has been shown to be applicable to a wide variety of analytes. ranging from small inorganic ions and molecules to biopolymers like proteins and oligonucleotides.

Capillary scale zone electrophoresis can be tracked back to the late 1950's and 1960's (1-3). In the 1980's Jorgenson *et al.* published several papers demonstrating the high separation efficiencies of this technique with the use of high field strengths and its application to protein digests in fused silica capillaries (4-6). Since then. the potentials of this technique have been more fully recognized and increasing numbers of research papers have been published on various aspects and applications of capillary electrophoresis. The attention attracted by capillary electrophoresis has been not only from academia. but also from industry. The first commercial CE instrument was introduced in 1988 by Microphoretic Systems (Sunnyvale. CA). And there are currently about a half dozen companies manufacturing CE instruments. The development of commercial instruments in turn has made the technique accessible to a larger group of scientists.

CE was principally derived from traditional electrophoresis with references to chromatography as well. Compared to slab gel electrophoresis. CE is faster. easier. simpler. can be more readily automated. and gives quantitative data. The major advantage of CE over HPLC is its applicability for the separation of widely different compounds.

2

inorganic ions, organic molecules and large biomolecules, using the same instrument and in most cases the same column while changing only the composition of the running buffer. Also, CE possesses the highest resolving power of any liquid separation technique. Furthermore, the amount of material needed for a CE experiment is minute, nanoliters of sample and microliters of buffer. This compares favorably to the other liquid separation techniques, which require microliters of sample and milliliters of solvent. Last but not least, ultra-sensitive detection can be achieved by combining CE with detection technique like laser-induced fluorescence (LIF) detection. Analysis at the single cell levels has been achieved by CE-LIF, which will be of great help toward accurate and reliable understanding of biological systems. These features of CE make CE a very attractive method for biological and clinical applications. Section 1.3 will cover some of the application fields.

CE now comprises a family of electrokinetic separation techniques that separate compounds based upon differences in electrophoretic mobility, phase partitioning, isoelectric point (pI), molecular size or a combination of these properties. However, despite the various separation mechanisms, there are two most important definitions in understanding CE: electrophoresis and electroosmosis, which will be discussed in the following section.

3

1.1.2 Electrophoresis and electroosmosis

1.1.2.1 Electrophoresis

Electrophoresis is the fundamental separation process in capillary electrophoresis. It describes the phenomenon that under an electric field. the cationic or anionic components will migrate toward the cathode or anode according to their electrophoretic mobility. Inside a capillary. the solute's mobility is determined by both its charge and the friction it encounters as it travels through the capillary which is correlated to the size of the ion. Therefore. ionic species can thus be separated into discrete zones through electrophoretic migration based on their charge-to-mass ratios. as shown in Figure 1.1A. The electrophoretic mobility. μ_{ep} (cm^2/sV) of an ion can be calculated as:

$$\mu_{ep} = \frac{V_{ep}}{E} = \frac{L_d \cdot t_r}{V \cdot L_c}$$

(1.1)

where V_{ep} is the electrophoretic velocity (cm/s). E is the electric field strength (V/cm). L_c is the length of the entire capillary. L_d is the length of the capillary from the injection end to the detection region. t_r is the migration time. and V is the voltage applied across the capillary.

1.1.2.2 Electroosmosis

Figure 1.1B shows another fundamental process called electroosmosis. In a fused silica capillary. there are ionizable silanol groups on the inner surface of the capillary wall. The degree of ionization of these silanols depends mainly on the pH of the buffer within the capillary. The pI of the silanol group is reported to be 1.5 [7]. Therefore. if a capillary is

4
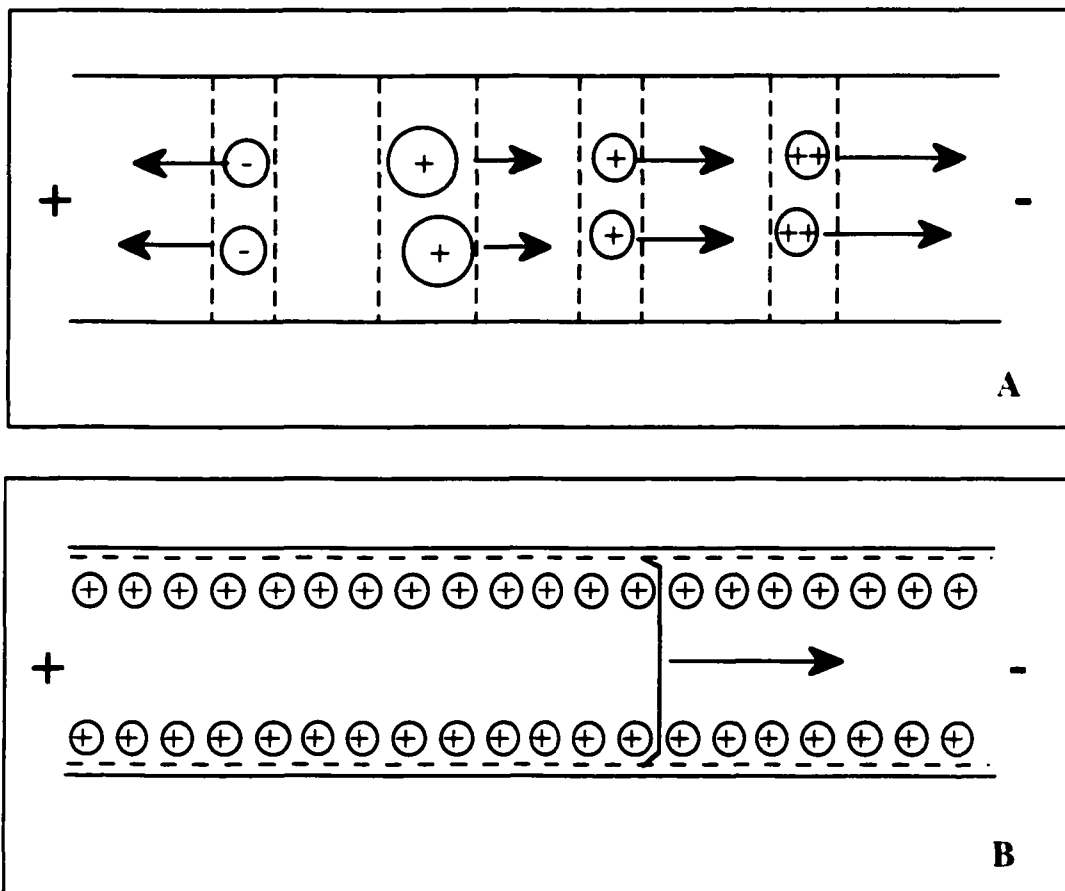
Figure 1.1 Electrophoresis (A) and electroosmosis (B). The size of the circle indicates the size of the ions, while + and − represent cationic and anionic compounds respectively. The valency of an ion is indicated by the number of +'s or −'s.

5

filled with alkaline buffer, the silanol groups deprotonate and a highly negatively charge surface results. The negatively charged capillary wall will then attract positively charged ions from the bulk buffer solution, creating an electric double layer. When an electric field is applied along the capillary, electroosmosis occurs, that is, the solvated cations in the diffuse layer migrate toward the cathode. In other words, electroosmosis moves the bulk buffer solution as a plug in the capillary toward the cathode. The electroosmotic mobility, μ_{eo} can be calculated as [7]:

$$\mu_{eo} = \frac{V_{eo}}{E} = \frac{\varepsilon\zeta}{4\pi\eta} \tag{1.2}$$

where V_{eo} is the electroosmotic flow velocity (cm/s), E is the electric field strength (V/cm), ε is the dielectric constant of the solution, η is the viscosity, and ζ is the zeta potential at the plane of shear close to the liquid-solid interface.

Since the pI of silanol groups is only 1.5, electroosmotic flow (EOF) is mainly from anode to cathode. Furthermore, the EOF is generally stronger than the electrophoretic mobility at neutral to alkaline pHs. The overall migration velocity $V_{overall}$ for each sample component is:

$$V_{overall} = V_{ep} + V_{eo} \tag{1.3}$$

Migration time t_r is defined as the time it takes a solute to migrate from the injection end of the capillary to the detection volume.

$$t_r = \frac{L_d}{V_{ep} + V_{eo}} \tag{1.4}$$

6

1.1.3 CE separation modes

CE can be classified into many different modes based on different separation and operation characteristics. The versatility of CE is greatly enhanced due to the availability of different modes. At present, the most often used modes of CE are capillary zone electrophoresis (CZE), micellar electrokinetic capillary chromatography (MECC), capillary gel electrophoresis (CGE), capillary isoelectric focusing (CIEF).

Each of the separation modes has unique characteristics and is good for different applications. In the following two sections, the basic principles of capillary zone electrophoresis (CZE), capillary gel electrophoresis (CGE), and sodium dodecyl sulfate capillary gel electrophoresis (SDS CGE) that are used in this thesis work will be discussed.

1.1.4 Basic principles of capillary zone electrophoresis (CZE)

CZE was introduced by Jorgenson and Lukacs in 1981 (5, 6, 8). Fundamental to CZE is the homogeneity of the buffer solution and constant electric filed strength in the capillary. Separation in CZE is based upon differences in net electrophoretic mobilities of analytes determined by differences in their charge-to-mass ratios. This leads to ionic solutes migrating in discrete zones of different velocities. Because all electrically neutral analytes have zero electrophoretic mobility and their migration through the capillary is purely based on the EOF, neutral components cannot be separated by CZE. However, CZE is good for almost all kinds of ionic species ranging from small inorganic ions and simple organic molecules to biopolymers like peptides and proteins. CZE analysis can be performed in the absence or the presence of electroosmosis and the separations primarily depend on the buffer and solvent employed. Chemical equilibria and affinities are also

7

employed to manipulate the electrophoretic mobilities of the solutes. and thus the separation. CZE has been the most popular CE mode to date. and studies using this technique account for 60% of the publications in the open literature.

1.1.5 Basic principles of capillary gel electrophoresis (CGE)

1.1.5.1 General aspects

Capillary gel electrophoresis (CGE) is employed to separate compounds with similar charge-to-mass ratios. such as DNA molecules [9, 10] and dodecyl sulfate-protein complexes [11, 12]. CGE combines the principles of slab gel electrophoresis with the instrumentation and small diameter capillaries of CZE and was introduced by Cohen and Karger in 1987 (11, 12). In the CGE mode. the capillary is filled with anticonvection medium (gel) and the EOF is suppressed so the gel will not be moving out of the capillary under the electric field. The gels form a porous solid. As charged solutes migrate through a gel-filled capillary due to electrophoresis. they are separated by a molecular sieving mechanism based on their sizes. Small molecules are able to pass quickly through the pores and thus elute first. In contrast. bigger molecules take longer time to pass through the gel and thus elute later. This is illustrated in Figure 1.2. Gels can be cross-linked polyacrylamide or noncross-linked entangled hydrophilic polymers also referred to as replaceable gels such as linear polyacrylamide (LPA). dextran. polyethylene glycol (PEG) and hydroxyethylcellulose (HEC). Replaceable gels are easy to introduce and replace. and are routinely employed.

8
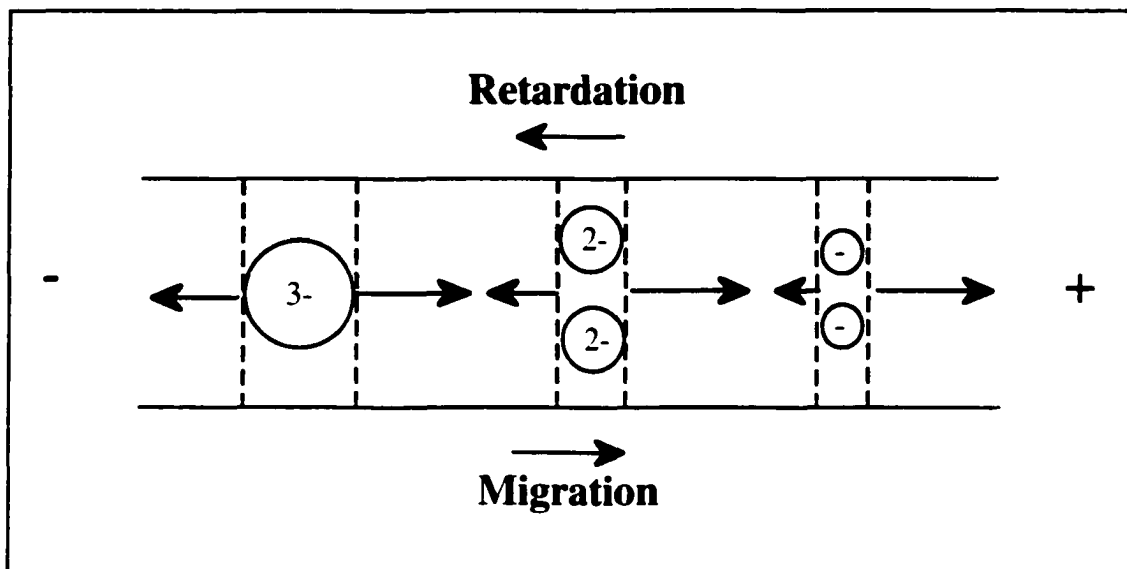
Figure 1.2 Illustration of CGE of anions. The sizes of the circles indicates the sizes of anions and different valences are indicated by $-$'s. Despite their differences in size and valence. all the three anions are of the same charge-to-mass ratios i.e. identical electrophoretic mobilities. However. when migrating through the pores of the gels. they each experience a different retardation force and they elute on the basis of their sizes. with the smallest ones migrating out first. Cations can also be separated by CGE by reversing the polarity.

9

1.1.5.2 CGE separations for DNA molecules

DNA molecules all possess similar charge-to-mass ratios independent of their molecular sizes: i.e. their electrophoretic mobilities are identical. Therefore, CZE separation of DNA fragments based solely on their electrophoretic mobility differences is not possible. There have been reports describing DNA separations in free solution using CZE by changing their mobilities with end-labeling techniques (end-labeled free-flow capillary electrophoresis (13). However, most DNA separations are achieved by CGE where a polymer matrix is sieved inside a capillary [14-16].

The basic principle of CGE separations of DNA molecules can be explained as depicted in Figure 1.2. During electrophoresis, DNA molecules collide with the sieving polymer and the interaction results in a retardation force in the opposite direction from the migration. In other words, the apparent mobility is reduced. Since different DNA fragments are of different sizes and interact differently with the sieving matrix, the resulting mobility change differs on the basis of molecular size. By the use of a sieving matrix, size-based separation of DNA molecules is achieved.

1.1.5.3 Sodium dodecyl sulfate capillary gel electrophoresis (SDS CGE) of proteins

The separation principle of protein separations using sodium dodecyl sulfate capillary gel electrophoresis (SDS CGE) is similar to DNA separations using CGE. However, an additional sample treatment step is required before introducing proteins into the gel-filled capillary. This is because native proteins do not have similar charge-to-mass ratios like DNA molecules. To separate proteins with SDS CGE, proteins are first denatured and SDS is added. SDS binds to denatured proteins with a constant ratio of 1.4 g of SDS to 1 g of denatured protein (17), which is equivalent to about one SDS molecule per two

10

amino acid residues (18). The consequences of this constant binding are proteins that are all highly negatively charged and have similar mass-to-charge ratios. Then the SDS-protein complexes are introduced into a capillary filled with sieving gels and separated based on their sizes. It is important that proteins are completely denatured when mixed with SDS because if the proteins contain disulfide bonds they will only bind in a ratio of 0.9 g to 1g of SDS to 1 g of protein (19).

1.2 CE system

1.2.1 Typical CE system setup

CE separations are typically carried out in an open tubular fused-silica capillary of about 25-75 μm inner diameter (I.D.) and 15-100 cm length. During analysis, the capillary is filled with buffer (typically of 10 to 100 mM-ionic strength) and the two ends are placed in two buffer-containing reservoirs. The liquid levels in the two reservoirs are kept the same to avoid unwanted hydrodynamic flow siphoning within the capillary. A platinum electrode is put into the buffer vial containing the injection end of the capillary while the waste reservoir is grounded. High voltage (positive or negative) is applied across the capillary. The high voltage end of the capillary is enclosed within a non-conducting box with a safety interlock to avoid electrocution hazards. Detection can take place either on-column or off-column. Figure 1.3 shows a typical CE system with on-column detection. However, post-column laser-induced fluorescence (LIF) detection is the major detection method used in this thesis because it achieves high sensitivity. This will be discussed in Section 1.2.2.

11
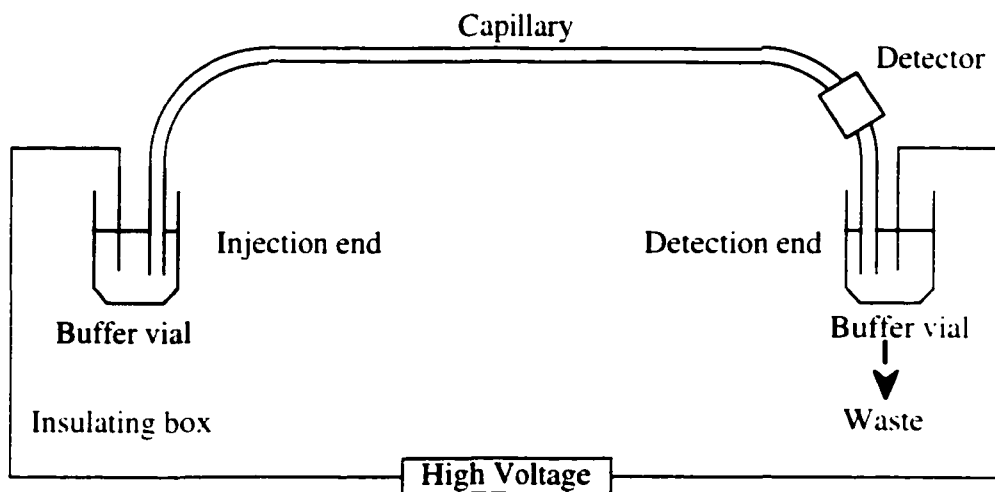
Figure 1.3 Schematic diagram of a typical capillary electrophoresis (CE) system with on-column detection. High voltage applied across the capillary can be either positive or negative.

1.2.2 Post-column laser-induced fluorescence (LIF) detection

Detection in CE is a significant challenge as a result of the small dimensions of the capillary. A number of detection methods have been employed to meet this challenge, many of which are similar to those used in liquid column chromatography. Table 1.1 has a list of several widely used detection methods for CE (20). From Table 1.1, it can be seen that laser-induced fluorescence (LIF) detection is the most sensitive detection scheme for CE among these widely applied detection methods. As monochromatic /narrow line excitation light sources, lasers have made spectacular improvements in detection limits in fluorescence measurements. The high spatial coherence of a laser allows very small sample volumes to be probed with high efficiency. When coupled with efficient collection and detection, minute amounts of analytes may be detected.

In 1985, Zare's research group reported the first application of on-column LIF detection in CE (21). Femtomole sensitivity was achieved for dye labeled amino acids. In on-column LIF approaches, a laser beam is directly focused onto the capillary and the fluorescence signal is collected at right angles to both the incident laser beam and the sample stream flowing in the capillary. The polyimide coating around the detection region has to be removed to decrease light scattering and thus increase the sensitivity. However, the change in refractive index at the capillary/buffer interface still produces a large amount of light scatter, which is responsible for the majority of the noise encountered in on-column detection.

To solve this problem, a post-column LIF detector using a sheath flow cuvette was designed for CE by this group and has been demonstrated to provide superior detection sensitivity. A simple schematic of the post-column LIF detection is shown in Figure 1.4. Different from on-column LIF detection, the capillary eluent is surrounded by a

13

Table 1.1 Common detection methods for CE (20).

Method	Mass detection limit (moles)	Concentration detection limit (mol/L)
Laser-induced fluorescence	$10^{-18} - 10^{-20}$	$10^{-14} - 10^{-16}$
Amperometry	$10^{-18} - 10^{-19}$	$10^{-10} - 10^{-11}$
UV-Vis absorption	$10^{-13} - 10^{-16}$	$10^{-5} - 10^{-8}$
Mass spectrometry	$10^{-16} - 10^{-17}$	$10^{-8} - 10^{-9}$

14
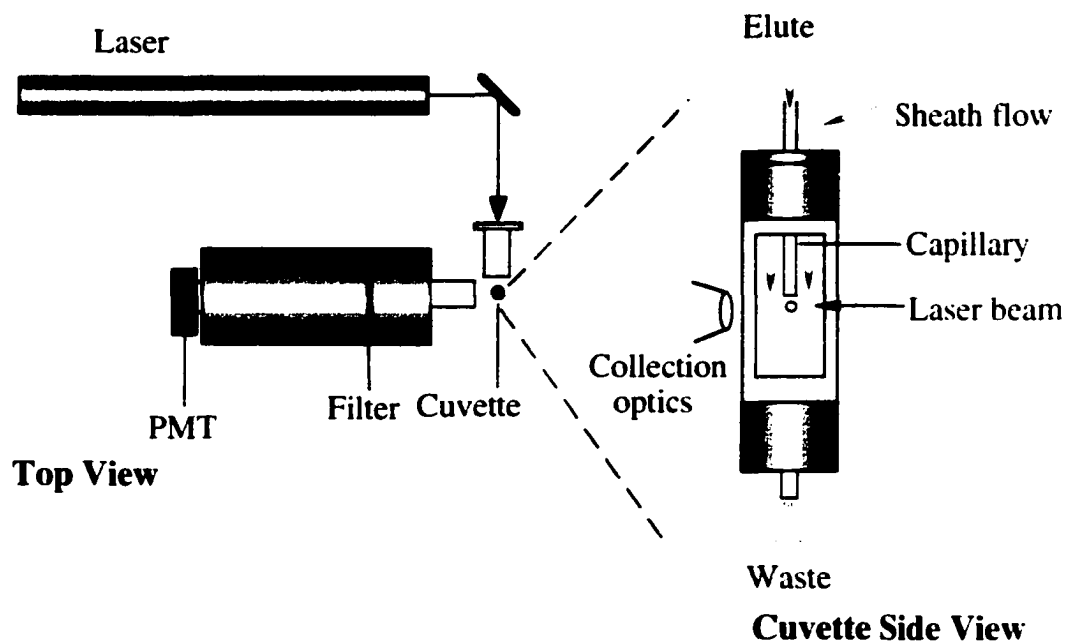
Figure 1.4 Schematic diagram of post-column laser-induced fluorescence (LIF) detection. Fluorescence signals are collected through confocal collection optics to discriminate the analyte signal from light scatter in other regions, filtered using a bandpass filter to remove light scatter in the same region, and then detected by a photo multiplier tube (PMT).

15

sheath flow (composed of the same electrophoretic running buffer as used for separation in most situations) of equal refractive index. Detection is carried out post-column at a position close to the capillary end. Therefore, the difference in refractive index at the capillary/buffer interface of on-column detection is eliminated. The major source of noise in sheath flow cuvette based post-column LIF detection is light scattering from the solvent, which is significantly less than the light scatter found in on-column detection. By this design, noise involved with LIF detection is reduced and sensitivity is increased greatly. Detection limits have been improved from sub-attomole (10^{-18} mole) in 1988 (22), to the low zeptomole (10^{-21} mole) range in 1992 (23) and to the yoctomole (10^{-24} mole) level in 1993. Single molecule detection has been achieved in some favorable cases (24-28).

With proper modifications, the LIF detection method can be used for a wide range of molecules including many of biological significance. LIF detection is also compatible with almost all the separation modes of CE. The great sensitivity of LIF, therefore, can have a big contribution to the fields of biological and clinical analysis. Without a specific statement to the contrary, LIF is used as the detection method for any CE separation in this thesis.

1.3 CE in biological and clinical applications

1.3.1 General information

When compared to chromatographic assays and slab gel electrophoretic techniques, CE has many attractive features. These include versatility, high resolution, efficiency, speed,

16

ease of automation, fast method development, very small sample volumes, use of small amounts of reagents and inexpensive columns. In addition, there is literally no restriction to the type of compounds that can be analyzed by CE. Because of these reasons, the popularity and importance of CE as an emerging technology in biological and clinical applications are steadily increasing and many new systems have been explored (29-35).

To date, there are innumerable papers exploring and promoting of CE applied to analyzing molecules of biological significance and employing CE in clinical applications (36-43). Based on the substances analyzed, applications can be classified into four major areas (i) inorganic ions, (ii) drugs, (iii) amino acids, peptides and proteins, and (iv) oligonucleotides (e.g. DNA fragments for the determination of genetic properties). In the following four sections, these four areas will be discussed with the emphasis on their separations by CE and potential clinical applications of CE for these molecules.

1.3.2 Inorganic ions

CZE and MECC are well suited for the separation of inorganic ions using indirect UV detection. Hjerten presented the first separation of 11 metal ions in 8 minutes (3). Since then, many studies have been published dealing with the separation of inorganic ions, acids, and bases (44-47). The separations of inorganic ions with CE are easy, fast and of high resolution. Separation of 36 anions was achieved in 3 min (44) and 37 anions were resolved in 12 minutes (45).

In terms of the determination of these small ions (e.g. Na^+, K^+, Ca^{2+}, nitrite, nitrate) in body fluids, clinical assays based upon ion-selective electrodes, ion chromatography, atomic absorbance spectrometry, as well as enzymatic and colorimetric reactions are typically employed. However, some of the routinely applied assays for these compounds

17

are time-consuming, expensive and lack selectivity, sensitivity and precision. Thus, the attractive separation features for these ions offered by CE are applied to a number of relevant clinical applications. The applications include the determination of ionized and total calcium in serum (48), of urinary oxalate and citrate (49), of urinary calcium and inorganic cations (50), of purine bases and nucleosides in human cord plasma (51), of nitrite and nitrate in blood (52), and many others (53-59).

1.3.3 Drugs

The measurement of drugs and other exogenous compounds in body fluids is essential in modern drug therapies, diagnostics, toxicology, drugs abuse testing and also in the research and development of new pharmacologically active compounds. Drug determinations by CE have been explored extensively (60-68). The separations are usually achieved by CZE or MECC in untreated fused-silica capillaries and aqueous buffer systems that may contain low amounts of an organic solvent or other additive. UV, LIF or mass spectrometry (MS) is usually used as the detection method coupled to the CE separations.

In clinical settings, most of the common drugs are analyzed by nonisotopic immunoassays that are highly automated, rapid and sensitive. However these methods have problems with cross-activities of related drugs, drug metabolites and other substances of similar structures. In addition, an immunoassay is typically designed for the determination of a drug only in a specific body fluid, blood, serum or urine and the development process is tedious. CE based assays, in contrast, are easy to develop and can selectively detect the analyte of interest with high sensitivity. In general, monitoring drugs in clinical applications using CE has two most important areas of interest: (i) the determination of specific drugs and/or research reasons; and (ii) the confirmation of drugs

18

of abuse and/or their metabolites in a specimen of clinical interest. A number of validated CE-based drug assays have been described. A few examples include metabolism studies of caffeine (69). dihydrocodein (70). zopiclone (71) and study of drugs such as tamxofen (72. 73). idarubicin (74). doxorubicin (75). ketoprofen (62) and methylphenidate (60) in plasma. serum and urine. CZE and MECC with UV. LIF and MS have been shown to comprise rapid. inexpensive and highly efficient analytical methods for drug studies.

In Chapter 4 of this thesis. a CZE based separation method was developed for nucleoside and nucleotides with LIF detection. This assay was used to study a key enzyme. deoxycytidine kinase (dCK). in the activation of nucleoside anti-cancer drugs.

1.3.4 Amino acids, peptides and proteins

The separation of amino acids. peptides. and proteins by CE has been a popular one. although not an easy one. The 20 common amino acids possess many different chemical properties. basic. acidic. polar. hydrophobic and hydrophilic. Therefore. MECC is the method of choice for the separation of a mixture of amino acids. In MECC. a surfactant such as SDS is added to affect the separation by introducing partitioning as a mechanism in addition to charge-to-mass ratios (23. 76). Peptide separations with CE were one of the first CE applications. Now many more studies have dealt with the separation of peptides and peptide mapping after enzymatic protein digestion (77. 78). CZE separations of proteins in untreated fused silica capillaries have not been very successful due to the interaction of the protein with the silanol groups on the inner capillary wall. Usually buffer modifiers or capillary coating steps are used to eliminate or suppress the protein/wall interaction (6. 79-82). Compared to CZE. the area of SDS CGE separation of proteins is relatively young. The first reports of this separation method only date back to 1987 (11. 12). Initially cross-linked polyacrylamide (PA) was employed as a sieving

19

matrix. Then came a shift to linear PA (LPA) sieving matrices for SDS CGE separations (83-85) and method development with many other different polymers such as dextran. poly(ethylene oxide) (PEO), and poly(ethylene glycol) (PEG) (86-88) has taken place.

For the analysis of peptides and amino acids in clinical labs, CE has found many successful examples such as the analysis of amine-containing compounds in cerebrospinal fluids by CE-LIF (89) and the determination of phenylalanine in pretreated serum (90). The general areas of protein analysis by CE in clinical research include separation, identification and quantification of serum proteins with CZE (91-94), lipoproteins with CZE and CITP (95-97), human hemoglobins with CZE and CIEF (98-100), urinary proteins with CZE (101-103) and other interesting applications (104, 105).

In Chapter 3 of this thesis, a CZE-LIF based assay was developed to quantify the plasma membrane protein hENT1 (human equilibrative nucleoside transporter protein 1). hENT1 is clinically important and is responsible for nucleoside drug resistance. The developed hENT1-CZE-LIF method was also successfully applied to study the hENT1 expression level changes during the cell cycle, as demonstrated in Chapter 5.

In Chapter 4 of this thesis, the traditional protein separation methods of SDS PAGE and 2-D gel electrophoresis techniques along with SDS CGE were employed to profile the overall protein expressions in different phases of HeLa cells. Differences in these separation methods were also compared.

1.3.5 DNA

The success of CE as an analytical technique for the separation of nucleic acids is based on CGE. CGE is an extremely powerful separation method for double-stranded and

20

single-stranded DNA fragments and PCR products. Hydroxyethylcellulose (HEC), hydroxymethylcellulose (HMC), polyvinyl alcohol (PVA), liquid polyacrylamide, and others have been used as liquid polymers (106, 107). The pore size of a sieving matrix can be changed by changing its concentration. Depending on the pore size, single oligonucleotide resolution (e.g. for sequencing of single-stranded DNA in the range of 20 to over 600 bases) as well as the resolution of DNA digests or PCR products (double-stranded DNA in the range of 50 to over 20.000 base pairs) can be obtained.

One of the most important biological applications of CGE is in the field of DNA sequencing. The realization of high throughput sequencing has come about with the development of multi-capillary CGE sequencing machines (108-110). Utilizing this technology, Celera Genomics has been able to sequence the entire human genome. This lab has been a pioneer in this area of interest.

Ever since the first validated clinical CGE assays for PCR products was described, PCR product analysis by CGE has been a field of growing importance. CGE can be used to study various mutations (111), polymorphism (112), determination of inherited genetic disease (113) and infectious diseases (114), to name but a few. CGE has also been used successfully in quantifying PCR products to measure the virus titer of clinical samples (115-118). The detection of low-level virus titers is an important clinical tool to guide therapy.

Furthermore, CGE represents the method of choice for analysis of antisense oligonucleotides, a new class of therapeutic drugs (119, 120).

21

In Chapter 2 of this thesis, a CGE based method was developed to accurately quantify PCR amplification product of duck hepatitis B virus (DHBV) DNA.

1.4 Thesis summary

The work in this thesis is dedicated to applying CE to biological and clinical research.

Chapter 2 presents the development of a CGE-LIF method for PCR quantification. DHBV was used as the model in this study. Quantification of PCR amplification products is key in determining clinical virus concentrations.

Chapter 3 presents the development of a CE-LIF based quantification method for the hENT1 protein. hENT1 is the major mediator of several major anti-cancer nucleoside drugs and its deficiency directly confers drug resistance and treatment failure. The work, once improved to an analysis at the single-cell level, will be extremely useful in understanding nucleoside drug resistance mechanism and helping cancer treatments.

Chapter 4 presents a study of a fluorescent dye labeled deoxycytidine as a substrate for measuring deoxycytidine kinase (dCK) activity. dCK is the key enzyme in nucleoside anti-cancer drug activation and toxicity. A series of studies were successfully carried out including the separation condition, substrate preparation, enzyme kinetics and substrate uptake and distribution. However, the preliminary results indicate that a better substrate is needed.

Chapters 5 and 6 illustrate the importance of cell synchronization techniques in understanding some cell cycle-dependent biological events. HeLa cells were successfully

22

synchronized with thymidine and nocodazole blockages. In Chapter 5, the CE-LIF based hENT1 quantification method was applied to the synchronized cells and differences in the hENT1 expression level were measured. In Chapter 6, overall protein expressions at different phases were probed with SDS-PAGE, 2D-gel electrophoresis and also a PEO-based SDS CGE assay. This chapter also demonstrates the differences in the separation capabilities of the three techniques in separating proteins.

1.5 References

1.   Turner, B. M. *Nature* **1957**, 179, 964-965.

2.   Turner, B. M. *Mikrochin. Acte III* **1958**, 305-318.

3.   Hjerten, S. *Chromatogr. Rev.* **1967**, 9, 122-219.

4.   Jorgenson, J. W.; Lukacs, K. D. *Clin. Chem.* **1981**, 27, 1551-1553.

5.   Jorgenson, J. W.; Lukacs, K. D. *Anal. Chem.* **1981**, 53, 1298-1302

6.   Jorgenson, J. W.; Lukacs, K. D. *Science* **1983**, 222, 266-272.

7.   *Introduction to Capillary Electrophoresis*. (Beckman Instruments, Inc., 1992)

8.   Jorgenson, J. W.; Lukacs, K. D. *J. Chromatogr.* **1981**, 218, 209-216.

9.   Chen, D. Y.; Harke, H. R.; Dovichi, N. J. *Nucleic Acids Res.* **1992**, 20, 4873-4880.

10.   Swerdlow, H. *Anal. Chem.* **1991**, 63, 2835-2841.

11.   Cohen, A. S.; Karger, B. L. *J. Chromatogr.* **1987**, 397, 409-417.

12.   Cohen, A. S.; Paulus, A.; Karger, B. L. *Chromatographia* **1987**, 24, 15-24.

13.   Ren, H.; Karger, A. E.; Oaks, F.; Menchen, S.; Slater, G. W.; Drouin, G. *Electrophoresis* **1999**, 20, 2501-2509.

14.   Sunada, W. M.; Blanch, H. W. *Electrophoresis* **1997**, 18, 2243-2254.

23

15. Dovichi. N. J. *Electrophoresis* **1997**. 18. 2393-2399.

16. Madabhushi. R. S. *Electrophoresis* **1998**. 19. 224-230.

17. Weber. K.; Osborn. M. *J. Biol. Chem.* **1969**. 244. 4406-4412.

18. Tanford. C. *The Hydrophobic Effect: Formation of Micelles and Biological Membranes* 2nd ed. Wiley: New York **1980**.

19. Pitt-Rivers. R.; Impiombato. F. S. A. *Biochemical Journal* **1968**. 109. 825-830.

20. Ewing. A. G.; Wallingford. R. A.; Olefirowicz. T. M. *Anal. Chem.* **1989**. 61. 292A-303A.

21. Gassmann. E.; Kuo. J. E.; Zare. R. N. *Science* **1985**. 230. 813-815.

22. Cheng. Y. F.; Dovichi. N. J. *Science* **1988**. 242. 562-564.

23. Zhao. J. Y.; Chen. D. Y.; Dovichi. N. J. *J. Chromatogr.* **1992**. 608. 117-120.

24. Chen. D. Y. PhD Thesis. Chemistry. University of Alberta. **1993**.

25. Castro. A.; Fairfield. F. R.; Shera. E. B. *Anal. Chem.* **1993**. 65. 849-852.

26. Nguyen. D. C.; Keller. R. A.; Jett. J. H.; Martin. J. C. *Anal. Chem.* **1987**. 59. 2158-2161.

27. Dovichi. N. J. *Trends in Anal. Chem.* **1991**. 3. 55-57.

28. Chen. D. Y.; Dovichi. N. J. *J. Chromatogr. B* **1994**. 657. 265-269.

29. Thormann. W.; Molteni. S.; Caslavska. J.; Schmutz. A. *Electrophoresis* **1994**. 15. 3-12.

30. Xu. Y. *Anal. Chem.* **1995**. 67. 463R-473R.

31. Jellum. E. *J. Cap. Electrophor.* **1994**. 1. 97-105.

32. Jenkins. M. A.; Guerui. M. D. *J. Chromatogr. B* **1996**. 682. 23-34.

33. Landers. J. P. *Clin. Chem.* **1995**. 41. 495-509.

34. Jangliaro. F.; Smith. F. P. *Trends in Anal. Chem.* **1996**. 15. 513-525.

35. Baba. Y. *J. Chromatogr. B* **1996**. 687. 271-302.

36. Issaq. H. J. *Electrophoresis* **2000**. 21. 1921-1939.

24

37.   von Heeren. F.: Thormann. W. *Electrophoresis* **1997**. 18. 2415-2426.

38.   Thormann. F.: Wey. A. B.: Lurie. I. S.: Gerber. H.: Byland. C.: Malik. N.:
       Hochemister. M.: Gehrig. C. *Electrophoresis* **1999**. 20. 3203-3236.

39.   Chen. S.-H.: Chen. Y.-H. *Electrophoresis* **1999**. 20. 3259-3268.

40.   Hadley. M. R.: Camiller. P.: Hutt. A. J. *Electrophoresis* **2000**. 21. 1953-1976.

41.   Krylov. S. N.: Dovichi. N. J. *Anal. Chem.* **2000**. 72. 111R-128R.

42.   Thormann. W.: Aebi. Y.: Lanz. M.: Caslavska. J. *Forensic Science International*
       1998. 92. 157-183.

43.   Watzig. H.: Degenhardt. M.: Kunkel. A. *Electrophoresis* **1998**. 19. 2695-2752.

44.   Jones. W. R.: Jandik. P. *J. Chromatogr.* **1992**. 608. 385-393.

45.   Jones. W. R.: Soglia. J.: McGlynn. M.: Haber. C.: Reineck. J.: Kotanovic. C. *Am.
       Lab.* **1996**. 28. 25-29.

46.   Janini. G. M.: Muschik. G. M.: Issaq. H. J. *J. Cap. Electrophor.* **1994**. 1. 116-120.

47.   Janini. G. M.: Chan. K. C.: Muschik. G. M.: Issaq. H. J. *J. Chromatogr. B* **1994**.
       657. 419-423.

48.   Zhang. R.: Shi. H.: Ma. Y. *J. Microcolumn Sep.* **1994**. 6. 217-221.

49.   Holmes. R. P. *Clin. Chem.* **1995**. 41. 1297-1301.

50.   Xu. X.: Kok. W. T.: Kraak. J. C.: Poppe. H. *J. Chromatogr. B* **1994**. 661. 35-45.

51.   Grune. T.: Ross. G. A.: Schmidt. H.: Siems. W.: Perrett. D. *J. Chromatogr. A*
       1993. 636. 105-111.

52.   Ueda. T.: Maekawd. T.: Sadamitsu. D.: Oshita. S.: Ogino. K.: Nakamura. K.
       Electrophoresis **1995**. 16. 1002-1004.

53.   Barbas. C.: Adeva. N.: Aguilar. R.: Rosillo. M.: Rubio. T.: Castro. M. *Clin.
       Chem.* **1998**. 44. 1340-1342.

54.   Evans. M. D.: Perrett. D.: Lunec. J.: Herbert. K. E. *Am. Clin. Biochem.* **1997**. 34.
       527-533.

55.   Garcia. A.: Barbas. C.: Aguilar. R.: Castro. M. *Clin. Chem.* **1998**. 44. 1905-1911.

56.   Hong. J.: Baldwin. R. P. *J. Cap. Electrophor.* **1997**. 4. 65-71.

57.   Vecchione. G.: Margaglione. M.: Grandone. E.: Colaizzo. D.: Cappucci. G.:
       Fermo. I.: D'Angelo. A.: Di Minno. G. *Electrophoresis* **1999**. 20. 569-574.

58.   Kiessig. S.: Vogt. C. *J. Chromatogr. A* **1997**. 781. 475-479.

59.   Viglio. S.: Valentini. G.: Zanaboni. G.: Cetta. G.: De Gregerio. A.: Cadarola. P.
       Electrophoresis **1999**. 20. 138-144.

60.   Bach. G. A.: Henion. J. *J. Chromatogr. B* **1998**. 707. 275-285.

61.   Bjornsdottir. I.: Kepp. D. R.: Tjomelund. J.: Hansen. S. H. *Electrophoresis* **1998**.
       19. 455-460.

62.   Friedberg. M.: Shihabi. Z. K. *J. Chromatogr. B* **1997**. 18. 1026-1034.

63.   Frost. M.: Kohler. H.: Blaschke. G. *Electrophoresis* **1997**. 18. 1026-1034.

64.   Lanz. M.: Theurillat. R.: Thormann. W. *Electrophoresis* **1997**. 18. 1875-1881.

65.   Sheppard. R. L.: Henion. J. *Anal. Chem.* **1997**. 69. 2901-2097.

66.   Thormann. W.: Lanz. M.: Casiavska. J.: Siegenthaier. P.: Portmann. R.
       Electrophoresis **1998**. 19. 57-65.

67.   Ramseier. A.: Siethoff. C.: Caslavska. J.: Thormann. W. *Electrophoresis* **2000**.
       21. 380-387.

68.   Ramseier. A.: Caslavska. J.: Thormann. W. *Electrophoresis* **1999**. 20. 2726-2738.

69.   Li. S.: Fried. K.: Wainer. I. W.: Lloyd. D. K. *Chromatographia* **1993**. 35. 216-
       222.

70.   Hufschmid. E.: Theurillet. R.: Martin. U.: Thormann W. *J. Chromatogr. B* **1995**.
       668. 159-170.

71.   Hempal. G.: Blaschke. G. *J. Chromatogr. B* **1996**. 675. 139-146.

72.   Carter. S. J: Li. X. F.: Mackey. J. R.: Modi. S.: Hanson. J.: Dovichi. N. J.
       Electrophoresis **2001**. in press.

26

73. Li. X. F.; Carter. S. J.; Dovichi. N. J. *J. Chromatogr. A* **2000**. 895. 81-85.

74. Hempal. G.; Haberland. S.; Schulze-Westhoff. P.; Mohling. N.; Blaschke. G.; Boos. J. *J. Chromatogr. B* **1997**. 698. 287-292.

75. Hempal. G.; Schulze-Westhoff. P.; Flege. S.; Laubrock. N.; Boos. J. *Electrophoresis* **1998**. 19. 2939-2943.

76. Chan. K. C.; Janini. G. M.; Muschik. G. M.; Issaq. H. J. *J. Chromatogr.* **1993**. 653. 93-97.

77. Issaq. H. J.; Chan. K. C.; Janini. G. M.; Muschik. G. M. *Electrophoresis* **1999**. 20. 1533-1537.

78. deGoor. T. V.; Apffel. A.; Chakel. T.; Hancock. W. in: Landers. J. P (Ed.) *Handbook of Capillary Electrophoresis* CRC Press. Boca Raton. FL **1998**. 213-258.

79. Neuhoff. V.; Schill. W. B.; Sternbach. H. *Biochem. J.* **1970**. 117. 623-627.

80. Hjerten. S. *J. Chromatogr.* **1985**. 347. 191-198.

81. Green. J. S.; Jorgenson. J. W. *J. Chromatogr.* **1989**. 478. 63-70.

82. Landers. J. P.; Oda. R. P.; Madden. B. J.; Spelsberg. T. C. *Anal. Biochem.* **1992**. 205. 115-124.

83. Wu. D.; Regnier. F. E. *J. Chromatogr.* **1992**. 608. 349-356.

84. Ganzler. K.; Greve. K. S.; Cohen. A. S.; Karger. B. L.; Guttman. A.; Cooke. N. C. *Anal. Chem.* **1992**. 64. 2665-2671.

85. Harvey. M. D.; Bandilla. D.; Banks. P. R. *Electrophoresis* **1998**. 19. 2169-2174.

86. Guttman. A.; Horvath. J.; Cooke. N. *Anal. Chem.* **1993**. 65. 199-203.

87. Benedek. K.; Thiede. S. *J. Chromatogr. A* **1994**. 676. 209-217.

88. Craign. D. B.; Polakowski. R. M.; Arriage. E.; Wong. J. C. Y.; Admadzaden. H.; Stathakis. C.; Dovichi. N. J. *Electrophoresis* **1998**. 19. 2175-2178.

89. Bergquist. J.; Gilman. S. D.; Ewing. A. G.; Ekman. R. *Anal. Chem.* **1994.** 66. 3512-3518.

90. Tagliaro. F.; Moretto. S.; Valentini. R.; Gambaro. G.; Antonioli. C.; Moffa. M.; Tato. L. *Electrophoresis* **1994.** 15. 94-97.

91. Jdliff. C.; Blessum. C. *Electrophoresis* **1997.** 18. 1781-1784.

92. Bossuyt. X.; Schiettekatte. G.; Bogaerts. A.; Blanckaert. N. *Clin. Chem.* **1998.** 44. 749-759.

93. Bossuyt. X.; Schiettekatte. G.; Blanckaert. N. *Clin. Chem.* **1998.** 44. 760-764.

94. Katzmann. J.; Clark. R.; Wiegert. E.; Sanders. E.; Landers. J. P.; Kyle. R. A. *Am. J. Clin. Pathol.* **1998.** 110. 503-509.

95. Macfarlane. R. D.; Bondarenko. P. V.; Cockrill. S. L.; Cruzado. J. D.; Koss.W.; McNeal. C. J.; Spiekerman. A. M.; Watkins. L. K. *Electrophoresis* **1997.** 18. 1796-1806.

96. Cruzado. I. D.; Cockrill. S. L.; McNeal. C. J.; Macfarlane. R. D. *J. Lipid Res.* **1998.** 39. 205-217.

97. Proctor. S. D.; Mamo. J. C. L. *J. Lipid Res.* **1997.** 38. 410-414.

98. Conti. M.; Gelfi. C.; Righetti. P. G. *Electrophoresis* **1995.** 16. 1485-1491.

99. Hempe. J. M.; Granger. J. N.; Craver. R. D. *Electrophoresis* **1997.** 18. 1785-1795.

100. Cotlon. F.; Lin. C.; Fontaine. B.; Gulbis. B.; Janssens. J.; Vertongen. F. *Clin. Chem.* **1999.** 45. 237-243.

101. Oda. R. P.; Clark. R.; Katzmann. J.; Landers. J. P. *Electrophoresis* **1997.** 18. 1715-1723.

102. Friedberg. M. A.; Shihabi. Z. K. *Electrophoresis* **1997.** 18. 1836-1841.

103. Jenkins. M. A. *Electrophoresis* **1997.** 18. 1842-1846.

104. Prasad. R.; Stout. R. L.; Coffin. D.; Smith. J. *Electrophoresis* **1997.** 18. 11814-1818.

105. Hiraoka, A.; Arato, T.; Tominaga, I.; Eguchi, N.; Oda, H.; Urade, Y. *J. Chromatogr. B* **1997**, 697, 141-147.

106. Righetti, P. G.; Gelfi, C. in: Righetti, R. G. (Ed.), *Capillary Electrophoresis in Analytical Biotechnology* CRC Press, Boca Raton, FL, **1996**, 431-476.

107. Righetti, P. G.; Gelfi, C. *Anal. Biochem.* **1997**, 244, 195-207.

108. Zhang, J.; Voss, K. O.; Shaw, D. F.; Roos, K. P.; Lewis, D. F.; Yan, J.; Jiang, R.; Ren, H.; Hou, J. Y.; Fang, Y.; Puyang, X.; Ahmadzadeh, H.; Dovichi, N. J. *Nucleic Acids Research* **1999**, 27, e36.

109. Dovichi, N. J.; Zhang, J. *Methods in Molecular Biology* **2001**, 162-163, 85-94.

110. Crabtree, H. J.; Bay, S. J.; Lewis, D. F.; Zhang, J.; Coulson, L. D.; Fitzpatrick, G. A.; Delinger, S. L.; Harrison, D. J.; Dovichi, N. J. *Electrophoresis* **2000**, 21,1329-1335.

111. Gelfi, C.; Righetti, P. G.; Cremonesi, L.; Ferrari, M. *Electrophoresis* **1994**, 15, 1506-1511.

112. Gelfi, C.; Righetti, P. G.; Leoncini, F.; Brunelli, V.; Carrera, P.; Ferrari, M. *J. Chromatogr. A* **1995**, 706, 463-468.

113. Lehmann, R.; Koch, M.; Pfohl, M.; Voelter, W.; Haring, I.-U.; Liebich, H. M. *J. Chromatogr. A* **1996**, 744, 187-194.

114. Felmlee, T. A.; Mitchell, P. S.; Ulfelder, K. J.; Persing, P. H.; Landers, J. P. *J. Cap. Electrophor.* **1995**, 2, 125-130.

115. Doglio, A.; Laffont, C.; Thyss, S.; Lefebvre, J. C. *Res. Virol.* **1998**, 149, 219-227.

116. Fernandez-Arcas, N.; Dieguez-Lucena, J. L.; Garcia-Villanova, J. G.; Pena, J.; Morell-Ocana, M.; Reyes-Engel, A. *J. Acquired. Immun. Defic. Syndr.* **1996**, 12, 107-111.

117. Zhang, N.; Yeung, E. S. *J. Chromatogr. B* **1998**, 714, 3-11.

118. Tan, W. G.; Tyrrell, D. L.; Dovichi, N. J. *J. Chromatogr. A* **1999**, 853, 309-319.

29

119. Leeds. J. M.: Graham. M. J.: Truong. L.: Cummins. L. L. *Anal. Biochem.* **1996.** 235. 36–43.

120. Cohen. A. S.: Bourque. A. J.: Wang. B. H.: Smisek. D. L.: Belenky. A. *Antisense Nucleic Acid Drug Devel.* **1997.** 7. 13-22.

30

CHAPTER 2

Quantitative Polymerase Chain Reaction Using Capillary

Electrophoresis with Laser-Induced Fluorescence Detection: Analysis of

Duck Hepatitis B Virus

31

2.1 Introduction

The development of polymerase chain reaction (PCR) has revolutionized the field of biology. PCR enables the amplification of a targeted DNA sequence with the use of two primers and DNA polymerase: the amount of target doubles with each cycle. This feature of exponential increase ensures the exquisite sensitivity of PCR amplification. However, it also makes quantification of the PCR product difficult. PCR-based amplification of nucleic acids is the tool of choice in clinical diagnosis of viral infection and monitoring of a patient's viral load (1-3). Many different methodologies have emerged in the last few years for PCR quantification; however, further improvement is needed for a highly sensitive, accurate, and reliable PCR quantification system (4-7).

Quantitative competitive PCR (QC-PCR) is widely used for the quantification of nucleic acids (5, 8-10). QC-PCR involves the use of a competitor sequence that is co-amplified with a target of interest in the same reaction tube and acts as an internal standard for the amplification reaction. The success of a QC-PCR assay depends exclusively on the design of a compatible competitor. If the amplification efficiency is identical for the target and the competitor, the amount of amplified target can be compared with the amount of amplified competitor to obtain accurate quantification of the initial target. On the other hand, minor differences in the efficiency between the target and competitor can result in serious errors in the overall quantification results. For example, ideally a sample doubles in concentration after each cycle. If the internal standard only amplifies 1.95 times each cycle, then there will be a 50% error in sample concentration after 25 amplification cycles. Furthermore, dynamic range and accuracy are mutually exclusive, unless an extremely large number of assays are performed with each sample.

32

More recently, a real-time quantitative PCR assay based on *Taq*Man chemistry was developed by Genentech and PE-Biosystems (11). In this method, a specific probe is used in addition to the two primers. This probe is labeled with a reporter fluorescence dye on one end and a quencher dye on the other. The probe hybridizes to a region between the two primers. During PCR amplification, *Taq Polymerase* extends the primers and cleaves the probe. The reporter dye is then liberated from the quencher dye and can be excited by a laser to emit fluorescence. The reporter dye signal is proportional to the amount of DNA produced and is measured at regular intervals during PCR. The entire PCR process is monitored in a real-time manner. Quantification of the initial target concentration is determined from the number of cycles necessary to generate a fluorescent signal that exceeds a threshold value. This method offers rapid, reproducible, and multiple sample quantification and has been used widely (12, 13). However, this method suffers from two limitations. First, mutation at the probe-binding region may decrease amplification efficiency and degrade experimental accuracy. Klein *et al.* reported in their studies that 3 or 4 base mismatches in the probe-binding region produced false negative results while the same samples were positive in gel electrophoresis analysis (4). Second, the probe must be tailored to each application.

Both QC-PCR and *Taq*Man require the synthesis of three specific oligonucleotides: the two PCR primers and either a competitor or a probe. The competitor or probe must be specific to the target sequence. In QC-PCR, the competitor must have similar amplification characteristics to the target. In *Taq*Man the probe must be synthesized with a fluorescent label at the 5' end and an appropriate quencher near the 3' end. The generation of such oligonucleotides is not always straightforward.

33

Interest here is focused on the development of an accurate and reliable PCR quantification assay using capillary electrophoresis. which requires the synthesis of only two PCR primers. Our method uses CE-LIF to monitor the amount of PCR product generated after each amplification cycle. Quantification of the initial target sequence is determined by noting how many cycles are required to generate product over a specified threshold value. To correct for variations in injection volume in capillary electrophoresis. a third oligonucleotide is employed. However. this internal standard is not involved in PCR amplification and is purely arbitrary in sequence. The method is applicable to all PCR analyses and involves simpler chemistry than the *Taq*Man system. In the present study. duck Hepatitis B virus (DHBV) DNA was successfully used as a model for quantification. This virus was chosen because it is a safe alternative to handling the human virus.

2.2 Experimental

2.2.1 DNA templates

A pAlter-W plasmid containing a wild type duck hepatitis B virus (DHBV) genome of 3021 base pairs (bp) was kindly donated by Dr. K. Fischer (Glaxo Heritage Research Institute. University of Alberta). The plasmid contained a 3021 bp monomer of the DHBV genome cloned into the *Eco*RI site of vector pAlter-1 (Promega. Madison. WI). A dilution series of this wild type plasmid DHBV DNA was used for the construction of the calibration curve in our study. Serum samples from two infected ducklings were also prepared using a commercial QIAamp Blood Kit (Qiagen. Missiassauga. ON. Canada)

34

and subjected to viral load determination. The DNA target in our study was 409 bp in length.

2.2.2 Injection standard

One 422 bp DNA fragment was prepared using a standard PCR protocol. After purification and quantification in a UV spectrometer at 260 nm, it was diluted to a final concentration of 2.7×10^{-8} mol/L and stored at $-20°C$ until analysis.

2.2.3 PCR assay

All PCR amplifications were carried out in a PCT-100 programmable thermal controller (MJ Research, Watertown, MA). Each PCR reaction was a 50 μL mixture containing 1.5 mM $MgCl_2$, standard PCR buffer, 300 μM dNTPs mix, 3 units of *Taq* DNA polymerase, 75 pmol of H2990 (5'AACTTACTATCCTTTCTTCT3') primer and 50 pmol of the primer HBVTa (5'GTGACTGTACCTTTGGTATG3') (Table 2.1). HBVTa was 5'-rhodamide-labeled for direct fluorescence detection. The PCR parameters were set as follows: initial denaturation for 5 min at 95°C; followed by 10 to 50 cycles of 50 s at 95°C, 1 min at 56°C and 1 min at 72°C, depending on the initial DNA copy number. In order to monitor the amplification process, a sample was prepared first and aliquoted into a series of PCR tubes. A tube was withdrawn at the end of each cycle and stored at -20°C. All the samples were then individually analyzed by CE-LIF without further manipulation.

35

Table 2.1 A Typical PCR Reaction Mixture

Components	Volume (µL)
10X PCR buffer	5
10 mM dNTP	1.5
50 mM MgCl$_2$	1.5
Primer 1 H2990 (25 pmol/µL))	3
Primer 2 HBVTa (25 pmol/µL)	2
Template	2*
Taq Polymerase	3
ddH$_2$O	32*
Total Volume	**50**

* For the negative control sample. 0 µL of template and 34 µL ddH$_2$O were used.

36

2.2.4. Capillary

A 30 cm long. 50 μm inner diameter (I.D.), 144 μm outer diameter (O.D.) DB-210 coated fused-silica capillary purchased from J&W Scientific (Folsom. CA) was used to carry out the separation. This coated capillary was previously tested and found to last for at least 400 runs without observable change in separation efficiency. The capillary was flushed with 0.1 M NaCl and buffer between runs and stayed in methanol during night.

2.2.5 Instrumentation and capillary electrophoretic conditions

An in-house built CE-LIF instrument was used for our study, and is described in detail elsewhere (14, 15). Each PCR product, without purification, was mixed with the injection standard and introduced electrokinetically into the capillary. 100 mM N-tris[Hydroxymethyl]methyl-3-aminopropanesulfonic acid (TAPS) at pH 8.0 (Sigma. Oakville, ON, Canada) was used as the electrophoresis buffer. A 0.8% (w/v) hydroxyethylcellulose (HEC: M_r 250,000) solution was prepared in electrophoresis buffer and filtered by a Millex-GS 0.45 μm filter unit (Millipore. Bedford. MA). HEC was introduced into the capillary as sieving matrix prior to sample injection. CE separation was performed with an electric field of (-)200 V/cm at room temperature. DNA molecules were excited with a Helium-Neon laser (Melles Griot Laser Group. Carlsbad. CA) with a single 543.5 nm emission line. Fluorescence was collected through a 580 nm bandpass filter of 40 nm bandwidth (580DF40. Omega Optical. Brattleboro. VI) and detected by a R1477 photomultiplier tube (PMT). Data was collected and analyzed using Igor Pro 2.04 (WaveMatrics, Lake Oswego, OR).

37

2.3 Results and Discussion

2.3.1 Analysis of PCR products by CE-LIF

Capillary electrophoresis has proven to be a powerful tool in DNA analysis (14-20). We employed a non-denaturing buffer system and hydroxyethylcellulose as the sieving medium. The PCR products, prior to CE analysis, were mixed with a 422 bp internal standard to correct for variations in the sample injection volume. In all experiments, PCR product signal was divided by the injection standard signal to produce the normalized signal used for further data processing. The theoretical plate number of the CE separation in our system was approximately 4×10^5. This high resolving power ensured that the PCR product, internal standard and excess primers were all well resolved, as shown in Figure 2.1.

Furthermore, since the target and the standard peaks were well separated from the primer peaks, measurements were simple and reliable. The requirement for a target-specific probe was also avoided due to the well-resolved separation. No purification step was required, which made the post-PCR process simple and fast.

2.3.2 Quantification parameters

During the exponential phase of PCR amplification, the number of molecules of PCR product, N, is related to the initial number of copies, N_0, the amplification efficiency, e, and the number of cycles, n:

$$N = N_0(1 + e)^n \qquad (2.1)$$

38
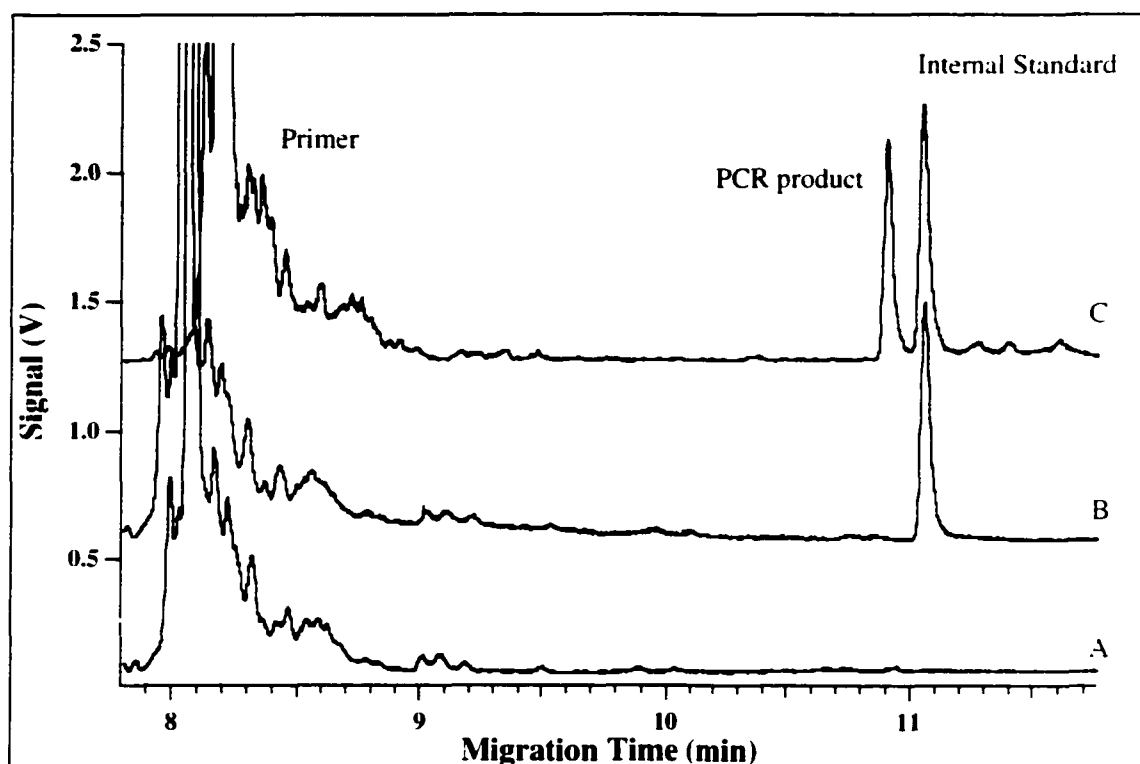
Figure 2.1 Analysis of PCR amplification products by CE-LIF. (-)1000 V was applied for
5 seconds to electrokinetically inject the sample into the capillary. CE separation was
done with an electric field strength of (-)200 V/cm. A: Negative control sample without
injection standard: B: Negative control sample with injection standard: C: PCR sample
with injection standard.

39

We determine the initial number of DNA copies by noting the number of cycles. Q_t. necessary to exceed a threshold number of copies. N_T:

$$N_T = N_0(1+e)^{Q_T} \tag{2.2}$$

For DNA samples with different numbers of initial copies. the number of cycles required to achieve the same N_T will vary as predicted by Equation (3):

$$Q_T = \frac{\log N_T}{\log(1+e)} - \frac{1}{\log(1+e)}\log N_0 \tag{2.3}$$

Assuming that the amplification efficiency at the threshold number for all the PCR reactions is the same then. as shown in Equation (2.3). Q_T is inversely proportional to the logarithm of the initial copy number. Q_T values can be used as the quantitative measurement of the input DNA concentration. From the calibration curve constructed using Q_T versus log(initial copy number). the amplification efficiency at this point can be obtained from Equation (2.4).

$$e = 10^{-\frac{1}{slope}} - 1 \tag{2.4}$$

2.3.3 Construction of the calibration curve

A dilution series of plasmid DHBV DNA ranging from 30 to 3.06×10^5 molecules per tube were amplified and detected to obtain a calibration curve for quantification. Figure 2.2 shows the amplification profiles of all these plasmid standards.

The copy numbers increased exponentially only during the initial cycles. Figure 2.3 presents a plot amplification profile along with the results of a least-squares fit of Equation (2.1) to the data for the sample containing an initial copy number of 3.06×10^5 viral particles per mL. The signal increased exponentially during approximately the first 20 cycles for this sample. During the early exponential period. all the amplification

40
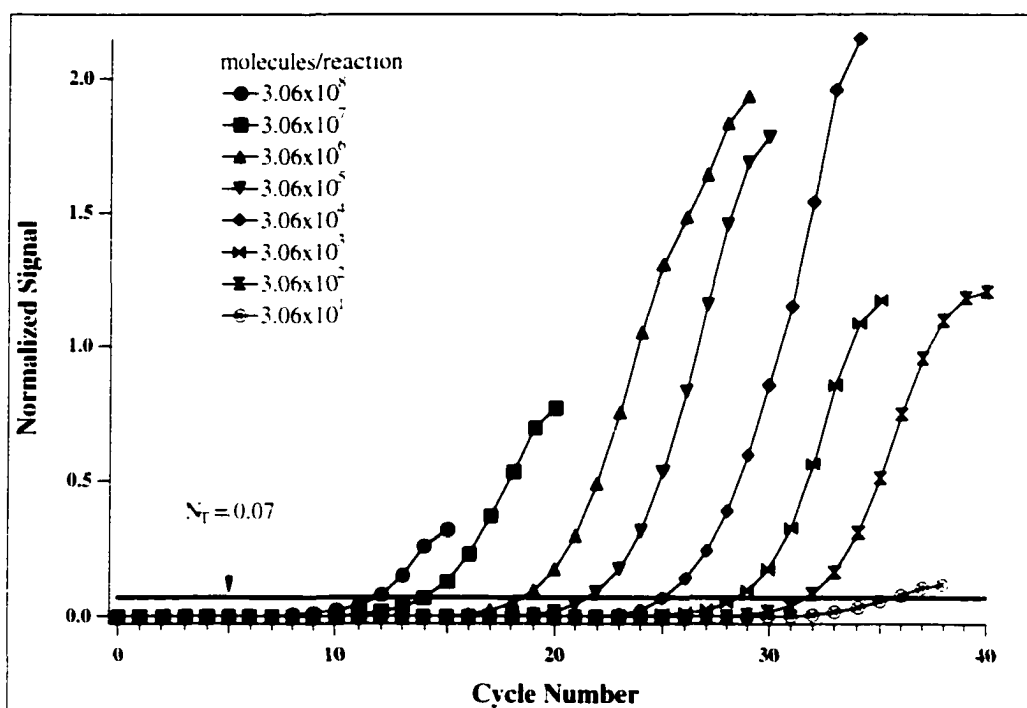
Figure 2.2 The PCR amplification profiles of the standard DNA samples. The curve shifted to the right with decreasing initial DNA copy number. Q_T values were obtained from Equation (2.3) using $N_T = 0.07$.

41
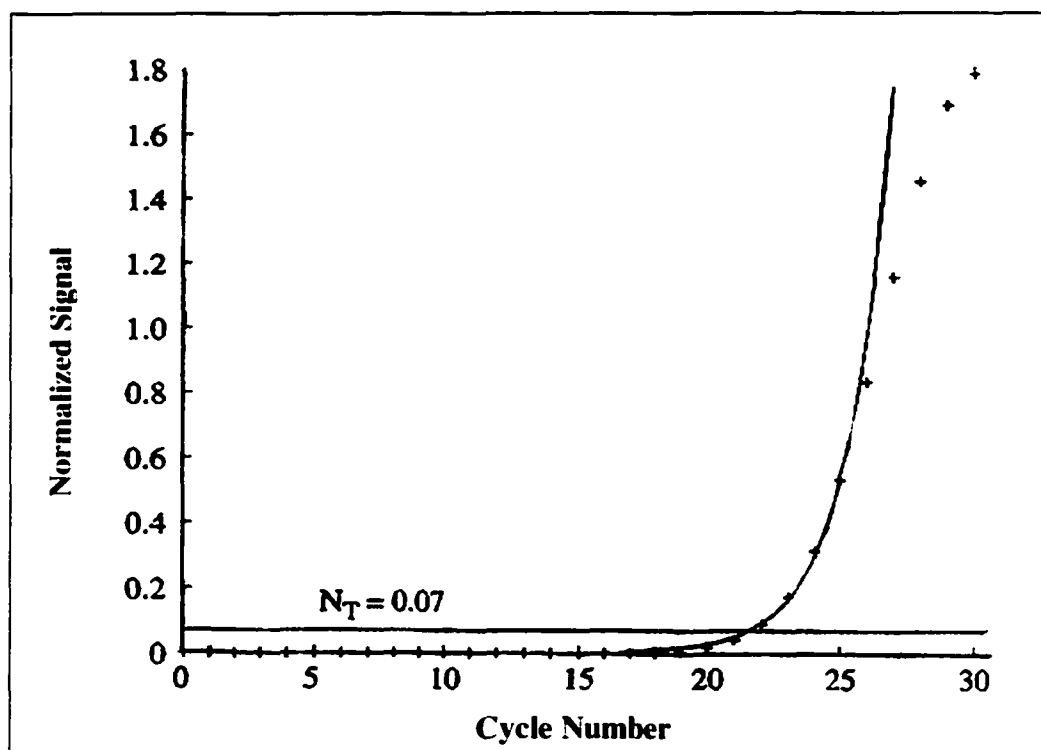
Figure 2.3 Least-squares fit of Equation 2.1 to the data for the 3.06×10^6 copy sample.

The smooth curve is the fit to cycle numbers 1 to 25, the crosses are the data points, and

the horizontal line at $N_T = 0.07$ corresponds to the threshold used for quantification.

curves were parallel. suggesting that the efficiency of amplification was constant at this stage. However, when the amplification was close to or in the plateau stage, the detected amount of amplified product was no longer proportional to the starting amount of target molecules. By monitoring PCR amplification at each cycle, more information can be obtained from the data points for each cycle.

To obtain the Q_T for the calibration curve, a threshold number N_T was assigned as 0.07 in our study. 0.07 was chosen as approximately 10 times the standard deviation of a typical CE run / internal standard signal.

A linear relationship between the Q_T value and the log (initial copy number) is shown in Figure 2.4. As low as 30 copies of target DNA could be quantified, indicating the good sensitivity of this quantitative assay. Since the quantification range is not limited by the linear response range of the detector, seven orders of linear range were obtained with $R^2 >$ 0.999. This large dynamic range and good linearity, in turn, ensures the precise and reliable quantification of the viral DNA concentration.

2.3.4 Single-blind study

To test the accuracy of the present quantification assay, a plasmid DNA template was prepared by another student in the lab and given to the author to determine the initial DNA concentration. 15 to 30 cycles PCR amplification product were plotted as shown in Figure 2.5 and the Q_T value obtained from the amplification plot was 22.6501. The initial DNA copy number was then calculated from the fitting equation of the calibration curve to be 1.51×10^5 molecules. The actual initial copy number was calculated from a UV
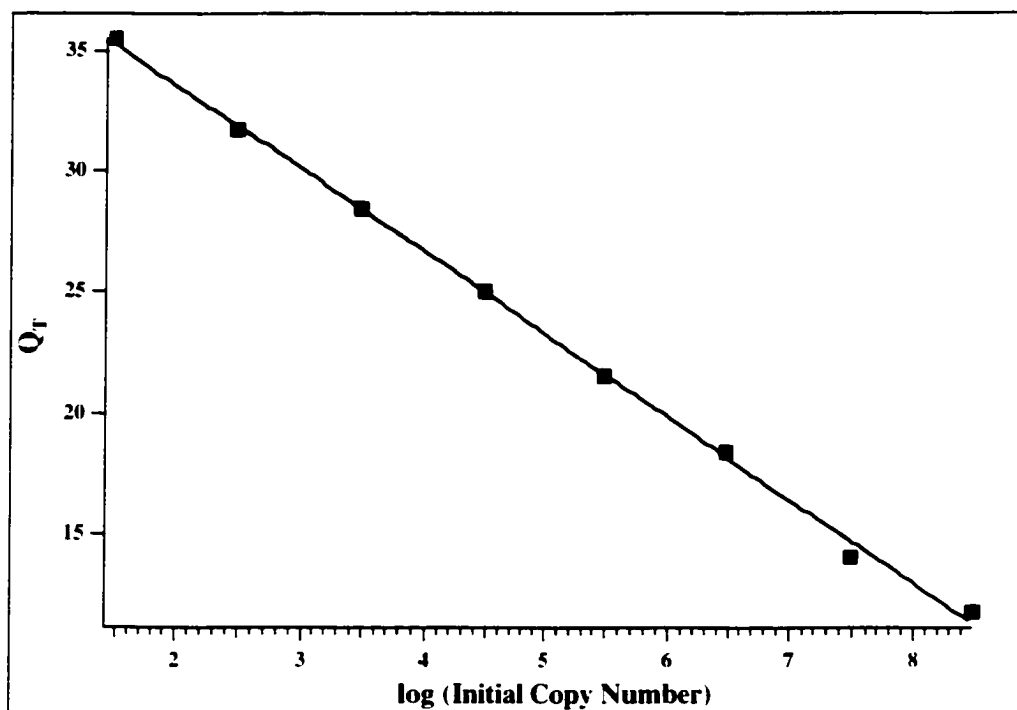
Figure 2.4 Calibration curve when N_T was assigned 0.07. The amplification efficiency calculated from Equation (2.4) is 0.956.

44
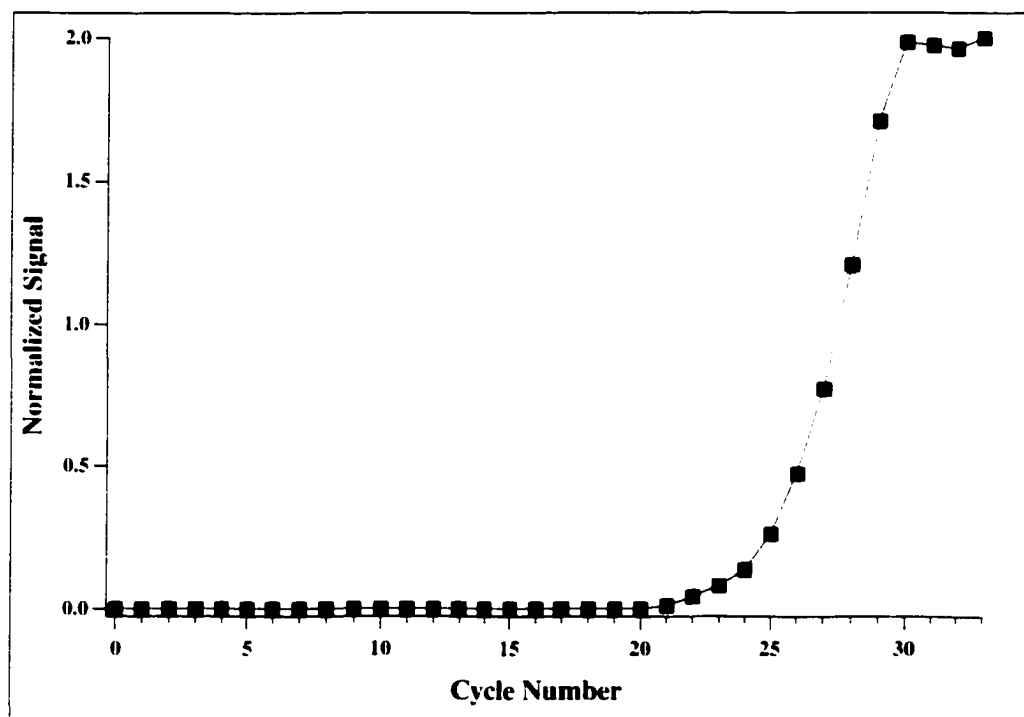
Figure 2.5 Amplification monitoring and quantification of the single-blind sample.

45

spectrometer measurement as 1.53×10^5 molecules. The error was only 1.3%, which suggests good accuracy for the technique for this amount of analyte.

2.3.5 Effects of N_T value on the quantification results

As shown in Equation (3). how N_T is assigned will directly affect the Q_T values, but N_i values will not alter quantification if efficiency is constant during the whole amplification process. However, when amplification is driven to the plateau phase, the efficiency decreases and variation increases due to parameters such as saturation of PCR product, strand reannealing, and incomplete product strand separation (21).

In our method, no competitor DNA is used to correct for fluctuations in amplification efficiency. Quantification is based on the assumption that at the threshold number N_i, all PCR reactions have the same efficiency.

When N_T is assigned at a lower number 0.07, the PCR amplification is at its early exponential phase. In this case, reagents are not limited. The amplification efficiency is close to 1 and relatively constant for all the amplifications with different initial DNA copy numbers. Quantification is still accurate without the competitor DNA. In the calibration curve shown in Figure 2.5, when we assume the amplification efficiencies are the same in all the amplifications, e was calculated as 0.956 from Equation (2.4). The linearity ($R^2>0.999$) of the calibration curve and the results of single-blind study strongly suggest that the assumption above is valid.

When N_T was assigned a much higher number e.g. 1.1, another calibration curve was obtained using the same group of samples, as depicted in Figure 2.6. The efficiency

46
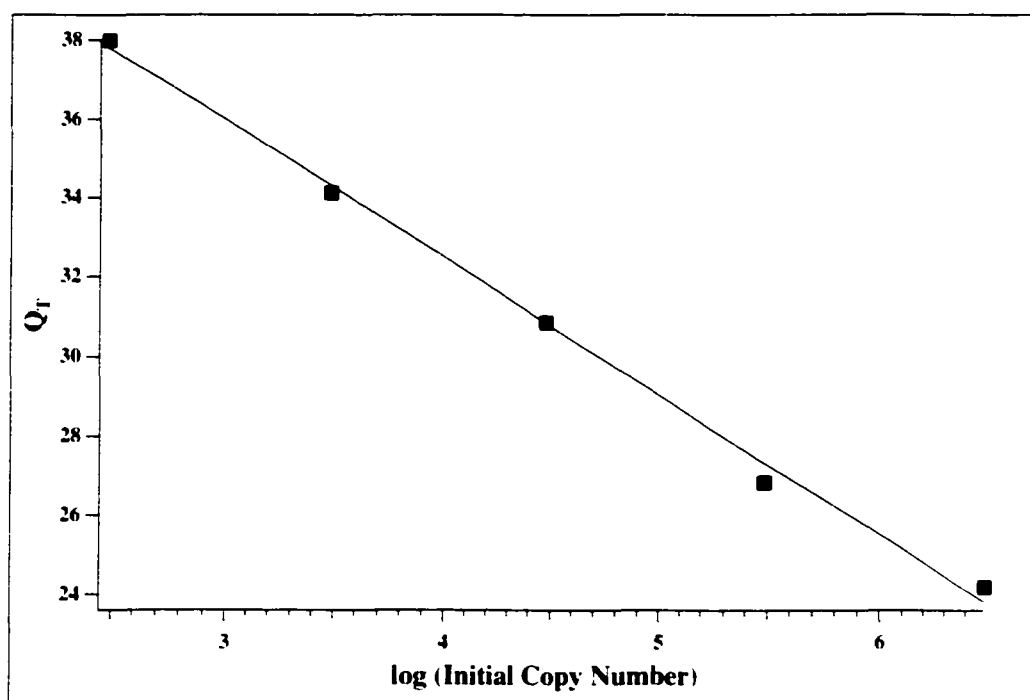
Figure 2.6 Calibration curve when N_T was assigned as 1.1. The amplification efficiency

calculated from Equation (2.4) is 0.934.

47

calculated using Equation (2.4) was 0.934. Amplification efficiency decreased when the cycle number approached the saturation level. More interestingly. when this curve was applied to the single-blind study, the calculated initial DNA copy number was 2.27×10^5 molecules with an error of 48.4%. The much higher error could be a result of the mismatch between the actual case and the assumption. When N_T approaches or is in the plateau region. between-assay variability is high and even minor differences in efficiency can have dramatic effects on the final yields. Table 2.2 shows that the quantification error increased with the increase of assigned N_T values.

Furthermore. because amplification in the plateau is difficult to control. the choice of N_T may also affect the linear quantification range. In our case. the linear range of the calibration curve was two orders of magnitude lower when N_T was defined as 1.1 instead of 0.07.

2.3.6 Quantification of DHBV DNA extract from sera of infected ducklings

Two DHBV samples from the blood serum of newly hatched ducklings were quantified using our method. Similar amplification plots to the standards applications were obtained and are shown in Figure 2.7. N_T was defined as 0.07. Once the Q_T values were determined. the initial target number could be calculated. The two animals that we investigated showed a virus titer of between 0.92×10^8 and 4.1×10^9 virus particles per mL of serum. These numbers are closely compatible to reported values obtained from other groups (Dr. David L.J. Tyrrell's group. unpublished results).

48

Table 2.2 Single-blind study results with different N_T values.

N_T	Q_T	Quantification Result (molecules)	Error (%)
0.07	22.6501	1.51×10^5	1.23
0.1	23.2977	1.48×10^5	3.10
0.2	24.5081	1.27×10^5	17.0
1.0	27.5267	2.06×10^5	34.9
1.1	27.7569	2.27×10^5	48.2

The actual initial copy number from UV detection was 1.51×10^5 molecules.

49
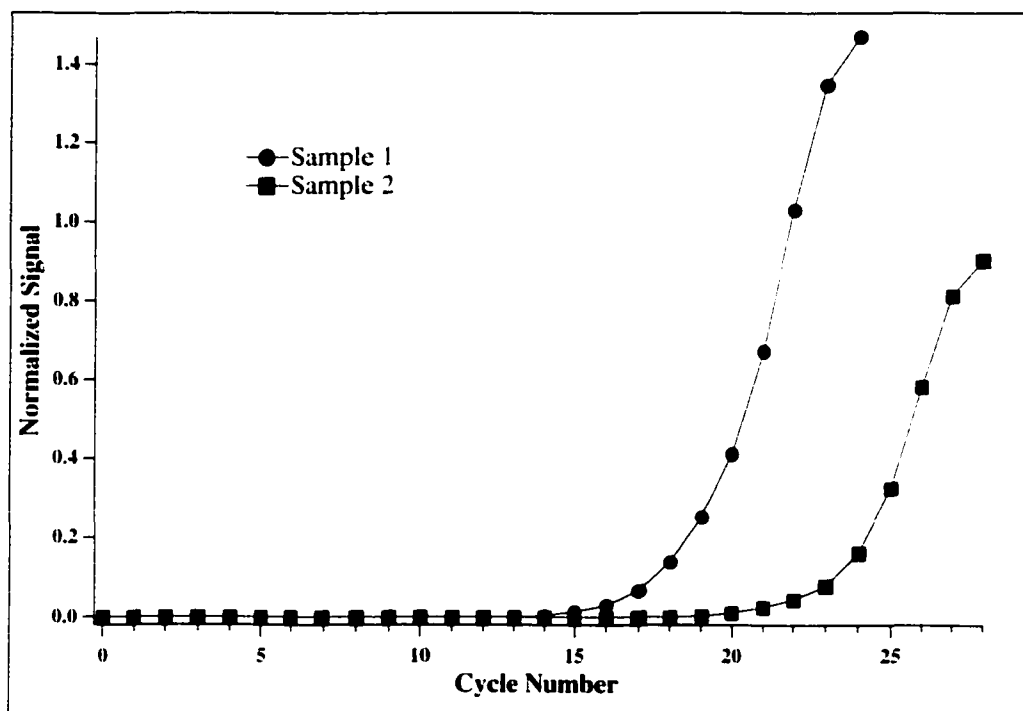
Figure 2.7 Amplification monitoring and quantification of two DNA samples extracted from HBV infected duck sera.

50

2.3.7 Precision of the quantification assay

The precision of the CE-LIF assay was determined by analysis of seven identical PCR samples with internal standards. Consecutive injections of these samples yielded a 2.7% relative standard deviation (RSD) for peak height precision (Table 2.3).

To obtain the overall PCR-CE-LIF precision and reproducibility, three aliquots were amplified in the same thermocycler for the same number of cycles. Each sample was then measured three times in the CE-LIF instrument. All together nine data points were used to calculate the RSD value. The 3.0% RSD includes the variability of both PCR amplification and CE-LIF detection (Table 2.4).

Both RSDs demonstrate the high precision of the assay, which is an important requirement for a reliable quantification method.

2.4 Conclusion

An accurate and reliable quantitative PCR method developed has been demonstrated here using capillary electrophoresis with laser-induced fluorescence detection. The assay was validated by evaluating its linearity, sensitivity, accuracy and precision. This technique uses much less expensive equipment and common reagents, but the quantitative precision and accuracy are compatible to the TaqMan assay. In practical terms, since no specific competitor or probe design is required, this method is more convenient and applicable to a wider variety of PCR amplifications than the TaqMan and QC-PCR assays.

51

Table 2.3 Precision of CE-LIF Detection

Sample	Normalized Signal
1	1.07
2	1.07
3	1.09
4	1.10
5	1.02
6	1.09
7	1.04
Relative Standard Deviation	**2.7%**

52

Table 2.4 Overall PCR-CE-LIF Precision and Reproducibility

CE Detection	PCR Sample		
	1	2	3
1	8.64	8.12	8.46
2	8.62	8.26	8.15
3	8.70	8.32	8.31
Relative Standard Deviation	3.0%		

53

In the present study, the use of capillary electrophoresis for DNA quantification of a single target was demonstrated. However, the capillary electrophoresis system is capable of resolving hundreds of amplified products in a single run. In principle, it will be possible to simultaneously detect and quantify a large number of targets from a single set of PCR amplifications, which is difficult to achieve with other quantification assays (23).

This method still requires some optimization. PCR monitoring was time-consuming: an aliquot was manually withdrawn from the thermocycler after each amplification cycle. internal standard was added to correct for variations in injection amount, and the mixture was analyzed by capillary electrophoresis. We believe that the system will be very useful when integrated into automated capillary array electrophoresis instruments (20, 24). These capillary array instruments could withdraw and analyze aliquotes from each well of a thermocycler at each temperature cycle. The use of very high electric field strength in capillary electrophoresis allows rapid separation of DNA fragments (25, 26). so that the separation time can be matched to the cycle time of the thermocycler.

2.5 References

1.   Mullis, K. B.; Ferré, F.; Gibbs, R. A. *Quantitative PCR: An Overview. In The Polymerase Chain Reaction* Birkhauser, Boston 1994, 67-88.

2.   Niemeyer, D. M. *Military Medicine* 1998, 163, 226-228.

3.   Reischl, U.; Kochanowski, B. *Molecular Biotechnology* 1995, 3, 55-71.

4.   Klein, D.; Janda, P.; Steinborn, R.; Müller, M.; Salmons, B.; Günzburg, W. H., *Electrophoresis* 1999, 20, 291-299.

54

5. Williams. S. J.; Schwer. C.; Krishnarao. A. S. M.; Heid. C.; Karger. B. L.; Williams. P. M. *Anal. Biochem.* **1996.** 236. 146-152.

6. Katz. E. D. *Molecular Biotechnology* **1996.** 6. 79-86.

7. Jalava. T.; Lehtovaara. P.; Kallio. A.; Ranki. M.; Söderlund. H. *BioTechniques* **1993.** 15. 134-139.

8. Köhler. T.; Rost. A. K.; Remke. H. *BioTechniques* **1997.** 23. 722-726.

9. Payan. C.; Véal. N.; Crescenzo-Chaigne. B.; Bélec. L.; Pillot. J. *J. Virol. Methods* **1997.** 65. 299-305.

10. Borson. N. D.; Strausbauch. M. A.; Wettstein. P. J.; Oda. R. P.; Johnston. S. L.; Landers. J. P. *BioTechniques* **1998.** 25. 130-137.

11. Heid. C. A.; Stevens. J.; Livak. K. J.; Williams. P. M. *Genome Res.* **1996.** 6. 986-994.

12. Takeuchi. T.; Katsume. A.; Tanaka. T.; Abe. A.; Inoue. K.; Tsukiyama-Kohara. K.; Kawaguchi. R.; Tanaka. S.; Kohara. M.. *Gastroenterology* **1999.** 116. 636-642.

13. Pongers-Willemse. M. J.; Verhagen. O. J. H. M.; Tibbe. G. J. M.; Wijkhuijs. A. J. M.; de Haas. V.; Roovers. E.; van der Schoot. C. E.; van Dongen. J. J. M. *Leukemia* **1998.** 12. 2006- 2014.

14. Swerdlow. H. P.; Wu. S. L.; Harke. H. R.; Dovichi. N. J. *J. Chromatogr.* **1990.** 516. 61-67.

15. Tan. W. G.; Tyrrell. D. L. J.; Dovichi. N. J. *J. Chromatogr.* **1999.** 853. 309- 319.

16. Butler. J. M.; McCord. B. R.; Jung. J. M.; Wilson. M. R.; Budowle. B.; Allen. R. O. *J. Chromatogr B.* **1994.** 658. 271-280.

17. Personett. D.; Sugaya. K.; Hammond. D.; Robbins. M.; McKinney. M. *Electrophoresis* **1997.** 18. 1750-1759.

18. Poirier-Toulemonde. A. S.; . Imbert-Marcille. B. M.; Ferré-Aubineau. V.; Besse. B.; Le Roux. M. G.; Cantarovich. D.; Billaudel. S.. *Molecular and Celluar Probes* **1997**. 11. 11-23.

19. Vincent. U.; Patra. G.; Therasse. J.; Gareil. P. *Electrophoresis* **1996**. 17. 512-517.

20. Zhang. J. Z.; Voss. K. O.; Shaw. D. F.; Roos. K. P.; Lewis. D. F.; Yan. J.; Jiang. R.; Ren. H.; Hou. J. Y.; Fang. Y.; Puyang. X.; Ahmadazdeh. H.; Dovichi. N. J. *Nucleic Acids Res.* **1999**. 27. E36.

21. Ferre. F. *PCR Methods and Applications* **1992**. 2. 1-9.

22. Jilbert. A. R.; Miller. D. S.; Scougall. C. A.; Turnbull. H.; Burrell. C. J. *Virology* **1996**. 226. 338-345.

23. Nasarabadi. S.; Milanovich. F.; Richards. J.; Belgrader. P. *BioTechniques* **1999**. 27. 1116-1118.

24. Crabtree. H. J.; Bay. S. J.; Lewis. D. F.; Coulson. L. D.; Fitzpatrick. G.; Harrison. D. J.; Delinger. S. L.; Zhang. J. Z.; Dovichi. N. J. *Electrophoresis* **2000**. 21. 1329-1335.

25. Rocheleau. M. J.; Dovichi. N. J. *J. Microcolumn Sep.* **1992**. 4. 449-453.

26. Yan. J. Y.; Best. N.; Zhang. J. Z.; Ren. H. J.; Jiang. R.; Hou. J.; Dovichi. N. J. *Electrophoresis* **1996**. 17. 1037-1045.

56

CHAPTER 3

Study of Nucleoside Anti-cancer Drug Uptake and Metabolism Using Capillary Electrophoresis with Laser-induced Fluorescence Detection: (I) Quantification of Human Equilibrative Nucleoside Transporter 1 (hENT1) Protein

57

3.1 Introduction

Cytotoxic chemotherapy is the mainstay of the clinical management of systemic cancers (1, 2). Among the several classes of anti-tumor agents, cytotoxic nucleoside drugs are potent anti-metabolites that display anti-tumor activities against both hematologic malignancies and solid tumors (3). The nucleoside anti-cancer drugs in routine clinical use are fludarabine (9-β-D-arabinosyl-2-fluoroadenine), cladribine (2-chloro-2'-deoxyadenosine), cytarabine (1-β-D-arabinofuranosyl cytosine), and gemcitabine (2', 2'-difluorodeoxycytidine) (4). The structures of these four drugs are shown in Figure 3.1. Each of these agents is a hydrophilic compound that requires cellular uptake by functional plasma membrane nucleoside transport (NT) proteins to permeate the plasma membrane and to interact with its intracellular targets (5-8).

Five distinct human NT proteins, varying in substrate specificity, sodium ion dependence, and sensitivity to inhibition by nitrobenzylthioinosine (NBMPR, structure shown in Figure 3.2) have been identified by molecular cloning and functional expression of cDNAs from human tissue (9). One type of transporter, the human equilibrative nucleoside transporter 1 (hENT1) protein, appears to be ubiquitous in human cells, has functional characteristics of es–mediated transport (equilibrative, and sensitive to inhibition by nanomolar concentrations of NBMPR) and mediates cellular entry of many cytotoxic nucleosides, including the four clinically used drugs described above (8-10). Because hENT1 appears to be the major mediator of nucleoside drug influx in normal and malignant human blood cells, it has been suggested that hENT1 deficiency is the most likely mechanism of transport-based nucleoside drug resistance (5, 11, 12).

58
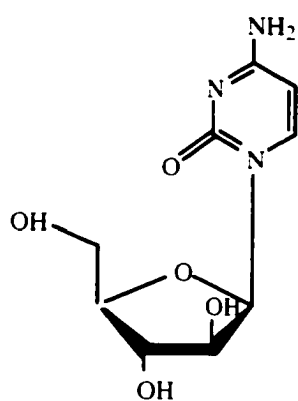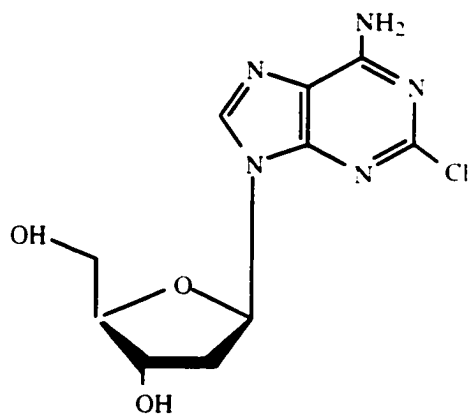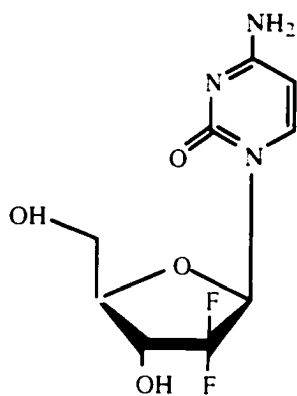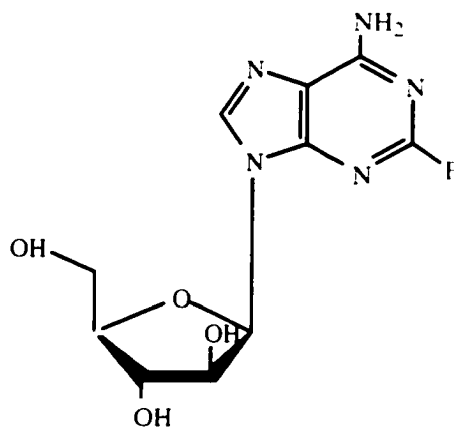
Figure 3.1 Structures of four anti-cancer nucleoside drugs.

59

NBMPR

5-(SAENTA-x8)-fluorescein
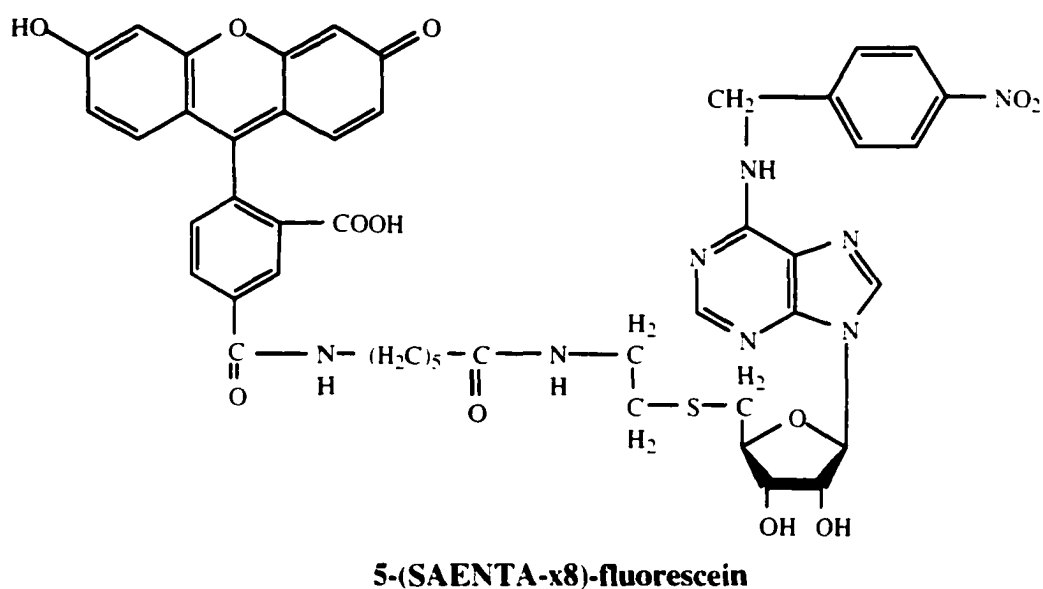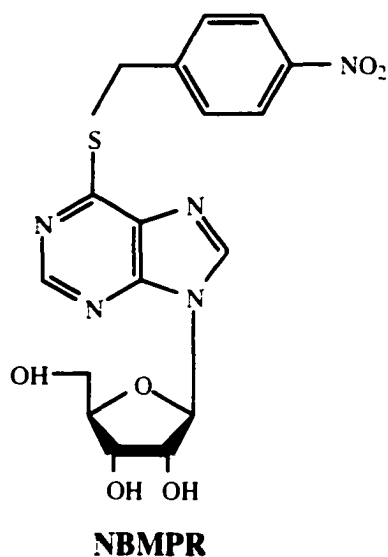
Figure 3.2 Structures of hENT1 inhibitors. 5-(SAENTA-x8)-fluorescein (5-Sx8f) is a modified form of NBMPR to which is attached a fluorescein molecule.

60

Shown in Figure 3.3. hENT1 is a 456-residue protein of M_r 50.249 DA with 11

transmembrane segments (N terminus intracellular and C terminus extracellular) and

three potential N-glycosylation sites (13). Enumeration of hENT1 sites on cells has

traditionally been estimated by steady-state binding of [^{3}H]NBMPR. a high-affinity (Kd

values. 0.1 – 1 nM) specific inhibitor of es-mediated transport of nucleosides in

mammalian erythrocytes and a variety of other cell types (14, 15). However. this assay

involves radiolabelled reagents and requires large numbers of cells (in excess of 10^8)

because of the relatively small numbers (10^4 – 10^6) of inhibitor binding sites per cell (16).

Recent studies that demonstrated tolerance for introduction of substituents at the 5'-

position of the ribosyl moiety of es transport inhibitors led to the development of 5'-S

–(2-Aminoethyl)-N^6–(4-nitrobenzyl)-5'-thioadenosine (SAENTA). a derivatizable

analog of NBMPR (17). Substituents at the 5'- position of NBMPR were shown to have

little effect on the potency of NBMPR as an inhibitor of nucleoside transport activity

(18). Conjugates of SAENTA in which the nucleoside analog is linked to fluorescein

have proven to be specific stains for cellular NBMPR binding sites (19-22). Thus. the

SAENTA-fluoresceins allow measurement of the relative abundance of NBMPR-binding

sites of cells by a procedure that requires only 10% of the cells needed for assays with

radiolabelled ligands (22, 23). However. despite the ability to quantify NBMPR-binding

sites using flow cytometry. the importance of deficiencies in nucleoside transport

capacity in clinical drug resistance remains unclear. in large part due to the problems

associated with quantifying NT proteins in malignant clones mixed with normal cells (9)

and the inability of flow cytometry to demonstrate subpopulations of transporter deficient

cells. Current assays cannot be applied to solid tumors because of the technical

difficulties in separating large numbers of malignant cells from contaminating benign

61

Extracellular Matrix

COOH

NH2

Cytoplasm
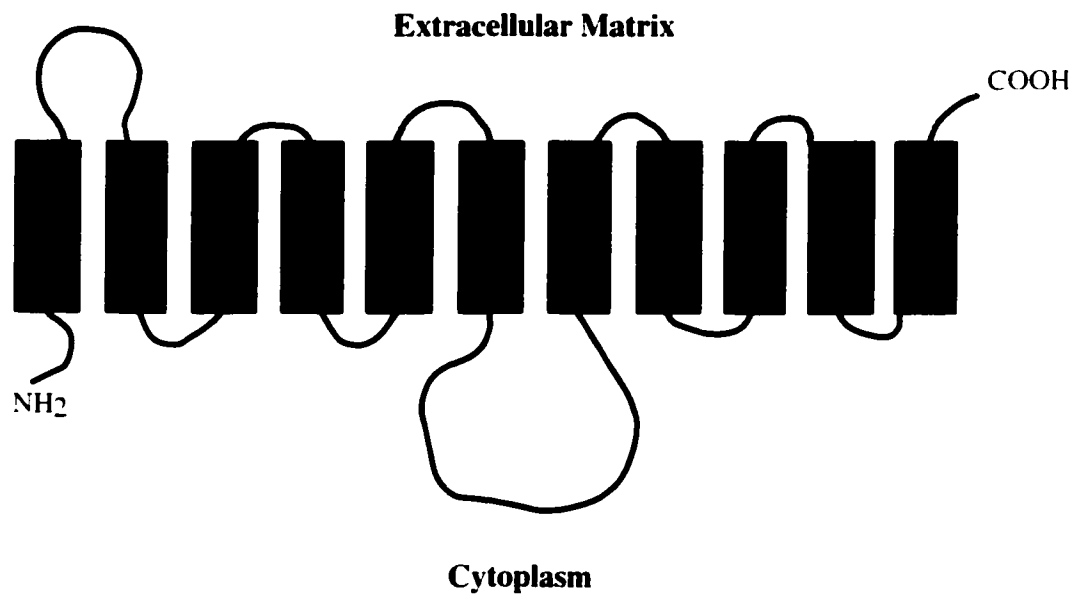
Figure 3.3 Structure of hENT1 protein.

62

stromal cells. For these reasons, we sought a new approach for hENT1 quantification that has the potential to quantify the hENT1 protein abundance in single cells.

Capillary electrophoresis (CE) has been proven to be a rapid, sensitive and reliable tool to separate, characterize and quantify membrane proteins (24-26). There have also been several reports of the use of capillary-based separations and fluorescence detection for the analysis of proteins from single cells (27-29). In this work, we demonstrate hENT1 quantification using CE followed by laser-induced fluorescence (LIF) detection based on 5-SAENTA-x8-fluorescein (5-Sx8f, structure shown in Figure 3.2), which binds with high affinity and specificity to hENT1 in a 1:1 stoichiometry (30, 31). Results obtained with the hENT1 CE-LIF assay were very similar to those obtained by flow cytometry (11). Theoretical calculations based on instrument detection limits also demonstrated the potential of the hENT1 CE-LIF assay for single-cell quantification of NBMPR-binding sites. Further refinement of this technique will thereby permit assays of clinical samples to i) quantify hENT1 on malignant cells admixed with normal cells; and ii) identify hENT1 deficient (and thereby nucleoside drug resistant) subclones among malignant cells. This information could then be used to validate the relationship between hENT1 quantity and clinical responsiveness in nucleoside-treated cancers, and potentially, to choose optimal candidates for nucleoside anti-cancer therapy.

63

3.2 Experimental

3.2.1 Chemicals and reagents

NaCl. KCl. sodium dodecylsulfate (SDS) and sodium tetraborate were obtained from BDH (Toronto, ON, Canada). Sigma (St. Louis, MO) supplied the bovine serum albumin (BSA) and octylglucoside. 4-(2-hydroxytheyl)-1-piperazineethanesulfonic acid (HEPES) was purchased from Fisher Scientific (Fair Lawn, NJ).

3.2.2 Buffers and solutions

The following buffers were used:

A. 5-Sx8f solutions were prepared with a buffer containing 10 mM HEPES. 100 mM NaCl and 5 mM KCl at pH 7.3:

B. Cells were suspended and washed with 10 mM HEPES. 100 mM NaCl. 5 mM KCl. 1 g/L glucose and 1 g/L BSA at pH 7.3:

C. 5-Sx8f bound to nonspecific sites on the cell other than hENT1 sites was removed by washing the cells with a non-ionic surfactant: 0.1% (v/w) n-octylglucoside with 1 g/L glucose and 1 g/L BSA:

D. CE electrophoretic buffer consisted of 10 mM Borate and 5 mM SDS. pH was adjusted with NaOH to 8.9.

All solutions were filtered through a 0.22 μm membrane filter (Millipore, Bedford, MA) before use.

64

3.2.3 Cell culture

Two human breast carcinoma cell lines (MCF-7 and MDA-MB-435s), a human colon carcinoma cell line (CaCo-2), and a human cervical carcinoma cell line (HeLa) were obtained from the American Type Culture Collection. CCI-180/1 cells were established from a biopsy of a stage Ib uterine squamous cell cervical cancer, courtesy of Dr. R. Britten (Cross Cancer Institute, Edmonton, Alberta, Canada). HeLa cells were grown in Roswell Park Memorial Institute (RPMI) supplemented with 10% fetal calf serum, and the other four cell lines were grown in Dulbecco's Minimal Essential Medium (DMEM) supplemented with 10% fetal bovine serum; all cultures were maintained at 37°C in a humidified atmosphere of 5% CO_2 and were free of mycoplasma. Cell concentrations were determined using a hemocytometer. Cultures were removed from dishes with trypsin-EDTA (0.05% trypsin, 0.53 mM EDTA•4Na) and subcultured every 3-4 days. Experiments were initiated with cells in the exponential growth phase.

3.2.4 hENT1 quantification assay

The solutions here were indicated as A, B, C and D, which were described as in 3.2.2. Because hENT1 is very hydrophobic, the following procedures were developed to avoid the direct detection of hENT1 protein to ensure accurate quantification. First, suspensions of intact cells (5×10^5) were added to 5-Sx8f solutions (A) with different concentrations ranging from 0 to 50 nM. 5-Sx8f is a non-permeating reagent because of its size and charge, and binds to plasma membrane NBMPR-binding sites. The equilibration of 5-Sx8f with membrane binding sites was allowed to proceed for 50 minutes at room temperature. Incubations were terminated by centrifugation at 150 g for 10 minutes. (All centrifugations were done under this same condition unless stated otherwise.) The pelleted cells were washed twice with buffer (B) to remove the unbound 5-Sx8f and once

65

with surfactant (C) to remove nonspecifically bound 5-Sx8f (17). Cells were then

centrifugally pelleted and lysed with CE buffer (D) releasing 5-Sx8f from the hENT1-5-

Sx8f binding complex. The lysate was centrifuged at 9,300 g for 10 minutes, and the

supernatants were sampled for CE measurement of 5-Sx8f binding content. Calibration

curves were constructed using a series of dilutions of a 5-Sx8f standard for quantification.

Three additional control samples were washed identically in order to obtain cell numbers.

Finally, 5-Sx8f binding content was correlated to NBMPR-binding content, which was

considered indicative of hENT1 binding sites. A cartoon of the assay procedure is

depicted in Figure 3.4.

3.2.5 Instrumentation and electrophoretic conditions

The same in-house built CE-LIF instrument described in Chapter 2 was used for our

study (32, 33). Each sample was mixed with an injection standard of fluorescein and

introduced electrokinetically into the capillary under an electric field of (+) 1000 V for 10

seconds. A 30 cm long, 50 μm inner diameter (I.D.), 150 μm outer diameter (O.D.)

uncoated fused-silica capillary purchased from J&W Scientific (Folsom, CA) was used

for the separation. Every five to six runs electrophoretic buffer was renewed to ensure the

CE reproducibility. All experiments were carried out applying a constant voltage of (+)

9 kV. 5-Sx8f was excited with an Argon-ion laser (Melles Griot Laser Group, Carlsbad,

CA) with a single 488 nm emission line. Fluorescence signal was collected through a 535

nm bandpass filter of 35 nm width (535DF35, Omega Optical, Brattleboro, VI, USA) and

detected by an R1477 photomultiplier tube (PMT). Data were collected and analyzed

using Igor Pro 2.04 (WaveMetrics, Lake Oswego, OR). In all experiments, the 5-Sx8f

signal was divided by the signal of the injection standard to get a normalized signal for

further data processing.

66
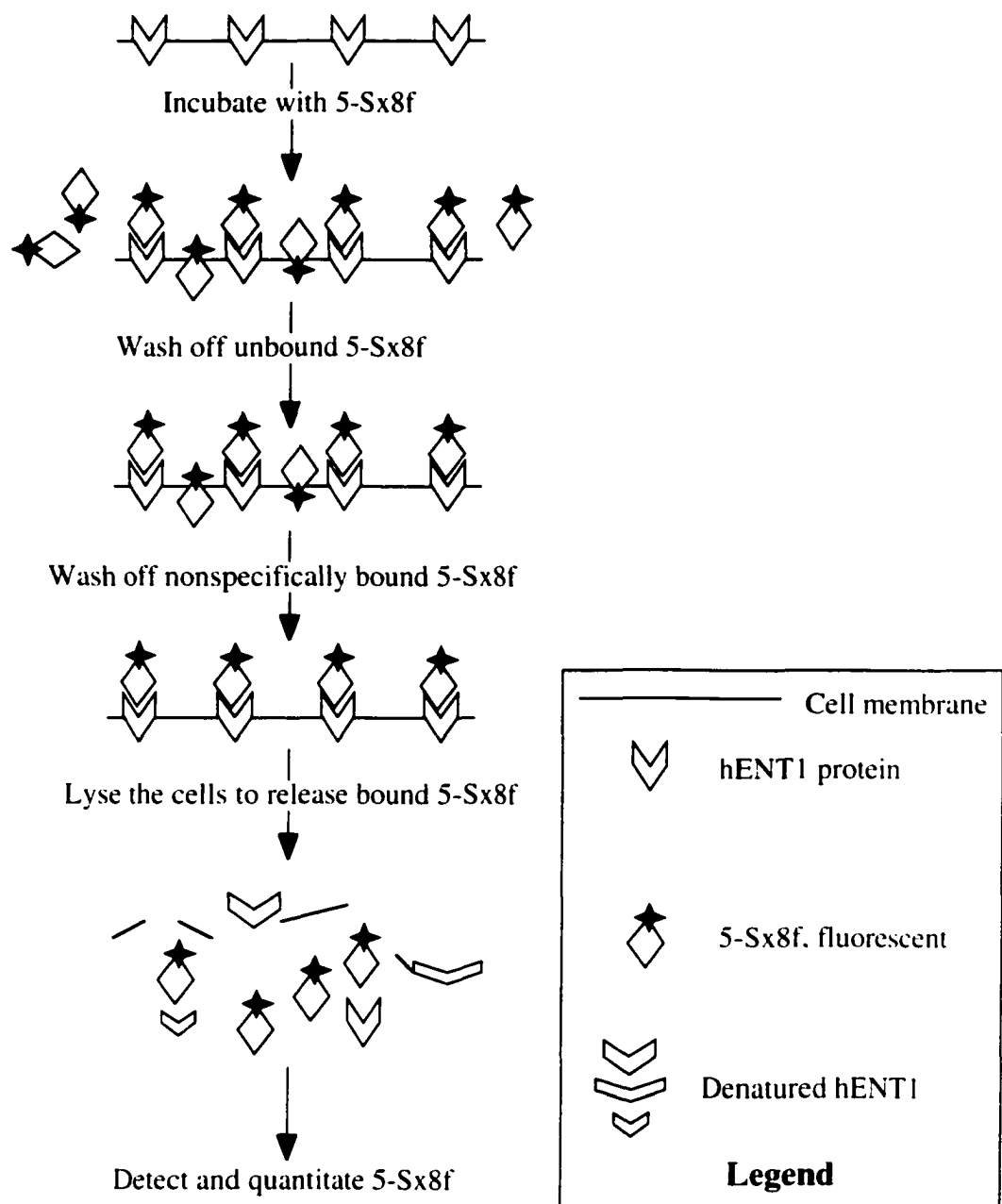
Figure 3.4 Process for quantification of hENT1 in the plasma membrane using 5-Sx8f as an impermeant inhibitor.

67

3.2.6 Flow cytometry

5-Sx8f was used for flow cytometric enumeration of transport sites on cultured human epithelial malignant cells maintained as described above (18, 34, 35). Trypsinized cells were washed and suspended in flow buffer (140 mM NaCl, 5 mM KCl, 10 mM HEPES pH 7.4, 1 g/L glucose and 1 g/L bovine serum albumin). Five hundred thousand cells were then incubated for 10 minutes at room temperature in the presence or absence of 1 mM NBMPR. Samples were then incubated in graded concentrations of 5-(SAENTA-x8)-fluorescein (final concentration of 1 nM-20 nM) at room temperature for 30 min. Cell-bound fluorescence and light scatter signals for 10,000 cells were analyzed on a FACSort instrument (Becton Dickinson Canada, Oakville, Ontario, Canada). Calibration curves were produced using fluorescein standard beads containing known numbers of fluorescein molecules. Mean fluorescence channel numbers were converted to molecules of equivalent soluble fluorescein (MESF; Flow Cytometry Standards Corporation, Research Triangle Park, NC). The specific values for bound fluorescence for each sample was divided by the 0.42, the previously validated MESF: NBMPR binding site ratio, to obtain plasma membrane hENT1 sites per cell (36).

3.3 Results and Discussion

3.3.1 Analysis of 5-Sx8f

CE offers fast and efficient separations. To correct for injection variation, fluorescein was used as an internal standard and was added to the CE samples prior to each injection. After introducing the samples electrokinetically into the capillary at 1000 V for 10 sec, 5-Sx8f was well resolved from the internal standard within five minutes (Figure 3.5).

68

3.3.2 Construction of calibration curve

A calibration curve of over two orders of magnitude was obtained with 5-Sx8f concentrations ranging from 1×10^{-10} mol/L to 2×10^{-8} mol/L and is shown in Figure 3.6(a).

All quantifications in this study were based on the low-range calibration curve shown in Figure 3.6(b). The correlation coefficients in both calibration curves are larger than 0.99.

3.3.3 Effect of incubation time

To obtain the optimal incubation time, quantification was carried out with eight different incubation times ranging from 0 to 180 minutes. As shown in Figure 3.7. 30 nM 5-Sx8f binds to hENT1 immediately upon its addition to the 180/1 cells. The signal at incubation time 0 minutes was already quite high due to the long centrifugation time. which also allowed the binding between 5-Sx8f and the hENT1 protein. Because it took approximately 30 minutes for the signal to reach 90% of its maximum. a 50 minute incubation time was chosen for all subsequent quantification studies.

3.3.4 hENT1 quantification on five cultured human cell lines

Quantification of hydrophobic proteins by CE is usually difficult because of a high degree of protein adsorption onto the capillary wall. In this report. the use of a specific inhibitor. 5-Sx8f. greatly simplified the quantification of the membrane protein hENT1. It has been previously demonstrated by flow cytometry that 5-Sx8f interacts with

69
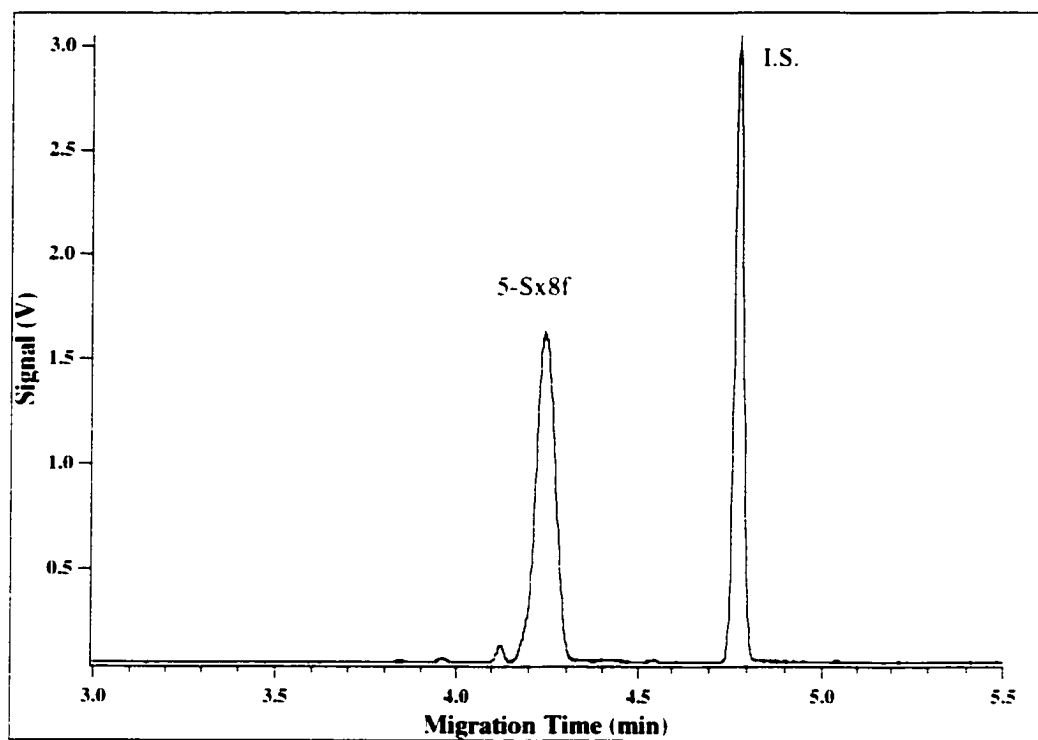
Figure 3.5 Separation profile of standard 5-Sx8f from internal standard.

70
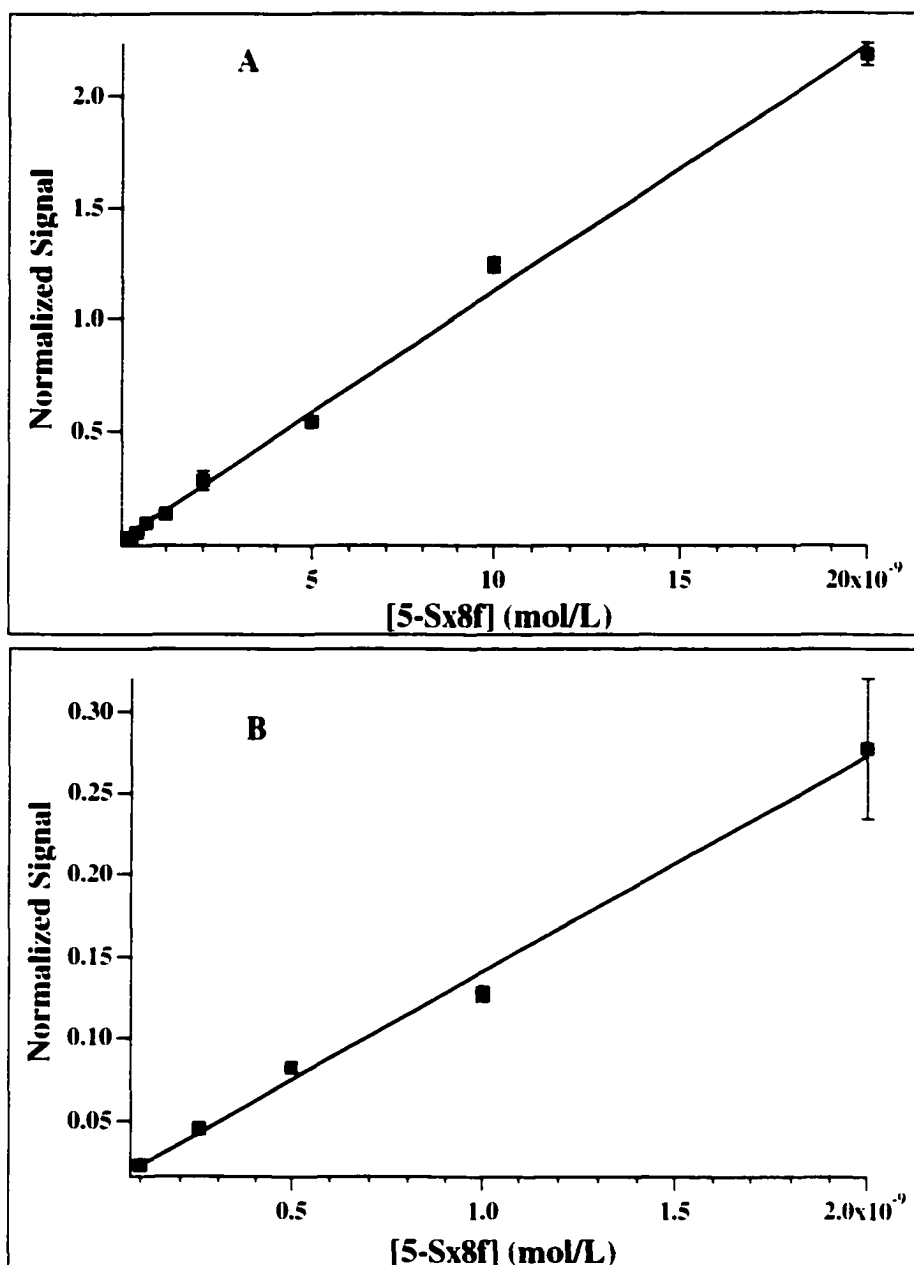
Figure 3.6 Calibration curves for 5-Sx8f. (A) Overall range calibration curve. The signal is linear with the initial 5-Sx8f concentration for about two orders of magnitude. (B) The low range calibration curve used for the quantification in our study. The error bar shows the standard deviation within three independent runs and may be smaller than the symbols.

71
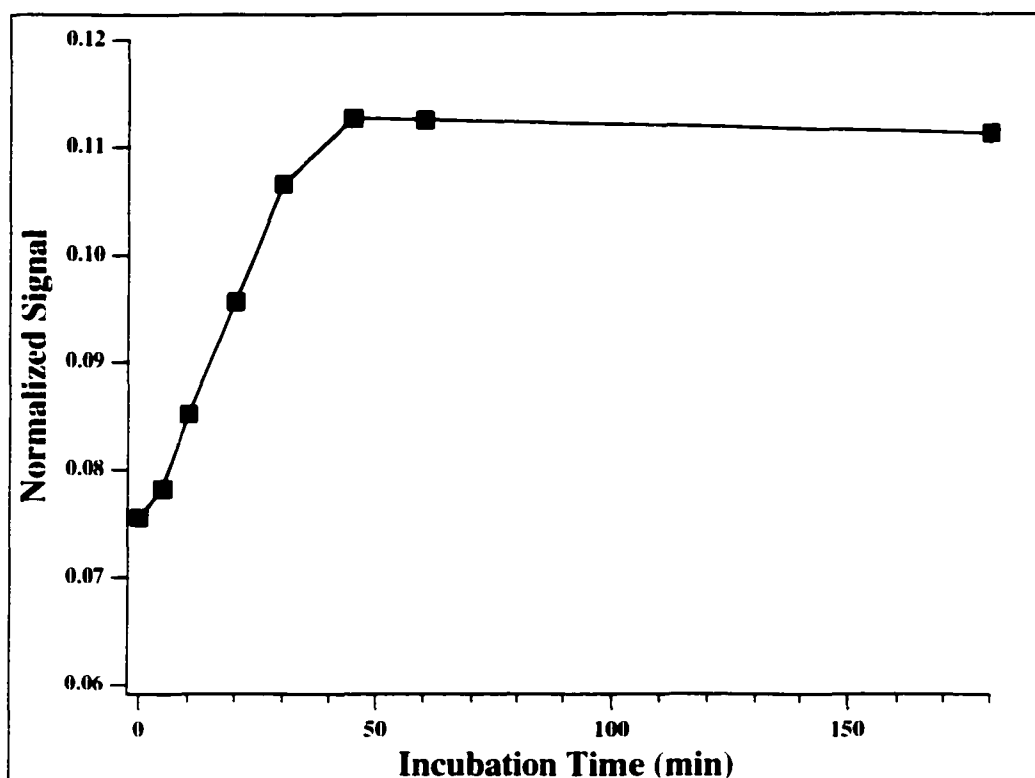
Figure 3.7 Effect of incubation time on the hENT1-5-Sx8f binding. 180/1 cells were used as a model in this experiment. And 5-Sx8f concentration was chosen as 30 nM.

72

NBMPR-binding nucleoside transporters with high affinity. The strong 1:1 hENT1-5-Sx8f binding complex was not dissociated until washing step (iii) where CE buffer contained 5 mM SDS was added (Figure 3.4). The site-bound 5-Sx8f released from the complex was then measured to quantify hENT1. Figure 3.8 shows the identification of 5-Sx8f released from binding complexes formed with 435S cells. When, as a negative control, 5-Sx8f was omitted from the incubation solution, no 5-Sx8f was detected as depicted in electropherogram (a). With 5-Sx8f present in the incubation mixture, hENT1 was recognized and bound by 5-Sx8f until dissociation, allowing the detection of 5-Sx8f as shown in electropherogram (b). Electropherogram (c) confirms the identification of 5-Sx8f by spiking with standard 5-Sx8f (positive control).

For 435S and MCF-7 cells, the normalized 5-Sx8f peak height was plotted against the initial 5-Sx8f concentration in the incubation mix. As depicted in Figure 3.9, the increasing 5-Sx8f signal as a function of initial concentration was saturable, suggesting interaction with a set of high-affinity binding sites. The abundance of NBMPR-binding sites, and therefore hENT1 protein, is known to differ among cell types. The different cell types used in experiments exhibited different binding profiles, as shown in Figure 3.9. Replicate profiles obtained from independent experiments with these cultured cells were consistent, despite variation in the number of cells studied. This could be explained by different K_d values for the different cell lines. K_d values obtained from my experimental data are shown in Table 3.1, where low-nanomolar values obtained for each of these cell lines indicate the high-affinity of the interaction between the hENT1 protein and 5-Sx8f.

To obtain the number of hENT1 binding sites, calculations were then done based on the plateau-signals obtained at saturation. Table 3.2 summarizes the cellular hENT1

73
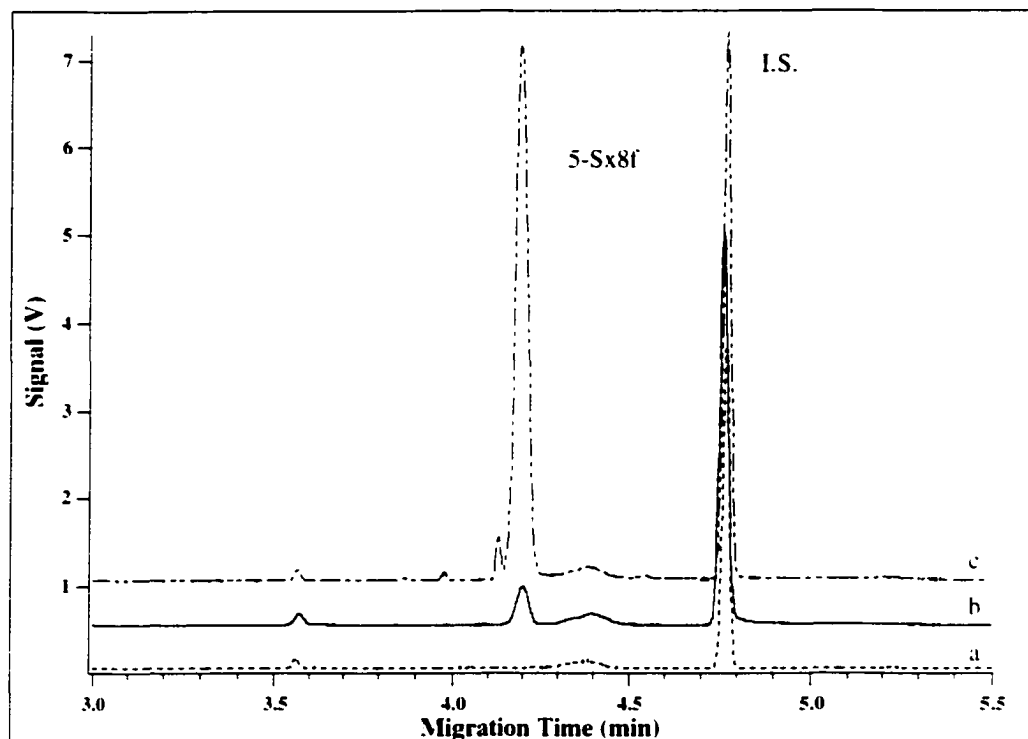
Figure 3.8 Detection of 5-Sx8f released from the binding complexes on 435S cells. (a).

Negative control sample in which no 5-Sx8f was added to the initial incubation mixture.

No 5-Sx8f signal was observed in this case. (b). CE sample prepared as described in

Section 3.2.4 in which a specified amount of 5-Sx8f was added to the initial incubation

mixture. (c) The sample from (b) was spiked with 5-Sx8f standard to confirm the

identification of 5-Sx8f.

74
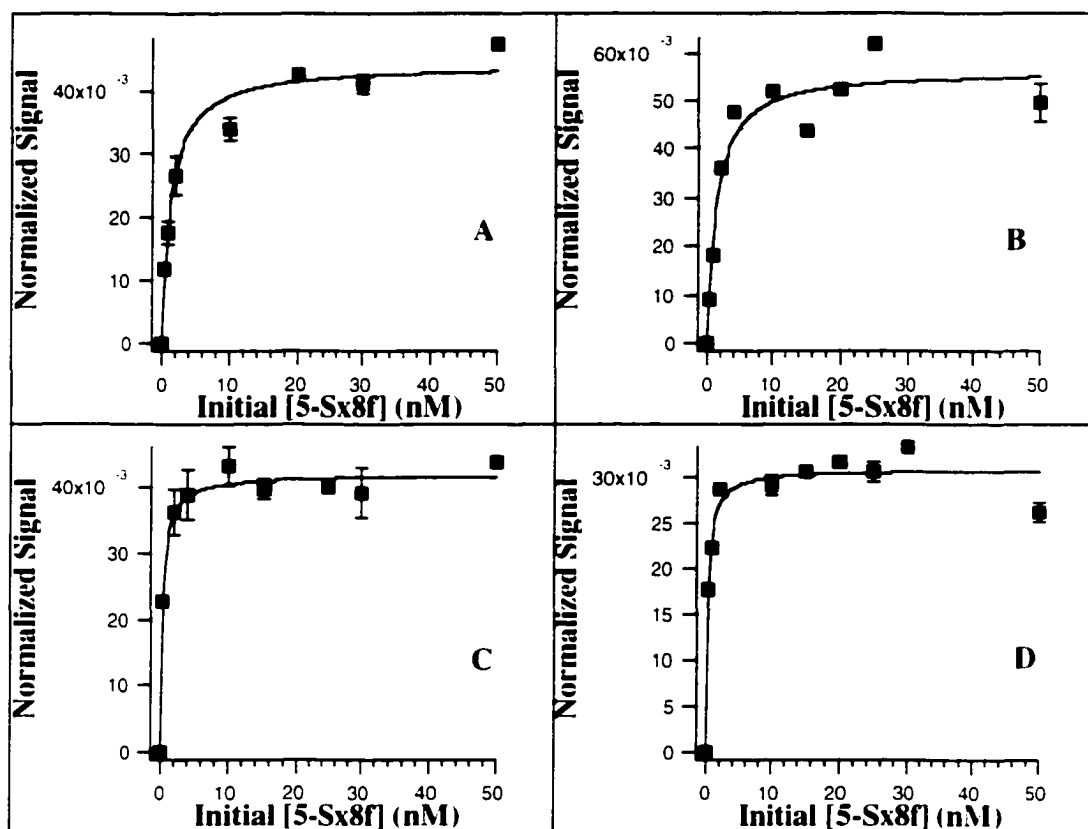
Figure 3.9 Equilibrium binding analysis of 5-Sx8f as a surrogate marker for the presence

of the hENT1 protein. (A). 2.5×10^5 435S cells. Kd = 1.30 nM. (B). 2.3×10^5 435S cells.

Kd = 1.33 nM. (C). 2.4×10^5 MCF-7 cells. Kd = 0.33 nM. (D). 1.5×10^5 MCF-7 cells.

Kd = 0.28 nM. All data points were averages of two independent measurements. The

error bars show the standard deviations and may be smaller than the symbols.

75

Table 3.1 Extracted K_d values for five cell lines.

Experiment Number	Kd Values (nM)				
	435S	HeLa	MCF-7	CaCo-2	180/1
1	1.3	1.0	0.3	1.1	1.8
2	1.3	0.9	0.3	0.8	0.8
3	2.9	2.1	1.4	0.9	0.9
Average	1.8	1.3	0.7	0.9	1.2

Although some numbers appear not to be very consistent and reproducible, this is entirely acceptable with cellular and biological systems.

76

Table 3.2 Quantification results on five cultured human cell lines

Cell Line	CE-LIF		Flow Cytometry[b]	
	hENT1-binding Sites / cell	RSDA	hENT1-binding Sites / cell	RSD
435S	2.0e5	19%	1.7e5	24%
HeLa	1.5e5	5.8%	1.1e5	41%
MCF-7	1.3e5	23%	1.5e5	44%
CaCo-2	2.0e5	17%	1.7e5	54%
180/1	2.4e5	16%	2.2e5	14%

a. The relative standard deviation (RSD) is calculated based on at least three independent experiments.

b. Flow cytometry results were obtained from reference paper 11 and each result was an average of three independent experiments.

77

quantification results of five cultured human cell lines. Results obtained from hENT1-CE-LIF assay are very similar to those obtained from flow cytometry measurements. The Pearson correlation coefficient between the CE hENT1 determination and flow cytometry results for these five cell lines is strong with r=0.84; however. the hENT1-CE-LIF assay demonstrated reproducibility superior to that of flow cytometry.

3.3.5 Reproducibility of the quantification assay

The reproducibility of the CE-LIF assay was determined by analysis of nine identical CE samples with internal standards. Consecutive injections of these samples yielded a 0.7% and 6.7% relative standard deviation (RSD) for migration times and normalized peak heights variations respectively (Table 3.3). These values confirm good CE reproducibility both qualitatively and quantitatively.

To obtain the overall hENT1-CE-LIF reproducibility. nine aliquots of 435S cells with the same amount of cell numbers were incubated with 20 nM of starting 5-Sx8f for 50 minutes. After washing off the extra 5-Sx8f and non-specifically bound 5-Sx8f. each sample was measured in the CE-LIF instrument. The RSD value was then calculated based on these nine data points. The 10.3% RSD includes the variability of the incubation. cell washes and CE-LIF detection (Table 3.4). This small RSD demonstrates the good quantification ability of the developed hENT1-CE-LIF assay.

3.3.6 Detection limit measurements

The assay was also tested by measurements of detection limits. Figure 3.10(A) and 3.10(B) depict individual CE electropherograms obtained when 2.1×10^4 fluorescein molecules and 1.2×10^5 5-Sx8f molecules were injected into the capillary.

78

Table 3.3 Reproducibility of CE-LIF Detection

Sample	Migration Time (min)	Normalized Peak Height
1	4.20	0.057
2	4.20	0.058
3	4.22	0.061
4	4.20	0.058
5	4.20	0.067
6	4.19	0.062
7	4.15	0.054
8	4.26	0.062
9	4.23	0.053
RSD	0.7%	6.7%

79

Table 3.4 Overall hENT1-CE-LIF Reproducibility

Sample	Normalized Peak Height
1	0.065
2	0.052
3	0.058
4	0.059
5	0.051
6	0.059
7	0.064
8	0.068
9	0.069
RSD	10.3%

80
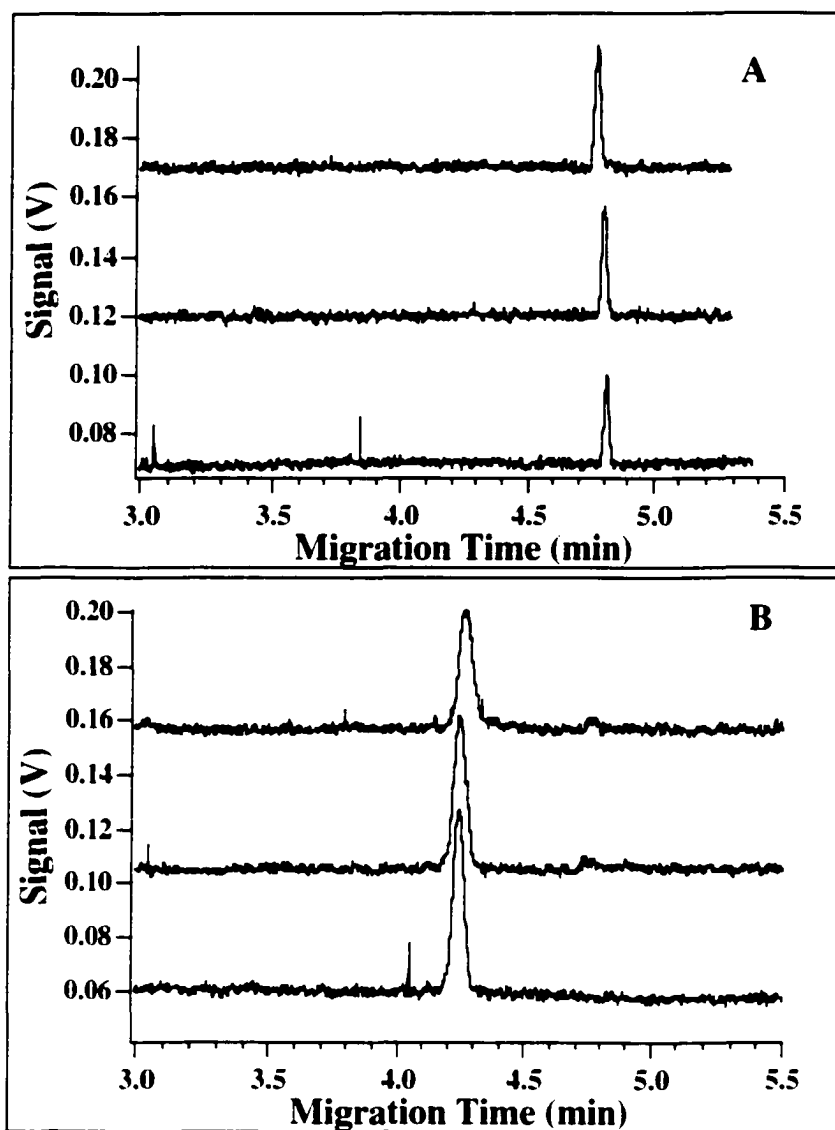
Figure 3.10 Instrument detection limit measurements of fluorescein and 5-Sx8f. All CE-LIF separation and detection parameters were the same as in the quantification assay. (A). Signal from 1.5×10^{-11} mol/L fluorescein (10 sec injection at 1000 V). (B). Signal from 7.5×10^{-11} mol/L 5-Sx8f (10 sec injection at 1000 V).

81

The limit of detection (LOD) was theoretically calculated (37) for fluorescein (1.600 molecules) and for 5-Sx8f (5.600 molecules). The results are consistent with the previous observation that the fluorescent quantum yield for 5-Sx8f is about 39% of that of fluorescein (38). More importantly, since the hENT1 quantity on single cells ranges from approximately 1.000 to 100.000, it will be possible to adapt the hENT1 CE-LIF assay to quantify hENT1 in samples with small numbers of cells and, eventually, in individual cells.

3.4 Conclusion

We developed a novel use of capillary electrophoresis to quantify 5-Sx8f binding as an indication of plasma membrane hENT1 protein abundance. This assay provides high precision and reliability in both qualitative and quantitative aspects. The developed hENT1-CE-LIF assay was validated by comparing the results obtained through conventional flow cytometry analysis and was successfully applied to study five cultured human cell lines.

The use of capillary electrophoresis for hENT1 quantification was still based on a large number of cells. However, the theoretical sensitivity of this method makes possible single-cell analysis of a nucleoside transporter. This will enable the analysis of single cells derived from heterogeneous cell populations, and will provide the opportunity to study malignant cells derived from clinical samples of solid tumors. Quantification of hENT1 protein using capillary electrophoresis with laser-induced fluorescence (CE-LIF) detection thereby warrants evaluation as a molecular predictive assay for clinical nucleoside analogue activity.

82

3.5 References

1.   Hanauske. A. R. *Anti-Cancer Drugs* **1996**. 7. 29-32.

2.   Baldwin. S. A.: Mackey. J. R.: Cass. C. E.: Young. J. D. *Mol. Med. Today* **1999**. 5. 216-224.

3.   Cheson. B. D. *Semin. Oncol.* **1992**. 19. 695-706.

4.   Allegra. C. J.: Grem. J. L. Antimetabolites. *In Cancer : principles and practice of oncology* (Devita VT. ed). Philadephia: Lippinocott-Raven. **1997**. pp 490-498.

5.   Gati. W. P.: Paterson. A. R. P.: Larratt. L. M. *et al. Blood* **1997**. 90. 346-353.

6.   Jamieson. G. P.: Snook. M. B.: Bradley. T. R.: *et al. Cancer Res.* **1989**. 49. 309-313.

7.   Sirotnak. F. M.: Barrueco. J. R. *Cancer Metastasis Rev.* **1987**. 6. 459-480.

8.   Mackey. J. R.: Mani. R. S.: Selner. M. *et al. Cancer Res.* **1998**. 58. 4349-57.

9.   Mackey. J. R.: Baldwin. S. A.: Young. J. D. *et al. Drug Resistance Updates* **1998**. 1. 310-324.

10.   Mackey. J. R.: Yao. S. Y. M.: Smith. K. M. *et al. J. Natl. Cancer Inst.* **1999**. 91. 1876-1881.

11.   Mackey. J. R.: Graham. K. A.: Wong. J. *et al.* unpublished results.

12.   Allay. J. A.: Spencer. H. T.: Wilkinson. S. L. *et al Blood* **1997**. 90. 3546-3554.

13.   Griffiths. M.: Beaumont. N.: Yao. S. Y. M.: Sundaram. M.: Boumah. C. E.: DAvies. A.: Kwong. F. Y. P.: Coe. I..; Cass. C. E.: Young. J. D.: Baldwin. S. A. *Nature Medicine* **1997**. 3. 89-93.

14.   Young. J. D. and Jarvis. S. M. *Biosci. Rep.* **1983**. 3. 309-322.

15.   Cass. C. E.: Belt. J. A.: Paterson. A. R. P. *Prog. Clin. Biol. Res.* **1987**. 230. 13-40.

16.   Griffith. D. A.: Jarvis. S. M. *Biochimica et Biophysica Acta* **1996**. 1286. 153-181.

17. Agbanyo, F. R.; Vijayalakshmi, D.; Craik, J. D.; Gati, W. P.; McAdam, D. P.; Asakura, J.; Robins, M. J.; Paterson, A. R. P.; Cass, C. E. *Biochem. J.* **1990**, 270, 605-614.

18. Peterson, A. J.; Brown, R. D.; Gibson, J.; Pope, B.; Luo, X. F.; Schutz, L.; Wiley, J. S.; Joshua, D. E. *Eur. J. Haema.* **1996**, 56(4), 213-220.

19. Schena, M.; Gottardi, D.; Ghla, P.; *et al. Leuk. Lymph.* **1993**, 11, 173-179.

20. Schena, M.; Larsson, L. G.; Gottardi, D.; *et al. Blood.* **1992**, 11, 2981-2989.

21. Wiley, J. S.; Brocklebank, A. M.; Snook, M. B.; Jamieson, G. P.; Sawyer, W. H.; Craik, J. D.; Cass, C. E.; Robins, M. J.; McAdam, D. P.; Paterson, A. R. P. *Biochem. J.* **1991**, 273, 667-672.

22. Jamieson, G. P.; Brocklebank, A. M.; Snook, M. B.; Sawyer, W. H.; Buolamwini, J. K.; Paterson, A. R. P.; Wiley, J. S. *Cytometry* **1993**, 14, 32-38.

23. Buolamwini, J. K.; Craik, J. D.; Wiley, J. S.; Robins, M. J.; Gati, W. P.; Cass, C. E.; Paterson, A. R. P. *Nucleosides & Nucleotides* **1994**, 13, 737-751.

24. Zolla, L.; Biancheti, M.; Timperio, A. M.; Mugnozza, G. S.; Corradini, D. *Electrophoresis* **1996**, 17, 1597-1601.

25. Scholz, E.; Pogany, G.; Ganzler, K.; Laurie, G. W. *J. Cap. Elec.* **1997**, 6, 287-292.

26. Vecchione, G.; Margaglione, M.; Grandone, E.; Colaizzo, D.; Cappucci, G.; Giuliani, N.; d'Addedda, M.; D'Andrea, G.; Nobile, M.; Amoriello, A.; Di Minno, G. *Electrophoresis* **1998**, 19, 1468-1474.

27. Zhang, Z.; Krylov, S.; Arriaga, E. A.; Polakowski, R.; Dovichi, N. J. *Anal. Chem.* **2000**, 72, 216-222.

28. Cheung, N. H.; Yeung, E. S. *Anal. Chem,* **1994**, 66, 929-936.

29. Colliver, T. L.; Brummel, C. L.; Pacholski, M. L.; Swanek, F. D.; Ewing, A. G.; Winograd, N. *Anal. Chem.* **1997**, 69, 2225-2231.

84

30. Wiley, J. S.; Cebon, J. S.; Jamieson, G. P.; Szer, J.; Gibson, J.; Woodruff, R. K.; McKendrick, J. J.; Sheridan, W. P.; Biggs, J. C.; Snook, M. B.; Brocklebank, A. M.; Rallings, M. C.; and Paterson, A. R. P., *Leukemia* **1994**, 8, 181-185.

31. Pressacco, J.; Wiley, J. S.; Jamieson, G. P.; Erlichman, C.; Hedley, D. W. *Br. J. Cancer* **1995**, 72, 9339-942

32. Swerdlow, H. P.; Wu, S. L.; Harke, H. R.; Dovichi, N. J. *J. Chromatogr.* **1990**, 516, 61-67.

33. Tan, W. G.; Tyrrell, D. L. J.; Dovichi, N. J. *J. Chromatogr.* **1999**, 853, 309-319.

34. Wiley, J.S.; Cebon, J. S.; Jamieson, G. P.; Szer, J.; Gibson, J.; Woodruff, R. K.; McKendrick, J. J.; Sheridan, W. P.; Biggs, J. C.; Snooke, M. B.; Brocklebank, A. M.;Ralling, M. C.; Paterson, A. R. P. *Leukemia* **1994**, 8(1), 181-185.

35. Jamieson, G. P.; Brocklebank, A. M.; Snooke, M. B.; Sawyer, W. H.; Buolamwini, J. K.; Paterson, A. R. P.; Wiely, J. S. *Cytometry* **1993**, 14, 32-38.

36. Sen, R. P.; Delicade, E. G.; Alvarez, A.; Brochlebank, A. M.;Wiley, J. S.; Miras-Portugal, M. T. *FEBS Letters* **1998**, 442, 368-372.

37. Giddings, J. C. *Sep. Sci.* **1969**, 4, 181-189.

38. Robbins, M. J.; Asakura, J.; Kaneko, M.; Shibuya, S.; Jackobs, E. S.; Agbanyo, F. R.; Cass, C. E.; Paterson, A. R. P. *Nucleosides & Nucleotides* **1994**, 13, 1627-1646.

CHAPTER 4

Study of Nucleoside Anti-cancer Drug Uptake and Metabolism Using

Capillary Electrophoresis with Laser-Induced Fluorescence Detection:

(II) The Possibility of Using [TAMRA]dCyd As A Substrate for

Deoxycytidine Kinase

86

4.1 Introduction

Four commonly used cytotoxic nucleoside drugs for cancer treatment, gemcitabine, cytarabine, cladribine and fludarabine were briefly introduced in Chapter 3. Each of these agents is a prodrug that requires: i) cellular uptake by nucleoside transport proteins, mediated predominantly by hENT1 (Chapter 3); and ii) phosphorylation by intracellular kinases to the active di- and tri-phosphate anabolites, which are subsequently incorporated into the DNA. The intracellular accumulation of nucleoside triphosphates is a critical determinant of cytotoxicity to both dividing and quiescent cells (1, 2).

Although the cellular pharmacology of different nucleoside analogs is different, the four nucleoside drugs listed above are all first phosphorylated by deoxycytidine kinase (dCK, E.C. 2.7.1.74), a step which constitutes the critical initial step in the activation of these drugs (3-6). dCK allows retention of nucleoside monophosphate residues within the cell, facilitating the formation of diphosphates and, ultimately the cytotoxic triphosphate residues. dCK activity is the rate-limiting step in the accumulation of intracellular triphosphates of these drugs (7, 8).

There is substantial and convincing evidence that dCK deficiency is an important and common mechanism of nucleoside drug resistance, both *in vitro* and *in vivo* (9-13). Variation in dCK expression also appears to explain some aspects of nucleoside cellular specificity (14, 15). For these reasons, dCK has attracted great attention in studies of drug resistance and sensitivity. It is thus essential to measure dCK activity in human cells and tissues.

87

Human dCK is a dimer of roughly 60 kDa. composed of two similar or identical 30 kDa units. and is constitutively expressed throughout the cell cycle. To date. the classic method for assessing dCK activity involves the use of radiolabelled deoxycytidine (dCyd) as a substrate (16-19). (In all of the following statements. dCyd is used for [^{3}H]dCyd and data on dCyd were obtained by using [^{3}H]dCyd as the substrate). An immunoassay method for direct dCK quantification was also developed (20). These two methods have been successfully applied to dCK quantification. activity measurement and comparison. and kinetic studies. However. similar to what is discussed in Chapter 3. these techniques require large numbers of cells and thus it is not possible to assess the dCK activity on clinical samples and solid tumors because of the technical difficulties in separating large numbers of malignant cells from contaminating benign cells. Therefore. a new approach is needed for dCK activity measurement that has the potential to be applied to the analysis in single cells.

Using CE-LIF. the goal of this project was the development of a metabolic cytometry assay for dCK enzymatic activity by the use of a fluorescently labeled dCyd as substrate. The studies described here were initiated in large part due to the great success demonstrated previously by our group on the enzymatic cascade studies with tetramethyl-rhodamine (TMR) labeled substrates at the single cell level (21. 22). The potential of using carboxytetramethylrhodamine (TAMRA) labeled dCyd ([TAMRA]dCyd) as a fluorescent substrate for dCK activity measurement was studied from several aspects including its generation. kinetic properties. cellular uptake. and intracellular distribution. It is clear that improvement of the substrate specificity by changing the position of the fluorescent dye or modifying the fluorescent dye itself is essential in deciding the fate of this project.

88

4.2 Experimental

4.2.1 Chemicals and reagents

[TAMRA]dCydTP and rhodamine 6G labeled dCydTP ([R6G]dCydTP) were obtained from Applied Biosystems (Foster. CA). [Fluorescein]dCydTP was purchased from Pharmacia (Quebec. Canada) and fluorescein from Molecular Probes (Eugene. OR). Calf intestinal alkaline phosphatase (CIAP) was supplied by Life Technologies (Gaimeisburg. MD). NaCl. $MgCl_2$ and sodium tetraborate were from BDH (Toronto. ON. Canada). From Sigma (St. Louis. MO) all of the following were purchased: tris(hydroxymethyl)-aminomethane (Tris). ATP. bovine serum albumin (BSA). levamisole. coformycin. 5-iodotubercidine and β-glycerophosphate. Purified dCK enzyme was a kind gift from Dr. Staffan Eriksson (Uppsala Biomedical Center. Uppsala University. Sweden). which was prepared as described by Bohaman and Eriksson (23). Microcon YM-30 centrifugal device filters were obtained from Millipore (Bedford. MA).

4.2.2 Cell culture

A2780 is a human ovarian carcinoma cell line (24). It was cultured in Dulbecco's modification of Eagle's medium (DMEM. Gibco. Paisby. UK) supplemented with 10% fetal bovine serum (FBS) at 37°C in a 5% CO_2 atmosphere. AG6000 is a highly nucleoside drug resistant variant of A2780 and was obtained as described previously (25). AG6000 was cultured under the same culture conditions as the A2780 cells.

89

4.2.3 Cell extract

To prepare cell extracts, 2×10^6 to 4×10^6 cells were homogenized in a micro-tissue grinder on ice for 10 minutes. The sample was centrifuged at 9,000 g for 10 minutes to remove cellular debris. The supernatant was then used for the enzyme assay. The protein concentration of the samples was determined using the BioRad Bradford protein assay (26).

4.2.4 Generation of [TAMRA]dCyd and [TAMRA]dCydMP standards

Since only [TAMRA]dCydTP is commercially available, an enzymatic reaction on [TAMRA]dCydTP was done to obtain the fluorescent nucleoside and nucleotide standards. Calf intestinal alkaline phosphatase (CIAP, 25 U/μL) was first 1/10,000 diluted with a buffer consisting of 100 mM NaCl, and 50 mM Tris at pH 8.0. Then 1 μL of the diluted enzyme and 0.5 μL of 400 μM [TAMRA]dCydTP were added to a siliconized tube containing 18.5 μL of the dilution buffer. The mixture was incubated at 37°C for different lengths of time ranging from 0 minutes to overnight. Each time, 1 μL sample was removed from the incubation mixture and added into 50 μL of ice-cold water/methanol (v/v 3:2) solution. Finally to remove the residual CIAP, this solution was filtered with a Microcon YM-30 by centrifuging at 13,600 g for six minutes. Samples were stored immediately at –20°C until analysis. From these treatment conditions, 5 min and 75 min incubation products were used as [TAMRA]dCydMP and [TAMRA]dCyd standards respectively.

90

4.2.5 Production of fluorescent substrate [TAMRA]dCyd for dCK analysis

CIAP enzyme was 1/100 diluted with the same dilution buffer used in Section 4.2.4. Into

a siliconized tube was added 30 μL of 400 μM [TAMRA]dCydTP and 2 μL diluted

enzyme. After gently mixing the solution. incubation was carried out at 37°C for 20

hours. Depending on specific situations. more enzymes or longer incubation times may

have been required. The incubation was checked once or twice to ensure completion.

When the reaction was finished. the whole product was mixed with approximately 200

μL water/methanol (v/v 3:2) and filtered with a Microcon YM-30 by centrifuging at

13.600 g for 20 minutes. The filtered solution was then lyophilized and the final product

was dissolved in 60 μL of ddH$_2$O. After the concentration was measured. the

[TAMRA]dCyd solution was stored at –20°C.

4.2.6 Calibration curve construction

[R6G]dCydTP was used as the internal standard (I.S.) in this study. Dilutions of

[TAMRA]dCydTP at different concentrations were mixed with the I.S. and subjected to

CE-LIF analysis. After normalizing the [TAMRA]dCydTP peak areas against those of

the internal standard. a calibration curve was plotted. This curve was used during the

study to measure the concentration of [TAMRA]dCyd and [TAMRA]dCydMP.

4.2.7 dCK enzyme assay

For the purified dCK enzyme. the reaction mixture contained 50 mM Tris-HCl (pH 7.5).

5 mM MgCl$_2$. 5 mM ATP. 2 mM DTT. 0.5 mg/mL BSA. 2 μg dCK enzyme and 12 μM

[TAMRA]dCyd in a final volume of 10 μL. The reaction was initiated with incubation of

the mixture at 37°C. The reaction rate at this specific substrate concentration could be

91

measured by incubating the mixture for different lengths of time. For each time point. 1 µL of solution was removed from the incubation and added into a pre-heated tube containing 100 µL of CE electrophoresis buffer. After heating at 90°C for another minute. the product was stored at -20°C until analysis. For assays with crude cell extracts. 2-4 × 10⁶ cells were first ground in 30 µL of the assay buffer (50 mM Tris-HCl (pH 7.5). 5 mM MgCl₂. 5 mM ATP. 2 mM DTT. 0.5 mg/mL BSA) along with five inhibitors (1mM levamisole. 35 µM coformycin. 1.2 µM 5-iodotubercidine. 60 µM β-glycerophosphate and 1 mM thymidine). Then [TAMRA]dCyd was added to the 30 µL of the extract to a final concentration of 12 µM. These mixtures were incubated at 37°C for different lengths of time to obtain the data for determining the reaction rate.

4.2.8 Kinetic study

A series of incubations with different concentrations of the substrate [TAMRA]dCyd were carried out. The reaction rates at each substrate concentration were obtained as described in Section 4.2.7. The kinetic data was then fit to a hyperbola. from which apparent Michaelis constant (K_m) and V_{max} values were extracted.

4.2.9 Study of phosphatase and other enzymes in the cell extracts

2-4 × 10⁶ cells were ground in 30 µL of the assay buffer (50 mM Tris-HCl (pH 7.5). 5 mM MgCl₂. 5 mM ATP. 2 mM DTT. 0.5 mg/mL BSA). Then 19.5 µL of supernatant was transferred into a siliconized tube. 0.5 µL of 400 µM [TAMRA]dCydTP was added and mixed gently with the extract solution. The mixture was incubated at 37°C for 14 time points ranging from 0 minutes to overnight. At each time. 1 µL of sample was removed

92

from the incubation mixture and added into 40 μL of ice-cold water/methanol (v/v 3:2) solution. Finally this solution was filtered through a Microcon YM-30 by centrifuging at 13,600 g for five minutes. Samples were immediately stored at $-20°C$ until analysis.

4.2.10 [TAMRA]dCyd uptake by cells

The A2780 and AG6000 cells were first grown to 80% confluence. After filter-sterilization, [TAMRA]dCyd was added to the media to reach a final concentration of approximately 25 μM. 18 and 36 hours of incubation were applied to A2780 and AG6000 cells respectively. When the incubation was finished, the cells were washed three times with phosphate buffered saline (PBS) to remove the residual substrate. A small portion of the cells was quickly ground and the extract was analyzed by CE-LIF. Also a 20 μL aliquot of each cell sample was examined by a model 2001 confocal laser scanning microscope (Molecular Dynamics, Sunnyvale, CA). An argon/krypton gas laser was used as an excitation source at 568 nm selected for TAMRA. The fluorescence of the aliquot was collected using a 100× objective.

4.2.11 Microinjection and intracellular distribution of [TAMRA]dCyd

To prepare [TAMRA]dCyd for microinjection, similar protocols to those described in Section 4.2.5 were used except an additional desalting step was applied. Before lyophilizing, the filtered [TAMRA]dCyd was loaded into a C-18 Sep Pak cartridge and washed with 2 mL of water for three times. Then the hydrophobic [TAMRA]dCyd was eluted from the cartridge with approximately 5 mL HPLC grade methanol. The product was then dried and dissolved in sterilized PBS for microinjection.

93

To prepare cells for microinjection, cells were set into 35×10 mm dishes (Falcon, Franklin Lakes, NJ) engineered with holes drilled into the bottom and 18×18 mm coverslips (Fisher Scientific, Nepean, ON, Canada) attached to the underside with glue (five minute epoxy). The cells were seeded at 1×10^5 cells in 2 ml DMEM and 10% FBS and grown for 3 to 4 days at 37°C, 5% CO_2 similar to regular cell culture (see Section 4.2.2). Then fresh media and 1 µL MitoTracker Green (Molecular Probes, Eugene, OR) were added to the cells. After 20 min. incubation at 37°C, 5% CO_2, the media was again changed and the cells were ready for injection.

To inject, electrodes were freshly pulled and filled with 1 µL [TAMRA]dCyd using an Eppendorf Microloader (Eppendorf, Hamburg, Germany). The electrode was prepared with the Faming/Brown micropipette puller (Sutter Instruments Co. Model P 87, Novato, CA) from an aluminosilicate filament (O.D. 1.0 mm, I.D. 0.68 mm, 10 cm in length) (Sutter Instrument, Novato, CA). Automated injections were done using the Eppendorf Micromanipulator 5171 in combination with the Transjector 5246. The injection parameters were: 150 hPa injection pressure, 30 hPa holding pressure and 0.5 s injection time.

After injection, media was changed again, the dish was sealed with parafilm and mounted on a prewarmed objective (Tempcontrol mini) set at 37°C. The injected cells were imaged using a 510 laser scanning microscope (Zeiss, Germany), 40× objective 1.3 N.A., and argon and HeNe lasers. The dish remained mounted throughout the imaging time.

94

4.2.12 Instrumentation and electrophoretic conditions

The same in-house built CE-LIF instrument described in Chapter 2 was used for this study (27). Each sample was mixed with an internal standard (I.S.) of [R6G]dCydTP and introduced electrokinetically into the capillary under an electric field of about (+) 33.3 V/cm for 5 seconds ([R6G]dCydTP was the I.S. unless otherwise stated). A 30 cm long, 20 μm inner diameter (I.D.), 150 μm outer diameter (O.D.) uncoated fused-silica capillary purchased from J&W Scientific (Folsom, CA) was used for the separation. The electrophoresis and sheath flow buffers were the same, containing 50 mM borate at pH 10. Every five to six runs, the electrophoretic buffer was renewed. All experiments were carried out applying a constant voltage of (+) 6 kV. Compounds were excited by a helium-neon laser (Melles Griot Laser Group, Carlsbad, CA) with a single 543.5 nm emission line. The fluorescence signals were collected through a 580 nm bandpass filter of 40 nm bandwidth (580DF40, Omega Optical, Brattleboro, VI) and detected by a R1477 photomultiplier tube (PMT). Data were collected and analyzed using Igor Pro 2.04 (WaveMetrics, Lake Oswego, OR). In all experiments, the TAMRA labeled nucleoside and nucleotides signals were divided by the signal of the internal standard resulting in a normalized signal for further data processing.

95

4.3 Results and Discussion

4.3.1 Generation of standards and concentration measurement

Currently there are no fluorescent dye-labeled dCyd or dCydMP available commercially. This originally appeared to be a large obstacle to begin this project. However, the problem was easily solved with an enzymatic treatment of [TAMRA]dCydTP (available from Applied Biosystems) using alkaline phosphatase (AP). AP, with the ability to hydrolyze 5'-phosphate groups from DNA, RNA, and nucleotides, enabled clear observation of a conversion from [TAMRA]dCydTP to [TAMRA]dCydDP to [TAMRA]dCydMP and eventually to [TAMRA]dCyd. The process was monitored with CE-LIF and these results are shown in Figure 4.1. It was observed that AP worked very efficiently even at very low concentrations and incubation products [TAMRA]dCydDP and [TAMRA]dCydMP were already generated with 0 minutes of incubation, having been formed during the short preparation process. The starting material [TAMRA]dCydTP which has a migration time at around 8.5 min gave the highest fluorescence signal when the treatment began. This signal kept decreasing and was not observable after approximately 10 min incubation under our conditions. A similar phenomenon was noticed with [TAMRA]dCydDP, while for [TAMRA]dCydMP, the signal increased first with the incubation and then decreased to almost zero after three hours. The fluorescence signal of the final product, [TAMRA]dCyd, kept increasing and became dominant after 60 min. incubation. The monitoring of the whole process allows the clear identification of [TAMRA]dCydDP, [TAMRA]dCydMP and [TAMRA]dCyd as assigned in the electropherograms. The process can also be illustrated by plotting the signal from each product against incubation time.

96
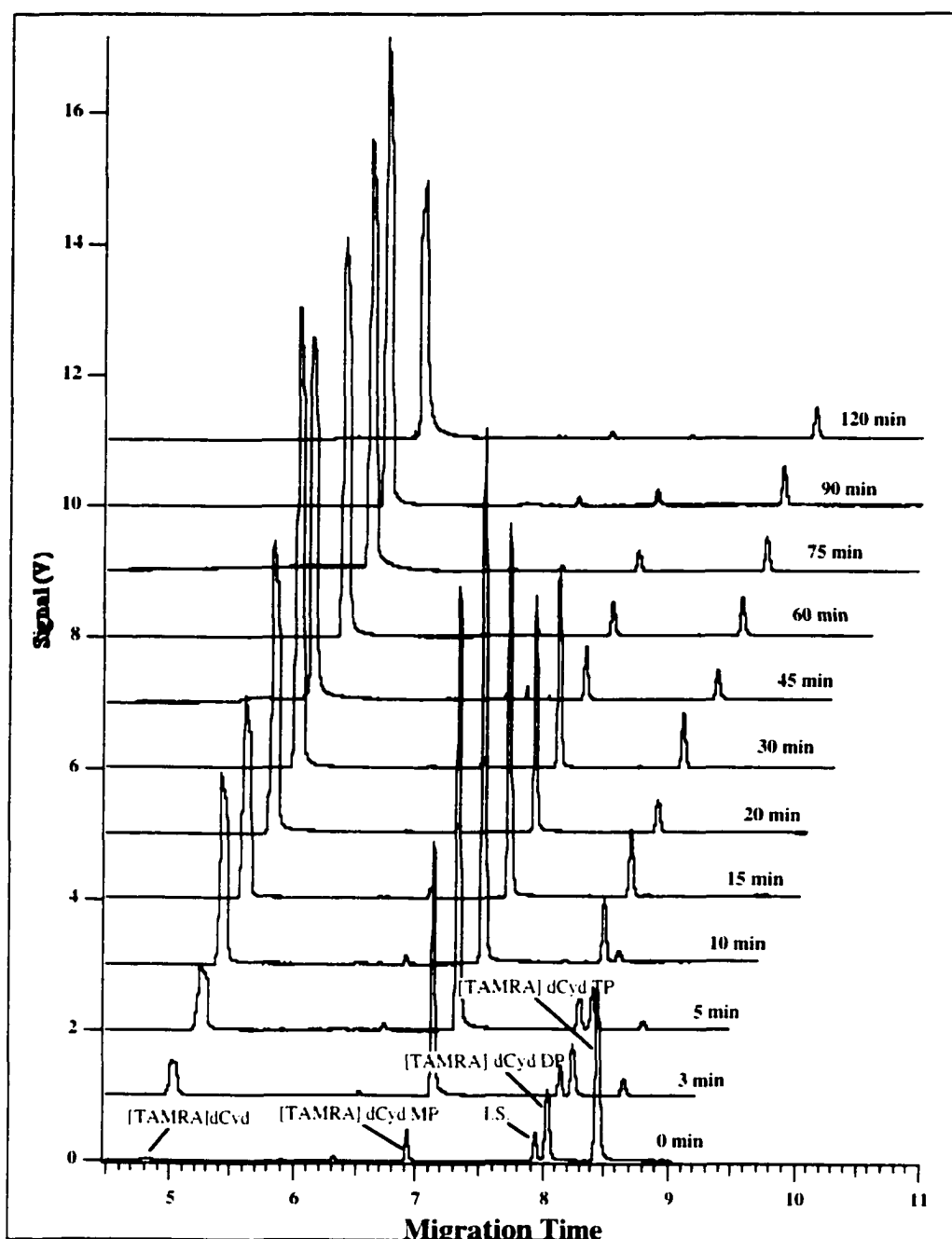
Figure 4.1 CE-LIF monitoring of [TAMRA]dCydTP enzymatic treatment by AP. Electropherograms are offset in time and signal for clarity; the time to the right of each electropherogram is the incubation time. Incubation and separation conditions are described in Sections 4.2.4 and 4.2.13, respectively.

97

As depicted in Figure 4.2. incubation product at 5 min. and 75 min. time points seem best for use as the standards for [TAMRA]dCydMP and [TAMRA]dCyd respectively.

After learning the characteristic migration time of each product. it was not difficult to prepare and confirm the production of pure [TAMRA]dCyd as substrate for dCK. Figure 4.3 compares the electropherograms of starting material and the generated product for dCK assay. After AP treatment. [TAMRA]dCyd was almost the only product. This pure [TAMRA]dCyd enabled accurate and reliable studies on dCK.

A problem with the generation of dCK substrate [TAMRA]dCyd and dCK enzymatic product [TAMRA]dCydMP by ourselves is the difficulty of knowing their concentrations because resulting amounts and volumes are too low for conventional UV measurement. To roughly measure the concentrations. a calibration curve was constructed using [TAMRA]dCydTP (Figure 4.4). Peak areas were measured to avoid the inaccuracy caused by different peakwidths of components with different migration times.

4.3.2 Kinetic study of [TAMRA]dCyd

The kinetic properties of dCK have been studied with a wide variety of purine and cytosine nucleosides. It is well known that dCyd is the best and preferred substrate of dCK enzyme with the highest V_{max} and K_m compared to other substrates such as deoxyadenosine (dAdo) and deoxyguanosine (dGuo). However. with the attachment of a bulky fluorescent tag. the kinetics of the substrate could certainly be changed. In addition. dCK activity has been found to be controlled by a complex pattern of substrate kinetics and end product inhibition (23. 28). For all of these reasons. it was essential to study

98
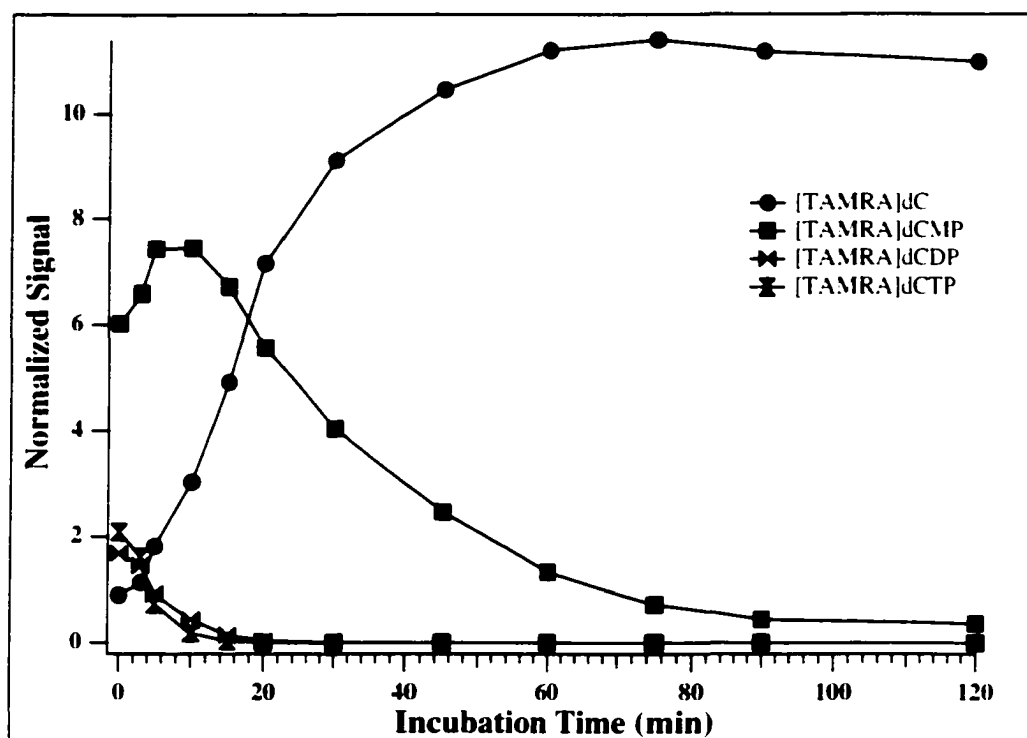
Figure 4.2 Changes in signal intensity from each product with incubation time. Based on this plot. 5 min. and 75 min. incubation products were used as [TAMRA]dCydMP and [TAMRA]dCyd standards respectively.

99
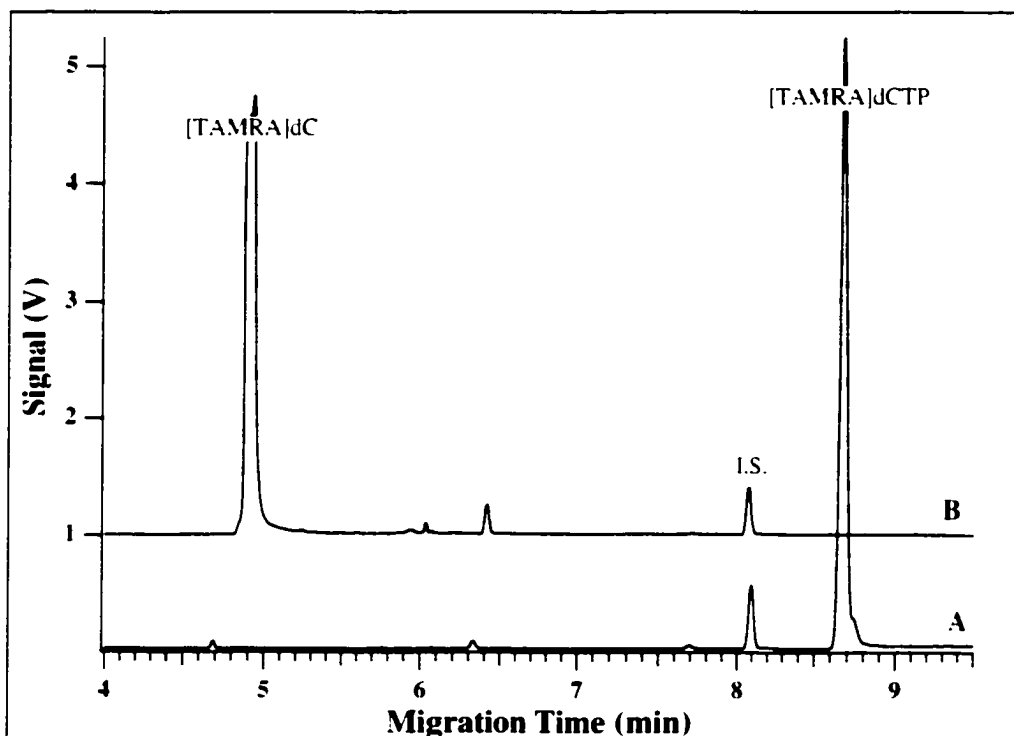
Figure 4.3 Generation of pure [TAMRA]dCyd from [TAMRA]dCydTP.

A: Standard [TAMRA]dCydTP + I.S.. [TAMRA]dCydTP is the major component:

B: Treated product + I.S.. [TAMRA]dCyd is the major component.

Treatment conditions were described in Section 4.2.5.

100
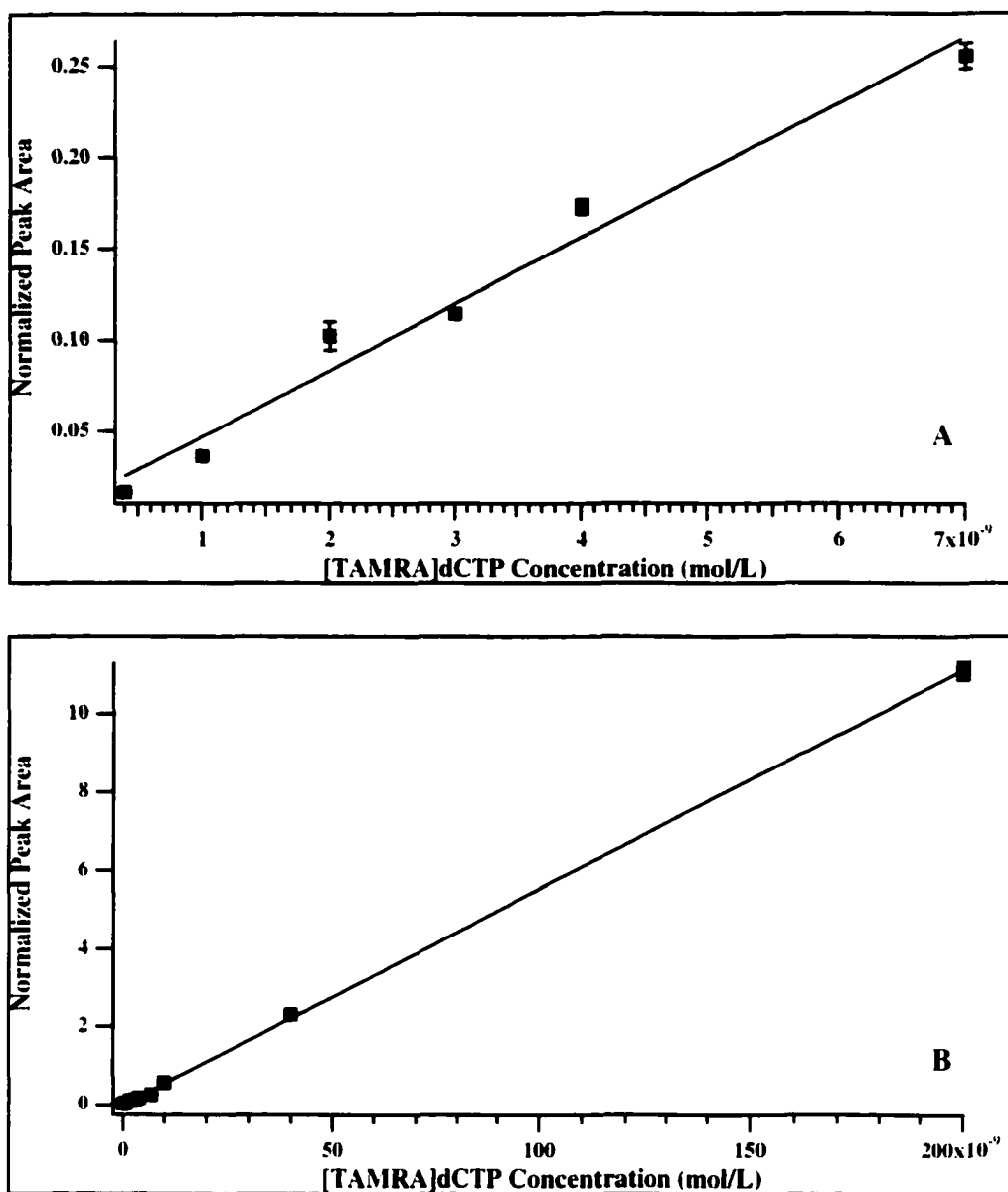
Figure 4.4 Calibration curves constructed with [TAMRA]dCydTP for [TAMRA]dCyd
and [TAMRA]dCydMP concentration measurements.

A: Lower range calibration curve; B: Overall range calibration curve.

The error bars show the standard deviation within three independent runs. Correlation
coefficients of both curves are 0.99.

101

the kinetic properties of [TAMRA]dCyd before applying this substrate to dCK activity measurements in cell extracts and further studies.

With a bulky dye molecule, [TAMRA]dCyd is much larger in size than dCyd. Therefore, it was very exciting and promising for us to see that [TAMRA]dCyd was still a substrate of dCK and could be phosphorylated by dCK. In fact, this is the first demonstration that the dCK enzyme molecule can use a fluorescently labeled dCyd as a substrate. As shown in Figure 4.5, a one hour incubation of [TAMRA]dCyd with purified dCK resulted in the clear generation of [TAMRA]dCydMP, giving a clean peak with a migration time around 7 minutes (electropherogram B). In contrast no such peak was detected when the reaction was not initiated (electropherogram A). However, in this reaction, approximately 2 μg of purified dCK and 12 μM substrate [TAMRA]dCyd were used. If the labeling had not affected the specificity of dCyd to dCK, the [TAMRA]dCydMP peak would be 1000-times higher, indicating that [TAMRA]dCyd may be up to 1000-fold less reactive than dCyd. To confirm this result and obtain more detailed kinetic information, five reactions were studied with substrate concentrations ranging from 6.25 μM to 50 μM. The reaction rate at each specific substrate concentration was obtained by varying the incubation time. The results are shown in Figure 4.6. In this plot, the rate was expressed as the change in normalized peak area per min (Δ(peak area)/min). After changing the units to nmol per hour based on the above calibration curve and the reaction volume, data were fitted to a hyperbola as shown in Figure 4.7, from which the kinetic parameters K_m and V_{max} were extracted.

102
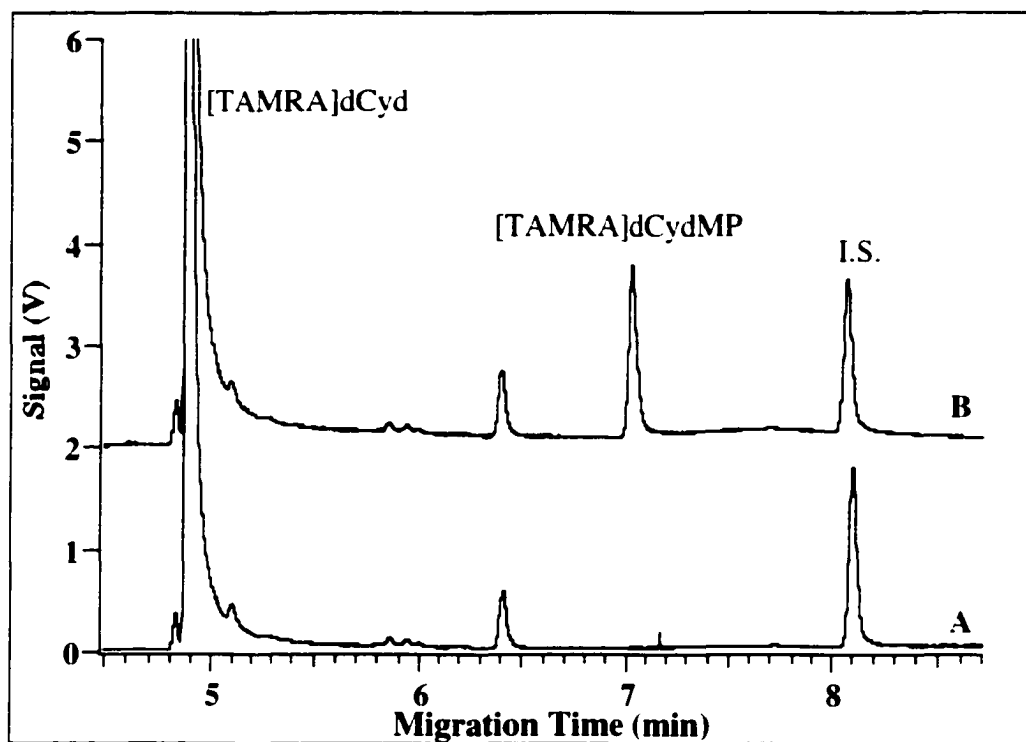
Figure 4.5 Generation of [TAMRA]dCydMP by incubating [TAMRA]dCyd with purified

dCK enzyme. The incubation conditions are described in Section 4.2.7.

A: 0 min incubation as negative control; no [TAMRA]dCydMP was detected.

B: 60 min incubation: [TAMRA]dCydMP was generated due to dCK enzyme activity.

103

The chart legend reads:

— ● — [S]=6.25 μM, v=0.0052426/min;
— ■ — [S]=12.5 μM, v=0.0078173/min;
— ◆ — [S]=18.75 μM, v=0.0088595/min;
— ✗ — [S]=25 μM, v=0.0086224/min;
— ▲ — [S]=50 μM, v=0.0094206/min.

Y-axis: **Normalized Peak Area** (2.0, 1.5, 1.0, 0.5, 0.0)

X-axis: **Incubation Time (min)** (0, 50, 100, 150, 200)

Figure 4.6 dCK reaction rate measurements at different fluorescent substrate

([TAMRA]dCyd) concentrations, [S]. The rate increases with the increases of [S]. Here

the rates are expressed in units of Δ(peak area)/min (see text). Experiment conditions are

described in Sections 4.2.7 and 4.2.8.
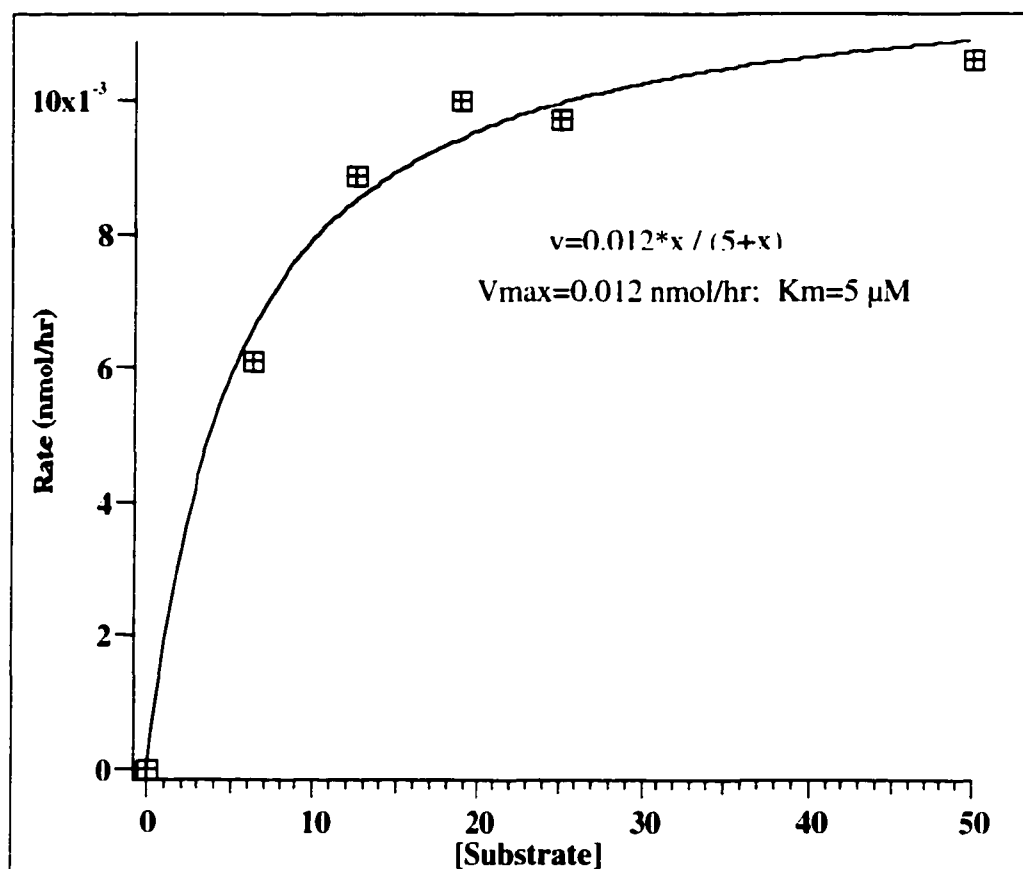
Figure 4.7 Kinetics of purified dCK on the substrate [TAMRA]dCyd. The change of rate change with [Substrate] was fitted to a hyperbola and V_{max} and K_m values were then extracted. The RSD (relative standard deviation) values for V_{max} and K_m are 4.9% and 21%.

Compared to a reported 145 nmol/min/mg V_{max} value for dCyd (23). V_{max} for

[TAMRA]dCyd (0.10 nmol/min/mg) is approximately 1,500 fold lower, while for K_m, the

value from [TAMRA]dCyd (5 μM) only shows a minimal difference from that reported

for dCyd (K_m = 1 μM) (23). The kinetic data obtained with purified dCK suggest that

[TAMRA]dCyd has a slightly smaller affinity for the dCK nucleoside binding site than

dCyd as indicated by the lower K_m of [T]dCyd as compared to the K_m of dCyd. However,

V_{max} is the major reason causing the significant loss of specificity of [TAMRA]dCyd to

dCK enzyme. The K_m value of [TAMRA]dCyd is actually lower than most other

substrates (23), i.e. has higher affinity to the enzyme binding sites than most of the other

substrates, as shown in Table 4.1.

Previous studies by Eriksson *et al.* showed that dCK phosphorylates analogues as long as

the base is a cytosine with only minor substitutions at the 5-position (29). Based on these

results, data obtained here could be explained by the fact that the TAMRA molecule is

attached to the 5-position of the base. (It is confirmed from the manufacturer and patent

information). This 5-position may be very important in orienting nucleosides for normal

phosphorylation. As a result, if the substitution molecule on dCyd is too bulky, the V_{max}

value will be decreased significantly while affecting minimally the binding affinity. The

other reason for the low V_{max} value might be the long and narrow tunnel structure of the

nucleoside binding site in dCK.

4.3.3 Enzyme activity study of cell extracts

When applying the dCK enzyme assay to the study of cell extracts, the effects caused by

many other enzymes have to be considered. To inhibit the major enzymes that may affect

dCK activity, up to five different inhibitors were used.

106

Table 4.1 Comparison of [TAMRA]dCyd's K_m value to those of other substrates.

Substrate	K_m (µM)
deoxycytidine (dCyd)	1
arabinosylcytosine	20
deoxyguanosine (dGuo)	150
deoxyadenosine (dAdo)	120
[TAMRA]dCyd	5

The K_m values were obtained from literature (23) except for that of [TAMRA]dCyd.

Levamisole. coformycin. 5-iodotubercidin. thymidine and β-glycerophosphate were used to inhibit alkaline phosphatase. adenosine deaminase. adenosine kinase. thymidine kinase and non-specific phosphatases respectively. The inhibitors were added to the dCK enzyme assay buffer before the first grinding step (see Section 4.2.7). In the presence of these inhibitors. [TAMRA]dCydMP. the dCK product from [TAMRA]dCyd. was detected. as shown in electropherogram B and C in Figure 4.8. The peak identification was confirmed by spiking the sample with standard [TAMRA]dCydMP (electropherogram D). The product signal was very low. which is predictable from the low V_{max} value of [TAMRA]dCyd because of the attached fluorescent tag. The reaction rate of dCK from the cell extract on [TAMRA]dCyd was also obtained by changing the incubation times as shown in Figure 4.9. The rate was calculated to be approximately 3×10^{-5} nmol/min/10^6 cells. This is about 3.000 fold lower than the 0.088 nmol/min/10^6 cells when using dCyd as the substrate (11) on the same cell line A2780. The rate difference in the cell extract was comparable to that obtained earlier using the purified dCK enzyme.

However. when comparing the dCK activity between the parental drug sensitive cell line A2780 and the variant drug resistant cell line AG6000. the results were not as predicted. No significant differences were observed between the two cell lines (as shown in Figure 4.10). This is contrary to up to 10-fold differences previously observed with conventional radio-labeled dCK assay (11). To explain this result. several possible reasons are proposed:

(1) The complexity of the enzyme in the crude extract may cause inaccurate dCK activity measurement. Although five kinds of inhibitors were included in the cell extract dCK

108
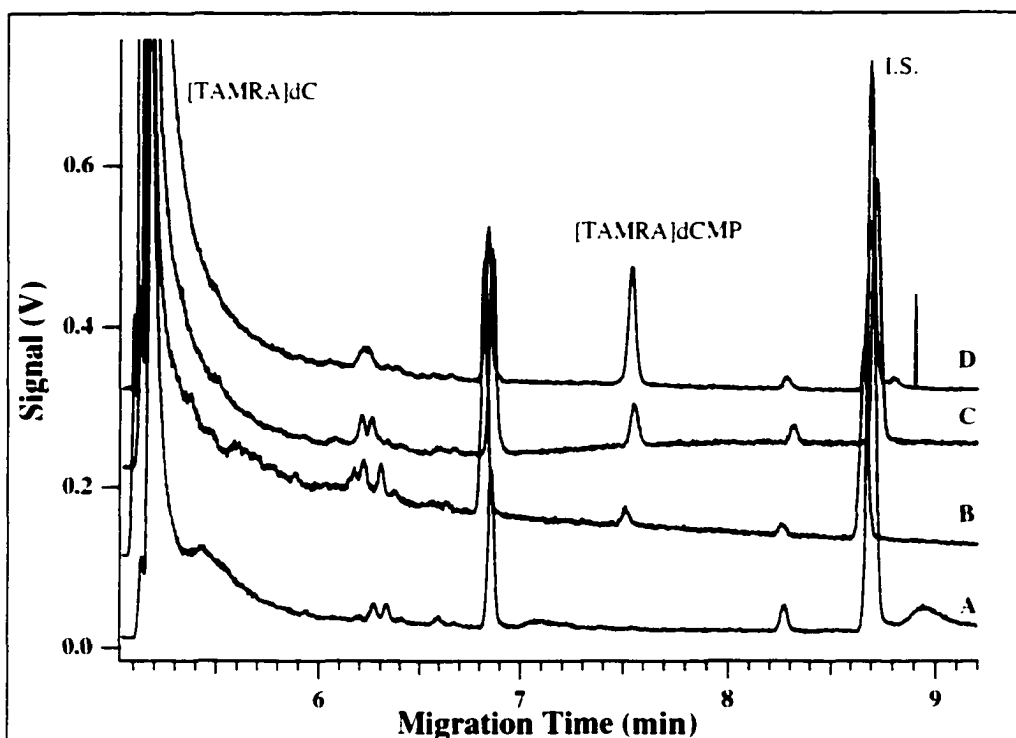
Figure 4.8 dCK activity measurement in A2780 cell extract. Experimental conditions are described in Section 4.2.7.

A: 0 min incubation as a negative control. No [TAMRA]dCydMP was detected:

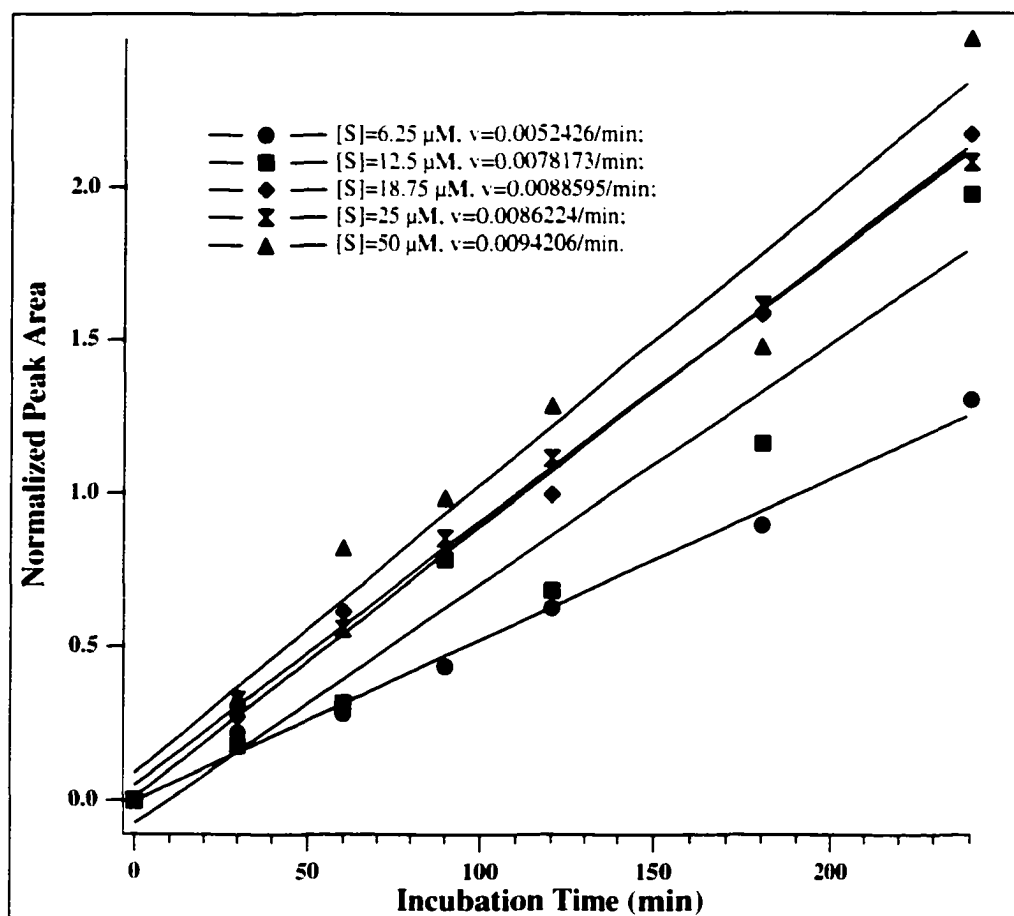B: 4 hours incubation. [TAMRA]dCydMP was generated due to the dCK activity in the cell extract:

C: 20 hours incubation. More [TAMRA]dCydMP was produced with this longer incubation time:

D: Sample B spiked with standard [TAMRA]dCydMP to confirm the peak identification.

109
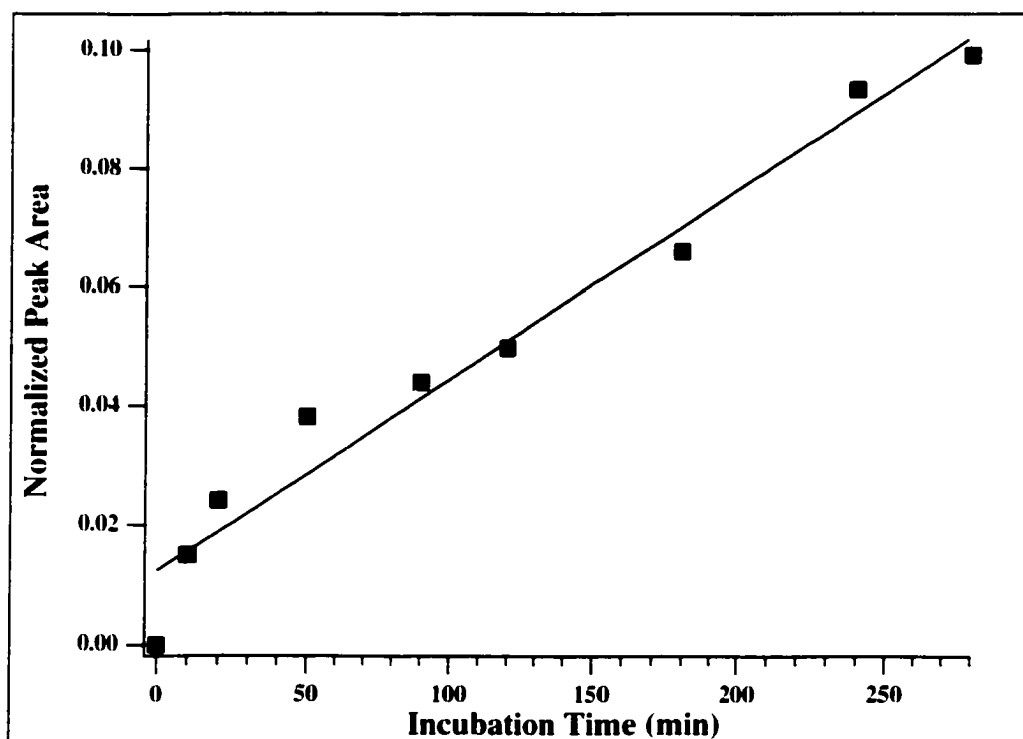
Figure 4.9 dCK enzymatic reaction rate measurement in A2780 cell extract at [S]=10

µM. The correlation coefficient is 0.98 and the rate is approximately 3×10^5 nmol/min/10^n

cells. Experimental conditions are described in Section 4.2.7.

Figure 4.10 Comparison of dCK enzyme activity between parental cell line A2780 and resistant cell line AG6000. Both were incubated overnight with substrate [TARMA]dCyd at a concentration of 10 μM.

A: Parental cell lineA2780: B: Resistant cell line AG6000.

No significant difference is observed.

111

assay, their concentrations and other assay conditions used in these two different cells were exactly the same. However, the enzymes in the cell extracts showed very different activities as depicted in Figure 4.11. In this experiment, [TAMRA]dCydTP was added in the crude extracts without any of the inhibitors. Therefore, the conversion of [TAMRA]dCydTP to [TAMRA]dCyd due to the activity of a series of phosphatase and nucleotidase and other enzymes was monitored by CE-LIF. With identical treatment and procedures, there was five times more [TAMRA]dCydTP left in the parental A2780 cell extract incubation product than that from the resistant AG6000 cells. Close to a 50 fold difference was observed in the amount of [TAMRA]dCyd left in the incubation products from these two cell extracts. These data suggest that the hydrolytic enzyme activities are very different in these two cell lines and different inhibitor conditions may be required for probing the dCK activity difference. Thus, no differences could be detected in our systems.

(2) Attachment of TAMRA to dCyd resulted in a significant loss of its phosphorylation efficiency by dCK enzyme. It might be possible that the modification increases other enzymes' efficiency, or does not affect their efficiencies to the same extent as it affects dCK. As a result, the interference caused by these enzymes may appear to be more significant, and therefore the inhibition conditions used in our assay are no longer efficient.

(3) It has been reported that 2'-deoxycoformycin, an adenosine deaminase inhibitor, showed an unexpected ability to inhibit purine and pyrimidine dideoxynucleoside phosphorylation; such inhibition was not competitive and was not observed when 2'-deoxycytidine was the substrate (30). This result suggests that the inhibitors used in our

112
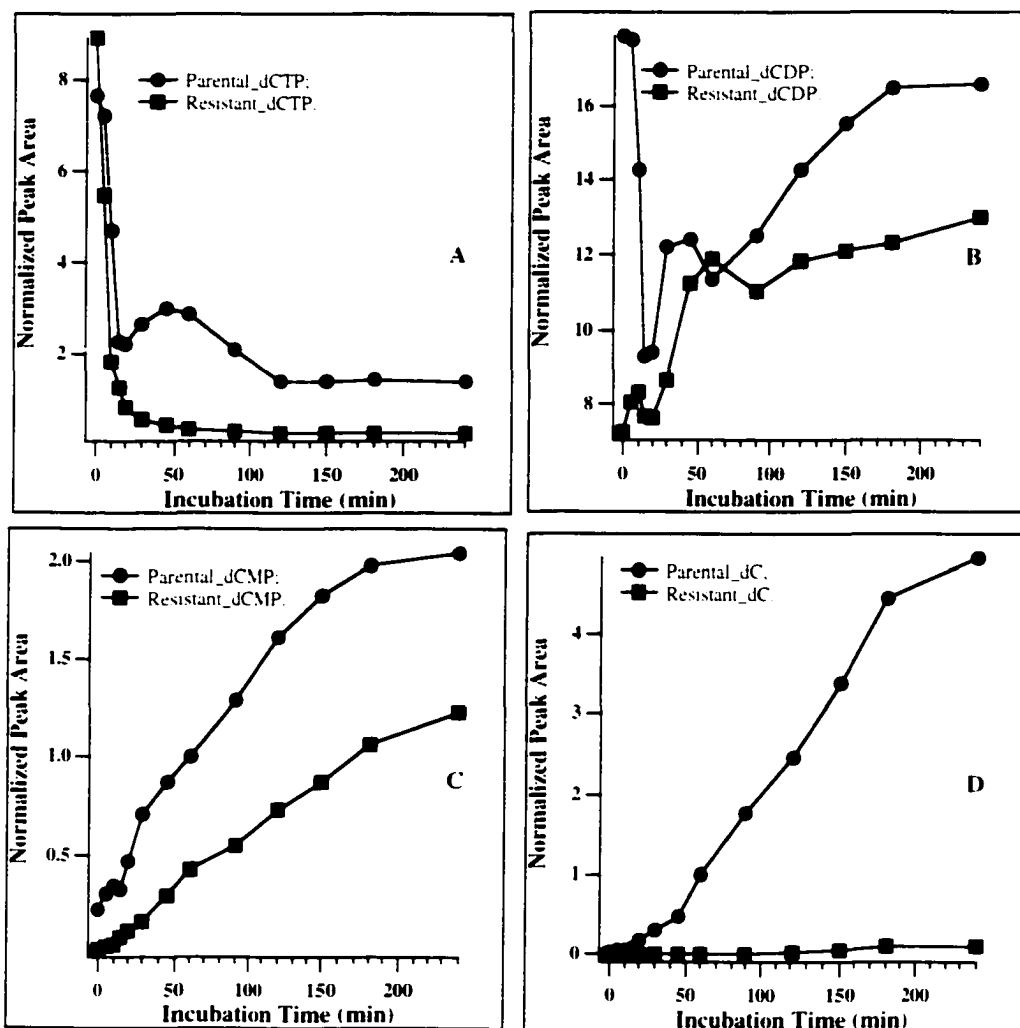
Figure 4.11 Differences of other enzyme activities between the parental A2780 cell line (indicated as P above) and the resistant AG6000 cell line (indicated as R above). Experimental conditions are described in Section 4.2.9.

113

system might inhibit the phosphorylation of [TAMRA]dCyd due to the large modification, which will in turn affect the accuracy of dCK activity measurements.

(4) A cell line established from an ara-C-resistant (ara-C is one of the nucleoside anti-cancer drugs) brown Norway rat model has been shown to be dCK deficient. preferentially with ara-C. but not with dCyd as a substrate (31). This may be another explanation for the inability of our method to probe the dCK expression difference by using [TAMRA]dCyd as the substrate.

Although [TAMRA]dCyd could be phosphorylated by dCK in the cell extracts, it may be premature to measure dCK activity based upon this assay. The changes to the substrate specificity and structure directly or indirectly affect the enzyme assay and cause inaccuracy in the activity measurements. It is essential to find a better fluorescent substrate for further study. This might be achieved by either changing the modification position of the dye or the dye itself.

In attempts to find a better substrate, another fluorescent substrate [Fluorescein]dCyd (similarly generated from [Fluorescein]dCydTP) was tried. Unfortunately, results with this substrate were worse than those with [TAMRA]dCyd. As shown in Figure 4.12A. virtually no [Fluorescein]dCydMP was generated from a 4-hour incubation with purified enzyme. A very small amount of [Fluorescein]dCydMP was seen in the overnight incubation product. On the other hand, a [TAMRA]dCyd incubation carried out under the identical conditions, generated a clear and sharp product peak in 4 hours as depicted in Figure 4.12B. It is known that the fluorescein molecule is attached to the 5-position of the base, the same as [TAMRA]dCyd (Shown in Figure 4.13). Therefore, the more significant loss of specificity of [Fluorescein]dCyd compared to [TAMRA]dCyd

114
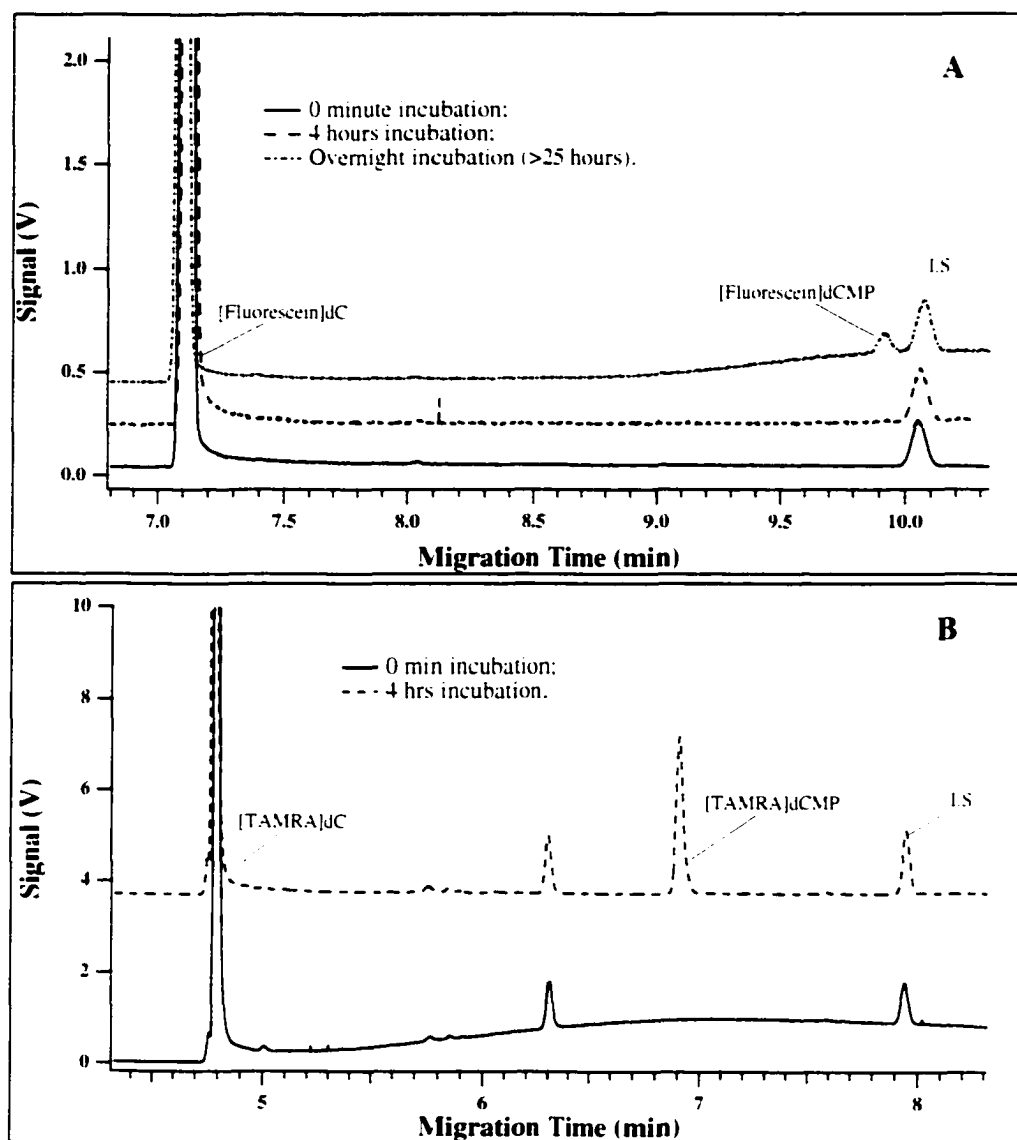
Figure 4.12 Test of [Fluorescein]dCyd as a substrate for dCK and its comparison with [TAMRA]dCyd. The same conditions ([S]=50 µM. 2 µg purified dCK enzyme) were used in both experiments.

A: [Fluorescein]dCyd as a substrate. The I.S. here is fluorescein. No [Fluorescein]dCydMP peak was detected until after 25 hours of incubation:

B: [TAMRA]dCyd as a substrate. A clear [TAMRA]dCydMP product peak was detected after 4 hours incubation.

115

[Fluorescein]dCyd
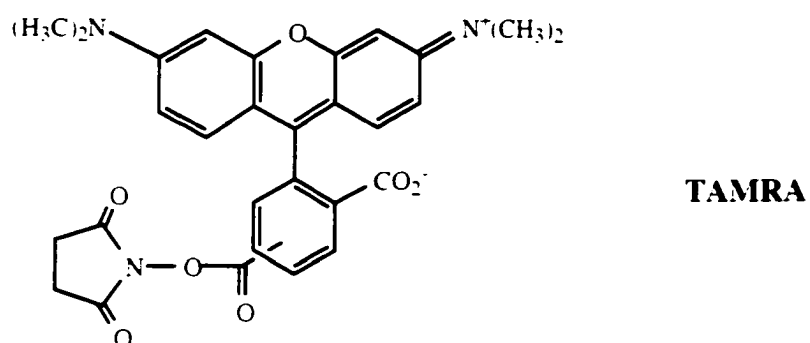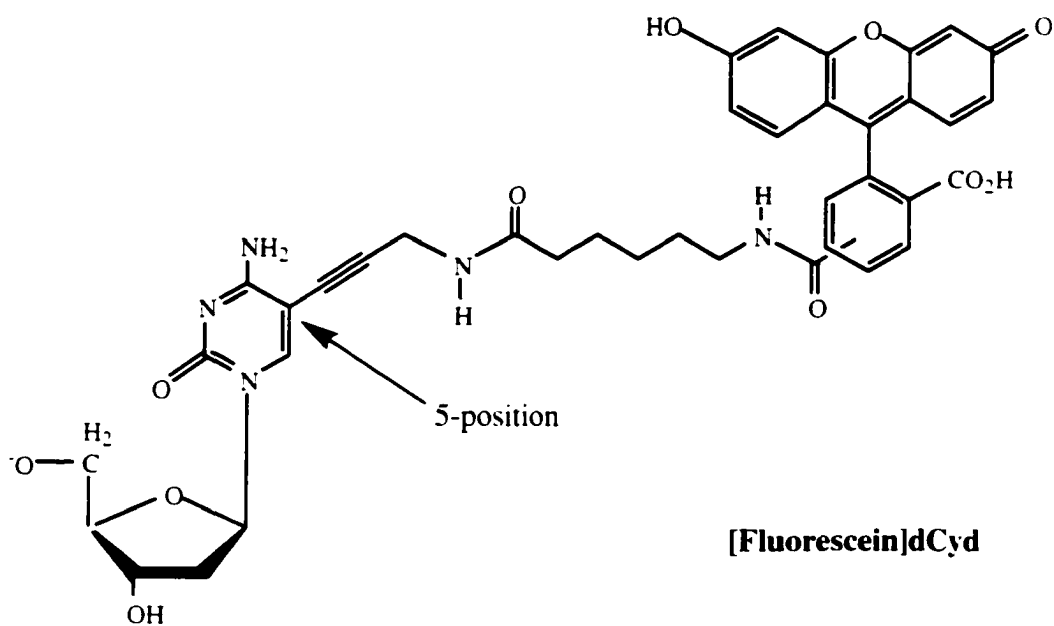
TAMRA

Figure 4.13 Structures of [Fluorescein]dCyd and TAMRA. In the case of [TAMRA]dC. the dye molecule is also attached to the 5-position same as [Fluorescein]dC while the linker may change.

116

must be a result of the native features of fluorescent tag such as its polarity, size, etc.

4.3.4 Cellular uptake of [TAMRA]dCyd

In addition to searching for a better fluorescent substrate and improving the enzyme assay conditions, cellular uptake studies on the fluorescent substrate were carried out in parallel since this plays a critical role in achieving the ultimate goal of enzyme activity measurement at the level of single cells. As shown in Figure 4.14, [TAMRA]dCyd was taken up by A2780 cells with an simple incubation step for 18 hours. The uptake was confirmed by CE-LIF measurement as shown in Figure 4.15. Similar results were obtained with the resistant AG6000 cells. At this point, the uptake mechanism is unclear. However, the low intensity of the fluorescence indicates that facilitated transport such as liposomal transport is required to improve the uptake efficiency.

Also observed was that the nucleus appeared to generate a stronger fluorescence signal than other organelles, and vesicles were formed inside the cells. These results were later found to be in agreement with the data obtained from microinjection and distribution studies (described in more detail in Section 4.3.5).

4.3.5 Intracellular distribution of [TAMRA]dCyd

dCK has been shown to be mainly localized in the cytoplasm. Whether or not [TAMRA]dCyd would remain in the cytoplasm after moving into the cells would directly affect the activity measurement results in future whole cell assays (i.e. uptake-incubation-lysis-detection instead of a traditional assay based on lysis-incubation-detection). Hence, the intracellular distribution of substrate [TAMRA]dCyd is another important property

117
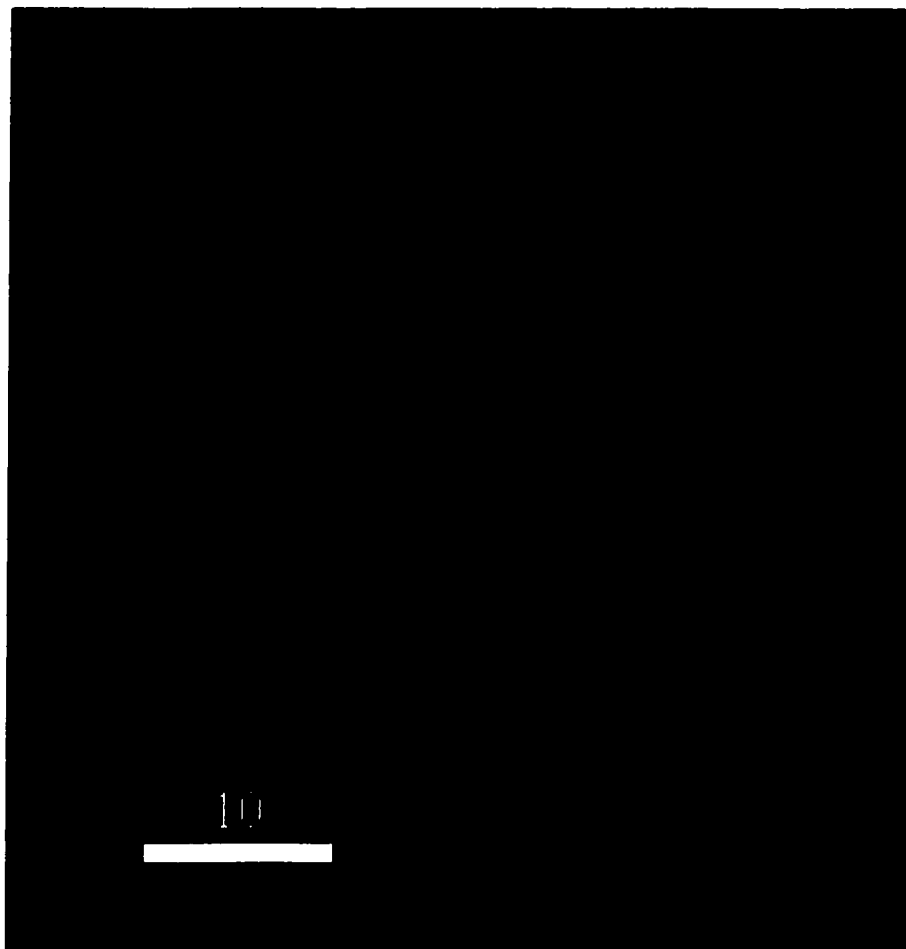
Figure 4.14 Confocal microscopy detection of [TAMRA]dCyd cellular uptake by A2780

cells. Experimental conditions are described in Section 4.2.10.

118
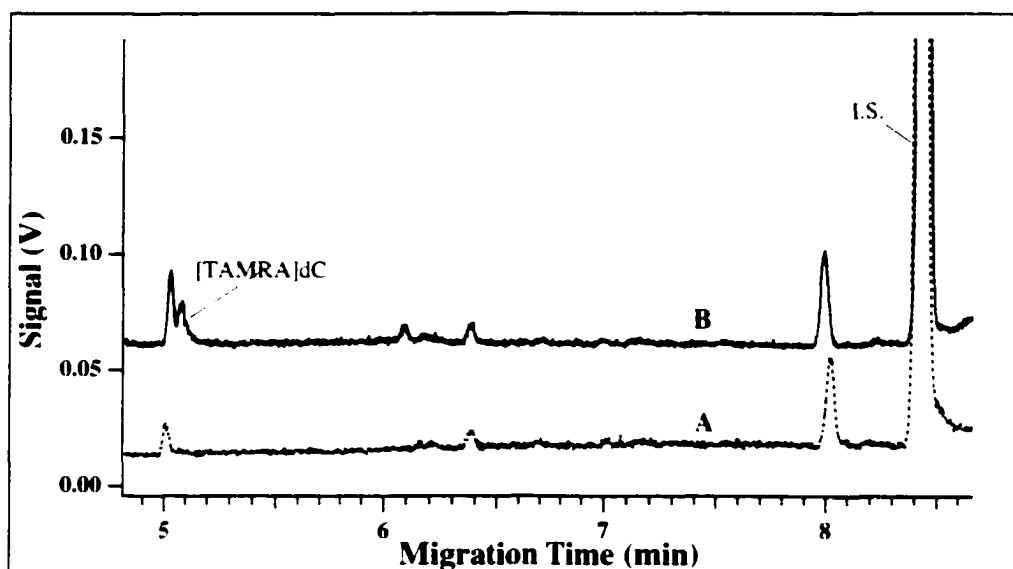
Figure 4.15 CE-LIF detection of [TAMRA]dCyd cellular uptake by A2780 cells.

A: Negative control. No [TAMRA]dCyd was present in the cell media during the incubation;

B: Uptake samples. Approximately 20 μM [TAMRA]dCyd was included in the cell media during the incubation.

which requires detailed study. In this work. the distribution was monitored by a laser scanning microscope after artificially injecting the substrate. [TAMRA]dCyd. into the cytoplasm.

Figures 4.16 and 4.17 are fluorescent images of both A2780 and AG6000 cells at different post-injection times. The green fluorescence is due to the mitotracker that stains the mitochondria inside the cells and indicates that the cells are still alive and healthy. The orange-red fluorescence is from the emission of TAMRA dye and shows the changes in [TAMRA]dCyd's intracellular distribution.

As shown in Figure 4.16. although the cell shape changed little during the monitoring process. cells were shown to be healthy by comparing the mitotracker green fluorescence signals in Figure 4.16 A and F. As for the intracellular distribution of [TAMRA]dCyd. it is clearly shown that the fluorescence signal from TAMRA was the strongest shortly after injection. specifically in the nucleus (Figure 4.16 B). With increasing post-injection time. less and less signal was detected as shown in Figures 4.16 B-D. indicating the loss of [TAMRA]dCyd. Almost no fluorescence signal from TAMRA was seen 140 min after injection. as shown in Figure 4.16 F. Comparing Figures 4.16 E and F seems to suggest that [TAMRA]dCyd was distributed more in the mitochondria regions. However. this might be an artifact or result from the mitotracker green.

Similar phenomena were observed with the AG6000 cell line. The fluorescent signal was much higher. as shown in Figure 4.17. This was most likely caused by the injection process during which the injection amount is hard to control. Fluorescence from TAMRA was also stronger in the nuclear area. and the overall fluorescent signal decreased with

120

121
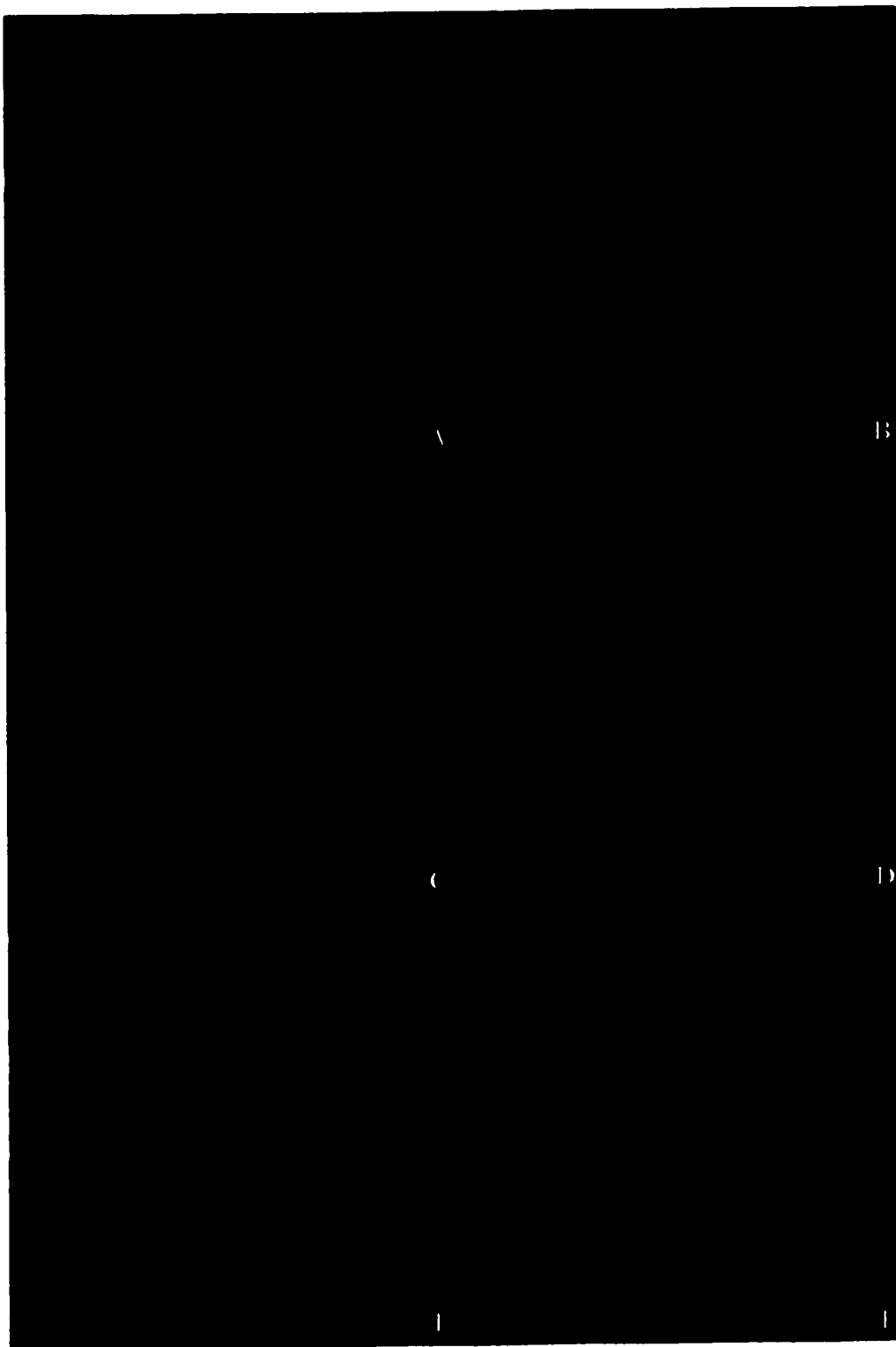
Figure 4.16 [TAMRA]dCyd microinjection into A2780 cells and its intracellular

distribution monitoring with post-injection time.

A. Mitotracker green staining of mitochondria. 10 min after injection.

B. Fluorescence signal from TAMRA. 10 min after injection.

C. Fluorescence signal from TAMRA. 40 min after injection.

D. Fluorescence signal from TAMRA. 75 min after injection.

E. Mitotracker green staining of mitochondria. 140 min after injection.

F. Fluorescence signal from TAMRA. 140 min after injection.

123
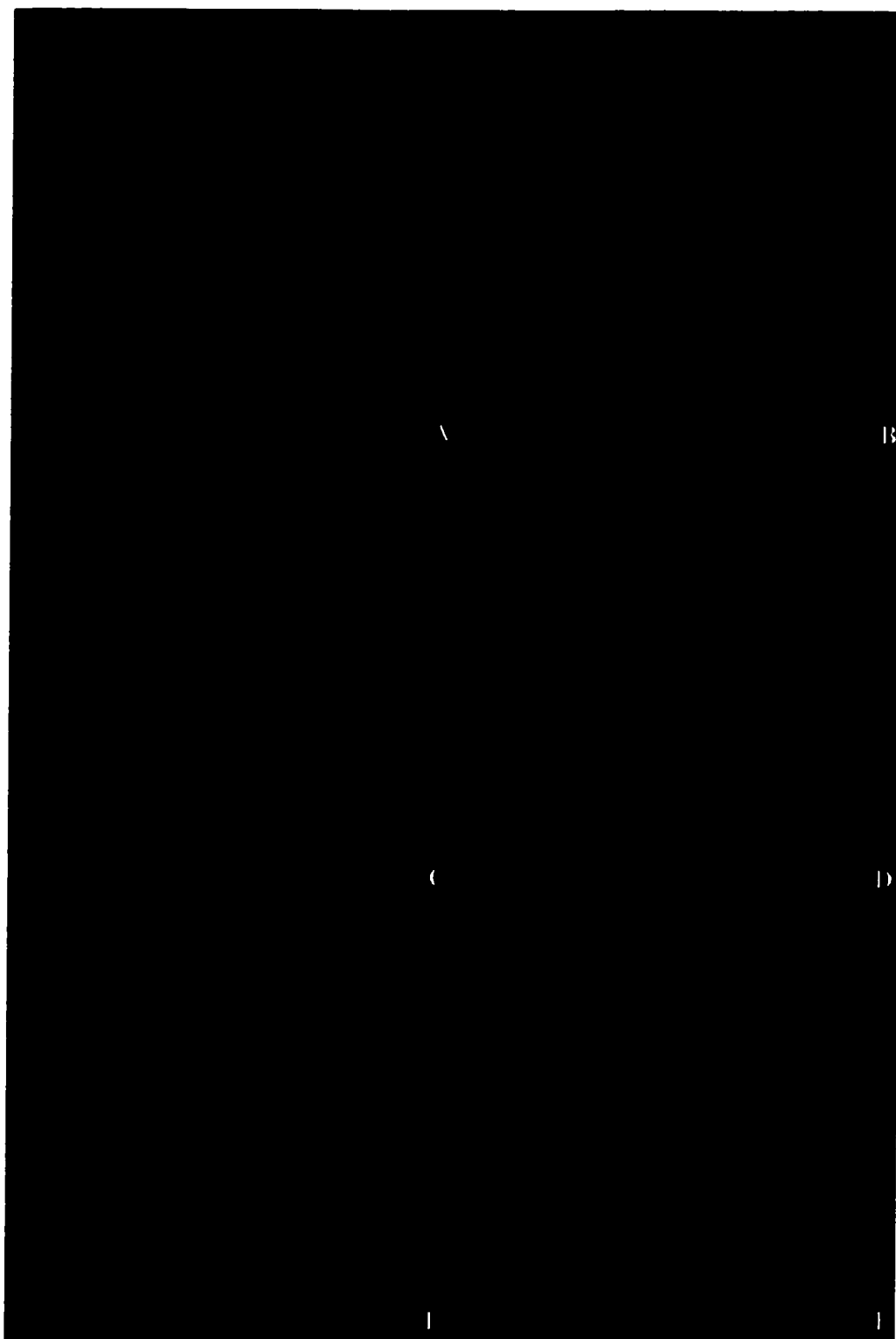
Figure 4.17 [TAMRA]dCyd microinjection into AG6000 cells and its intracellular

distribution monitoring with post-injection time.

A. Mitotracker green staining of mitochondria. 30 min after injection.

B. Fluorescence signal from TAMRA. 30 min after injection.

C. Fluorescence signal from TAMRA. 60 min after injection.

D. Fluorescence signal from TAMRA. 90 min after injection.

E. Mitotracker green staining of mitochondria. 160 min after injection.

F. Fluorescence signal from TAMRA. 160 min after injection.

124

post-injection time. Furthermore, vesicles were formed inside the cell. It is possible that the cells were forming vesicles to expel [TAMRA]dCyd by exocytosis.

4.4 Conclusion

The overall goal of this project was to detect dCK activity at a single-cell level with the help of the exquisite sensitivity of CE-LIF. The initial step toward this ultimate goal is to find a suitable and efficient fluorescent substrate for dCK.

In this preliminary study, [TAMRA]dCyd was generated from an enzymatic treatment. CE separation of [TAMRA]dCyd and its phosphates was efficient and rapid. Using purified dCK, kinetic data for its interaction with [TAMRA]dCyd were obtained and the lower V_{max} and higher K_m values were proposed to arise through structural modification. Although product generated from dCK enzyme activity was observed in the cell extract, the inability to distinguish the difference between the parental sensitive A2780 and the variant resistant AG6000 cells indicated a need for improvements. The improvements will mainly include the seeking of a better fluorescent substrate and inhibitor working conditions. Other aspects associated with the potential for using fluorescently dye labeled dCyd, specifically [TAMRA]dCyd in this study, as a substrate for dCK activity measurement at the level of single cells were also studied. These include its cellular uptake and intracellular distribution. It is suggested from the preliminary data that [TAMRA]dCyd uptake has to be assisted to obtain better efficiency. Furthermore, [TAMRA]dCyd's intracellular distribution requires a further and more detailed study to explain the significant decrease of [TAMRA]dCyd concentration observed inside cells.

125

At this stage of the study. it has been concluded that [TAMRA]dCyd is not an ideal substrate for dCK and analysis using it to measure cellular dCK enzyme activity was not successful. Attachment of TAMRA to dCyd changes its kinetics. possibly the working conditions of other enzyme inhibitors. the uptake mechanism. and also intracellular distribution. All these factors either directly or indirectly lead to difficulties in succeeding with dCK activity measurements. More effort is required not only from analytical chemists and oncologists. but also from organic chemists. to find a suitable fluorescent substrate for dCK. which will lead to the success of the overall project goals.

4.5 References

1.   Kufe. D.: Spriggs. D.: Egan. E. M.: Munroe. D. *Blood* **1984**. 64. 54-58.

2.   Zittoun. R.: Jean-Pierre. M.: Delanian. S.: Suberville. A.-M.: Thevenin. D. *Oncology* **1987**. 14. 269-275.

3.   Heinemann. V.: Hertel. L. W.: Grindey. G. B.*et al. Cancer Res.* **1988**. 48. 4024-31.

4.   Leiby. J. M.: Snider. K. M.: Kraut. E. H. *et al. Cancer Res.* **1987**. 47. 2719-2722.

5.   Arner. E. S. J.: Eriksson. S. *Pharmac. Ther.* **1995**. 67. 155-186.

6.   Kawasaki. H.: Carrera. C. J.: Piro. L. D. *et al. Blood* **1993**. 81. 597-601.

7.   Cheson. B. D.: Keating. M. J.: Plunkett. W. *Nucleoside Analogs in Cancer Therapy* Marcel Dekker. Inc.. **1997**.

8.   Abbruzzese. J. L.: Grunewald. R.: Weaks. E. A. *et al. J. Clin. Oncol.* **1991**. 9: 491-498.

9.   Dumontet. C.: Fabianowska-Marjewska. K.: Mantincic. D. *et al. Br. J. Haematol.* **1999**. 106. 78-85.

10. Stegmann. A. P.; Honders. M. W.; Willemze. R. *et al. Leukemia* **1995**. 9. 1032-1038.

11. Ruiz van Haperen. V. W.; Veerman. G.; Eriksson. S. *et al. Cancer Res.* **1994**. 54. 4138-4143.

12. Flasshove. M.; Strumberg. D.; Ayscue. L. *et al. Leukemia* **1994**. 8. 780-   785.

13. Eriksson. S.; Arner. E. S.; Spasokoukotskaja. T. *et al. Advances in Enzyme Regulation* **1994**. 34: 13-25.

14. Spasokoukotskaja. T.; Arner. E. S.; Brosjo. O. *et al. Eur. J. Cancer* **1995**. 2: 202-208.

15. Singhal. R. L.; Yeh. Y. A.; Szekeres. T. *et al. Oncol. Res.* **1992**. 4. 517-522.

16. Arner. E. S.; Eriksson. S. *Pharmac. Ther.* **1995**. 67. 155-186.

17. Kim. M.-Y.; Ives. D. H. *Biochemistry* **1989**. 28. 9043-9047.

18. Momrarler. R. L.; Fischer. G. A. *J. Biol. Chem.* **1968**. 243. 4298-4304.

19. Hughes. T. L.; Hahn. T. M.; Reynolds. K. K.; Shewach. D. S. *Biochemistry* **1991**. 30. 7540-7547.

20. Kawasaki. H.; Carrera. C. J.; Carson. D. A. *Anal. Biochem.* **1992**. 207. 195-196.

21. Le. X. C.; Tan. W. G.; Scaman. C. H.; Szpacenko. A.; Arriaga. E.; Zhang. Y.; Dovichi. N. J.; Hindsgaul. O.; Palcic. M. M. *Glycobiology* **1999**. 9. 219-225.

22. Krylov. S. N.; Zhang. Z.; Chang. N. W. C.; Arriaga. E.; Palcic. M. M.; Dovichi. N. J. *Cytometry* **1999**. 37. 15-20.

23. Usova E. V.; Eriksson. S. *Eur. J. Biochem.* **1997**. 248. 762-766.

24. Pizao. P. E.; Lyaruu. D. M.; Peters. G. J. *et al. Br. J. Cancer* **1992**. 66. 660-665.

25. Ruiz van Haperen. V. W. T.; Veerman. G.; Eriksson. S.; Stegmann. A. P. A.; Peters. G. J. *Seminars in Oncology* **1995**. 22. 35-41.

26. Bradford. M. M. *Anal. Biochem.* **1976**. 72. 248-254.

27. Tan. W. G.; Tyrrell. D. L. J.; Dovichi. N. J. *J. Chromatogr.* **1999**. 853: 309-319.

28. Sarap. J. C.; Fridland. A. *Biochemistry* **1987**. 26. 590-597.

29. Eriksson. S.; Wang. J.; Gronowitz. S.; Johansson. N. G. *Nucl. Nucleotides* **1995**. 14. 507-510.

30. Johnson. M. A.; Johns. D. G.; Fridland. A. *Biochem. Biophys. Res. Commun.* **1987**. 148. 1252-1258.

31. Richel. D. J.; Colly. L. P.; Arkesteijn. G. J. A.; Arentsen-Honders. M. W.; Kerster. M. G. D.; ter Riet. P. M.. Willemze. R. *Cancer Res.* **1990**. 50. 6515-6519.

128

CHAPTER 5

Study of Cell Cycle Phase Dependent Biological Events Using Cell Synchronization Techniques: (I) hENT1 Protein Expression Variation with Cell Cycle Phase

129

5.1 Introduction

The basic unit of life. the cell. is a complex and dynamic entity. Typically cells have to go through four different phases to replicate. namely a gap after division and before DNA synthesis (G_1). a period of DNA synthesis (S). a gap after DNA synthesis and before mitosis (G_2) and a period of mitosis (M) (1). As cells progress through the replication cycle. marked changes occur in terms of their characteristics and their functions (2).

Exponentially growing cultures are generally asynchronous. i.e.. each cell progresses through the cell cycle independently of neighboring cells. As a result. cell synchronization is particularly useful for investigating cell cycle-regulating or cell cycle-dependent events in cell biology.

The purpose of synchronization is to create a population of cells enriched at a single stage of the cell cycle. These cells will then be able to continue through the cell cycle with as little disruption of normal events as possible. At present. there are numerous methods available for collection of synchronous cultures *in vitro* (For review. see reference 3). Generally they can be classified into two major methods. The first is so-called "induction synchrony" in which the cells of a normal asynchronous culture are induced to divide synchronously. This can be done by environmental changes (e.g. temperature or light) or by blocking a stage of the cycle (DNA synthesis or mitosis) and then releasing the block (4-6). The second main method of producing synchronous cultures is by selection of cells at a particular stage of the cycle from a normal asynchronous culture. which are then grown up as a synchronous culture (7.8).

130

In Chapter 3, I described a CE-LIF method that was successfully developed to quantify hENT1 protein in five cultured human cell lines. The developed protocol employs the use of 5-Sx8f, a fluorescent analogue of NBMPR. NBMPR is a specific inhibitor of hENT1 protein and the quantity of NBMPR binding sites is usually taken as the hENT1 quantity (9,10). Results in Chapter 3 demonstrate the high-affinity binding between the 5-Sx8f and hENT1. The hENT1 quantification results calculated based on the 5-Sx8f binding sites were very compatible to those obtained from flow cytometry studies (See Table 3.6). However, the results are still averages of hENT1 expression level across all four phases.

Previous studies by other researchers have shown that numbers of NBMPR binding sites or nucleoside uptake rates are cell cycle-dependent (11-13). In this chapter, effort was undertaken to further assess the fluctuation in hENT1 abundance during the four phases of the cell replication cycle. Methods of synchronizing cells by means of a thymidine block and mitosis inhibition were adapted to the HeLa human cell line. This enabled us to obtain relatively homogenous cells at all four cycle phases. The developed hENT1-CE-LIF assay was then applied to quantify hENT1 expression and study the variation. A RT-PCR experiment was also done to probe mRNA changes that might happen during the cycle. The HeLa cell line was chosen as the model because it is a commonly used tumor cell line with well-known characteristics concerning cell cycle and maintenance of the culture (14,15).

5.2 Experimental

131

5.2.1 Chemicals and reagents

Thymidine. methyl[5-(2-thienylcarbonyl)-1H-benzimidazole-1-yl] carbamate

(nocodazole). sucrose. trisodium citrate. propidium iodide (PI). spermine

tetrahydrochloride and tris(hydroxymethyl)aminomethane (Tris) were all obtained from

Sigma (St. Louis. MO). BDH (Toronto. ON. Canada) supplied $MgCl_2$. $CaCl_2$ and $ZnCl_2$.

Trypsin. trypsin inhibitor and RNaseA were purchased from Life Technologies

(Gaimersburg. MD).

5.2.2 Standard cell culture

HeLa is a human cervical carcinoma cell line that possesses *es* activities. We obtained

HeLa cells from the American Type Culture Collection. They were grown in Roswell

Park Memorial Institute (RPMI) conditioned media supplemented with 10% fetal calf

serum. Culture was maintained at 37°C in a humidified atmosphere of 5% CO_2 in air and

was free of mycoplasma. Cell concentrations were determined using an Improved

Neubaure Counting Chamber. Cultures were removed from dishes with trypsin-EDTA

(0.05% trypsin. 0.53 mM EDTA•4Na).

5.2.3 Cell characterization

Cells were first treated with thymidine for 24 hours to allow all the cells to progress

through the cell cycle and stop at G_1/S. Then cells were released from the thymidine

block by simply washing off the thymidine-containing media. Once released. the cells

synchronously progress through the cell cycle starting from the S phase. The cells were

sampled periodically every 30 minutes after the thymidine release and analyzed by

fluorescence-activated cell sorting (FACS) and mitotic index (MI) staining (See Section

5.2.5). For synchronization of cells at M phase. nocodazole was added five hours after the

132

release and the cells were incubated for different lengths of time and then also analyzed by FACS and MI staining. For these analyses. we know the exact time points at which to harvest the cells to obtain the highest fraction in the desired phase.

5.2.4 Cell synchronization

The synchronization protocol is shown in Figure 5.1. 1.7×10^6 HeLa cells were plated with approximately 30 mL of media and grown for 24 hours. The next day. 750 µL of 100 mM thymidine was added to reach a concentration of 2.5 mM. After another 24 hours. the thymidine-containing medium was replaced with fresh regular media. Cells at S. G_2 and G_1 phases were obtained by harvesting the cells 1.5. 6.5 and 12 hours after the thymidine release respectively based on the characterization results. M phase cells were obtained by adding 30 µL of 0.5 mg/mL nocodazole to the media 5 hours after the release from thymidine and then incubating for 10 hours and 20 minutes.

5.2.5 Synchronization assessment

5.2.5.1 Fluorescence-activated cell sorting (FACS) analysis

Cells were prepared for FACS using the method of Vindeløv with several modifications (16). The composition and the preparations of all the buffers and solutions used are shown in Table 5.1. For each sample. 1×10^6 cells were scraped and collected by centrifugation at $200 \times g$ for 5 min at room temperature. After removal of the supernatant. cells were resuspended in 100 µL citrate buffer with DMSO and 900 µL of solution A. Then the cells were incubated for 10 min at room temperature during which the tube with all these solutions was inverted gently for five or six times to allow the

133

Asynchronous HeLa cells

Grow in standard media for 24 hours

Add thymidine into the media

Grow in the thymidine-containing media for 24 hours

Change the thymidine-containing media back to standard media

———Grow for 1.5 hours— **S phase cells**

┌———Grow for 5 hours———

Add nocodazole into the media

———Grow for 6.5 hours— **G2 phase cells**

Grow for another 10 hours
and 20 minutes

M phase cells

———Grow for 12 hours— **G1 phase cells**

Figure 5.1 Synchronization methods utilized on HeLa cells.

134

Table 5.1 Buffers and solutions used in FACS analysis and their compositions.

Buffers and Solutions	Composition
Citrate buffer	250 mM sucrose. 40 mM trisodium citrate•2H$_2$O. 0.5% (v/v) DMSO. pH 7.6
Solution A	15 mg trypsin in 500 mL stock solution. pH 7.6
Solution B	250 mg trypsin inhibitor. 50 mg RNaseA. 500 mL stock solution. pH 7.6
Solution C*	208 mg propidium iodide. 580 mg spermine tetrahydrochloride. 500 mL stock solution. pH 7.6
Stock solution	2 g trisodium citrate. 2 mL (0.1% v/v) spermine tetrahydrochloride. 121 mg Tris(hydroxymethyl)aminomethane. 2 L water. pH 7.6

*Solution C should be protected from light.

135

good mix of the contents. Then 750 µL of solution B was added and same incubation and inverting procedures were applied. At last, 750 µL of ice-cold solution C was added and the solution, after mixing, was filtered into a tube wrapped in tinfoil. Samples were then kept at 4°C until analysis.

5.2.5.2 Mitotic index (MI) determination

The composition and preparation of all the buffers and solutions used here are shown in Table 5.2. From each sample 2×10^6 cells were scraped and collected, then pelleted at 200 $\times g$ at room temperature. The pellet was resuspended in 100 µL of the hypotonic buffer and incubated at room temperature for 10 min. Then 10 µL of fixing solution, 1 µL of 0.5 mg/mL propidium iodide (PI) solution and 20 µL of 1 mg/mL RNaseA were added. The mix was placed in a 37°C water bath for 30 min to allow fixing and staining to occur.

Finally an approximately 10 µL aliquot was dropped onto a glass slide. The slide was visualized under a microscope and searched for cells with mitotic figures with condensed nuclear material and a lack of nuclear membrane. The data were represented as the observed percentage of mitotic cells in the total number of cells. Generally between 200 to 300 cells were scored for each sample (17).

5.2.6 hENT1 quantification assay

The buffers and quantification method used in this study are the same as described in Section 3.2.1 and Section 3.2.3. Basically, a fluorescent impermeant inhibitor, 5-Sx8f, was used to recognize and bind to hENT1 protein in the cell membrane. After washing off non-bound and non-specifically bound 5-Sx8f, the 5-Sx8f molecules that bound to hENT1 were released and detected.

136

Table 5.2 Buffers and solutions used in MI analysis and their compositions.

Buffers and Solutions	Composition
Hypotonic buffer	20 mM Tris[hydroxymethyl]aminomethane. 1 mM $MgCl_2$, 1 mM $CaCl_2$, 1 mM $ZnCl_2$, pH 7.5
Fixing solution	3:1 (v/v) methanol : acetic acid
Staining solution	0.5 mg/mL propidium iodide in water
RNaseA	1 mg/mL RNaseA in water

Hypotonic buffer and fixing solution were stored at 4°C until use:

Staining solution and RNaseA solution were stored at -80°C until use:

137

5.2.7 Instrumentation and electrophoretic conditions

The same in-house built CE-LIF instrument described in Chapter 2 was used for our study (18, 19). Each sample was mixed with an injection standard of fluorescein and introduced electrokinetically into the capillary under an electric field about 33.3 V/cm for 10 seconds. A 30 cm long, 50 μm I.D., 150 μm O.D. uncoated fused-silica capillary purchased from J&W Scientific (Folsom. CA) was used for the separation. Electrophoretic buffer was renewed every five to six runs. All experiments were carried out applying a constant voltage of 9 kV. 5-Sx8f was excited with an argon-ion laser (Melles Griot Laser Group. Carlsbad. CA) with a single 488 nm emission line. Fluorescence signal was collected through a 535 nm bandpass filter of 35 nm band width (535DF35, Omega Optical. Brattleboro. VI. USA) and detected by a R1477 photomultiplier tube (PMT). Data were analyzed using Igor Pro 2.04 (WaveMetrics. Lake Oswego. OR). In all experiments. the 5-Sx8f signal was divided by the signal of the injection standard to get a normalized signal for further data processing.

5.3 Results and Discussion

5.3.1 Cell generation time and phase duration time determination

In this study. the exponential HeLa cell doubling time was about 24 hours. To obtain the duration of each cell cycle phase. FACS analysis was carried out on the exponentially growing population of HeLa cells. Figure 5.2 shows a typical experimentally determined DNA-histogram of the asynchronous HeLa cells. The percentage of cells in the different phases of the cell cycle has been determined by computer fitting. Evaluation of data reveals 43% of cells in G_1. 30% of cells in S and 27% in G_2/M. Using these results

138
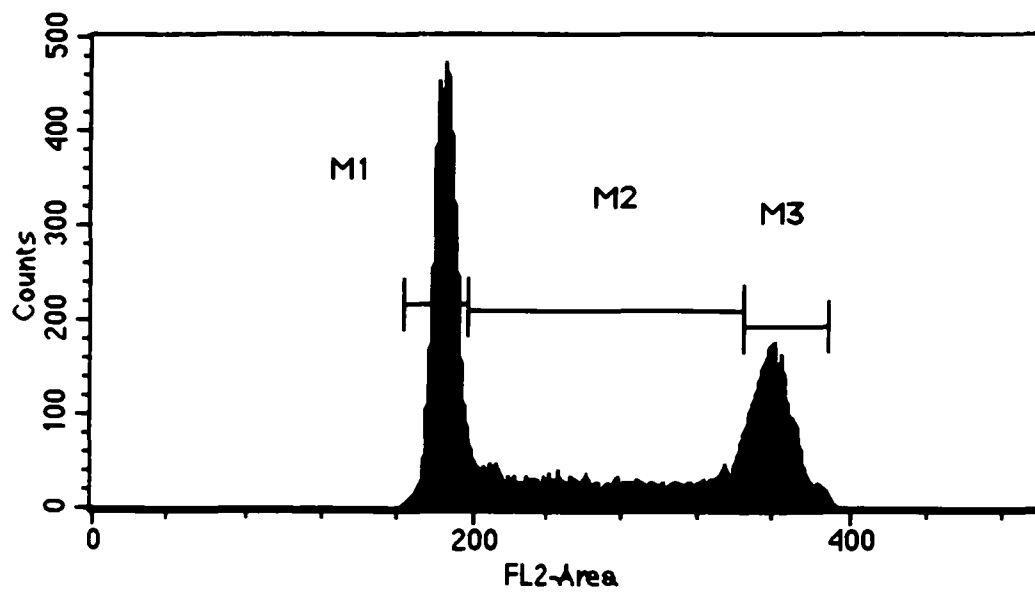
Figure 5.2 A typical DNA histogram of exponentially growing nonsynchronized HeLa cells. The gated M1 area represents the population in G_1 phase. while M2 and M3 represent populations in S and G_2/M respectively.

139

and the observed generation time. phase durations are calculated to be 10.3 hours for G_1. 7.2 hours for S and 6.5 hours for G_2/M. Numbers obtained here are consistent with literature reports (15, 20, 21).

5.3.2 Cell cycle characterization

In order to find the precise times at which cells could be sampled with the maximum numbers at each phase. cells were characterized under the synchronization conditions and evaluated by determination of cell concentration and synchronization efficiencies.

Excess thymidine is commonly used to induce synchronous growth (22). By washing off the thymidine. the process can be fully reversed and cells begin to progress through the cell cycle and replicate. As shown in Figure 5.3. no cell loss happened after the block and cell concentration increased along with the increase in the time after release. This treatment apparently does not harm cellular physiology.

In order to obtain cells at each phase with the highest synchrony. distributions of cells throughout the first cycle after the release from the thymidine block were monitored by FACS and MI. The changes in percentages of cells at G_1. S and G_2 phases with the time after release are shown in Figure 5.4. Based on these plots. 1.5-hour. 6.5-hour and 12-hour released times were chosen to synchronize HeLa cells at S. G_2 and G_1 phases in this study. As for M-phase synchronization characterization. similar monitoring was done except nocodazole was added to the medium 5 hours after the release from the thymidine block. A further 10 hour 20 minute incubation with nocodazole resulted in the highest percentage of M-phase cells (shown in Figure 5.5).

140
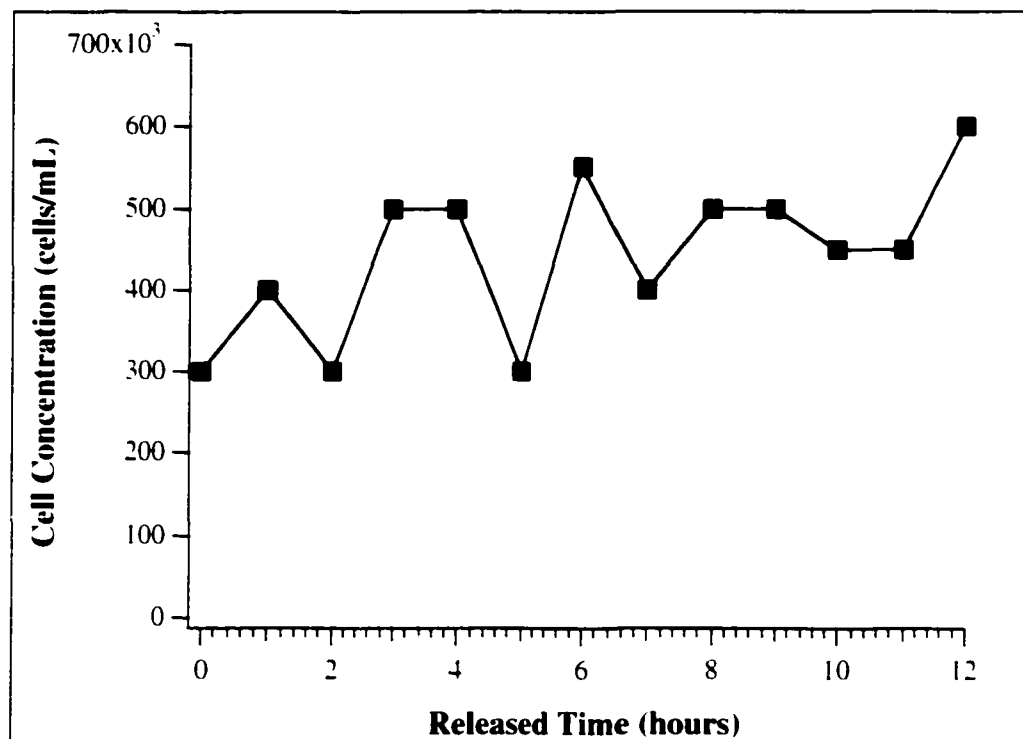
Figure 5.3 Cell concentration monitoring after thymidine block. The x-axis is the time

after thymidine release. the y-axis shows the cell concentration at that specific time point.

141
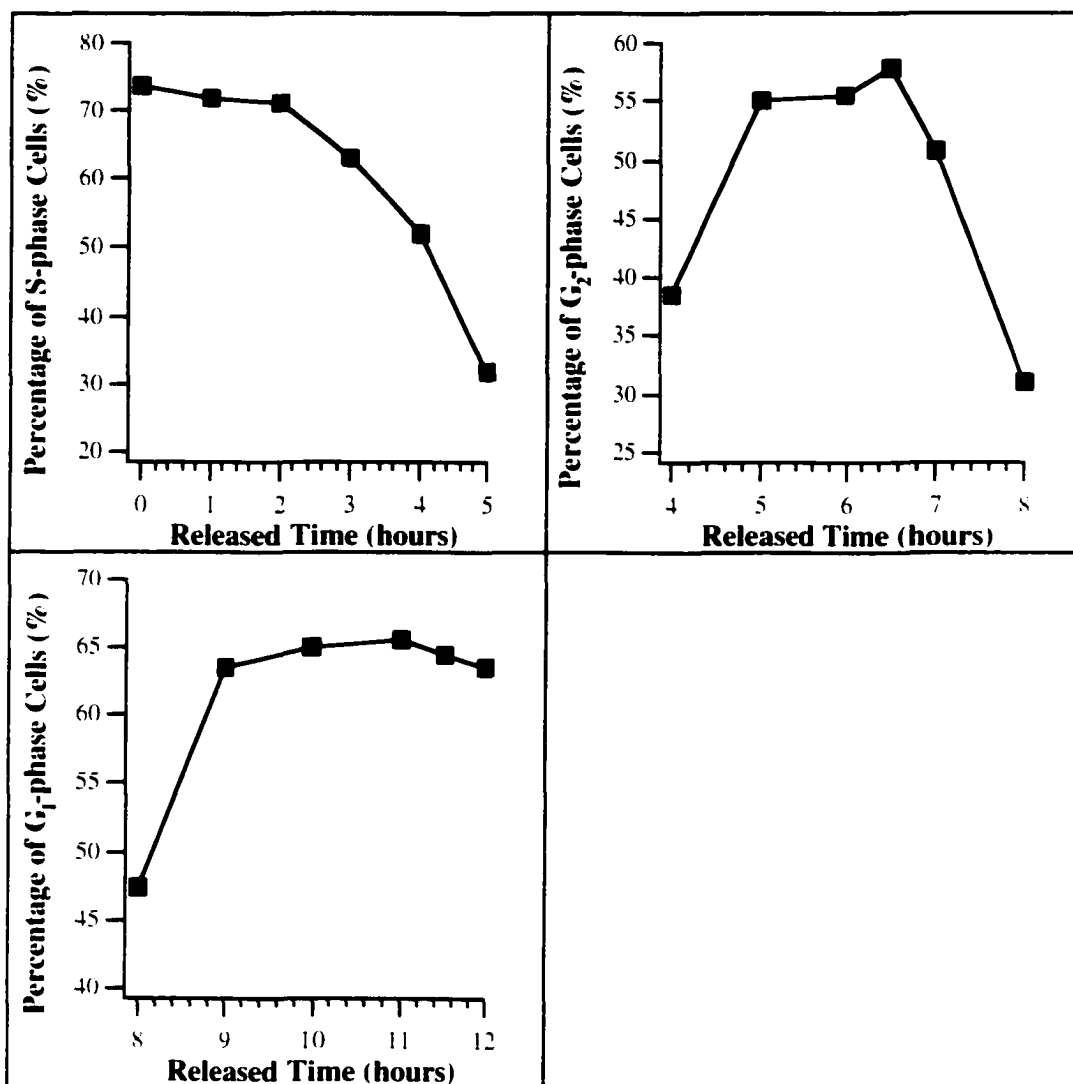
Figure 5.4 Characterization of synchronization efficiency to S, G_1 and G_2 phases against time after release from thymidine block. The percentages were calculated based on the FACS analysis for S and G_1 phases. For G_2 phase, the MI readings were combined with the FACS results to assess the synchrony.

142
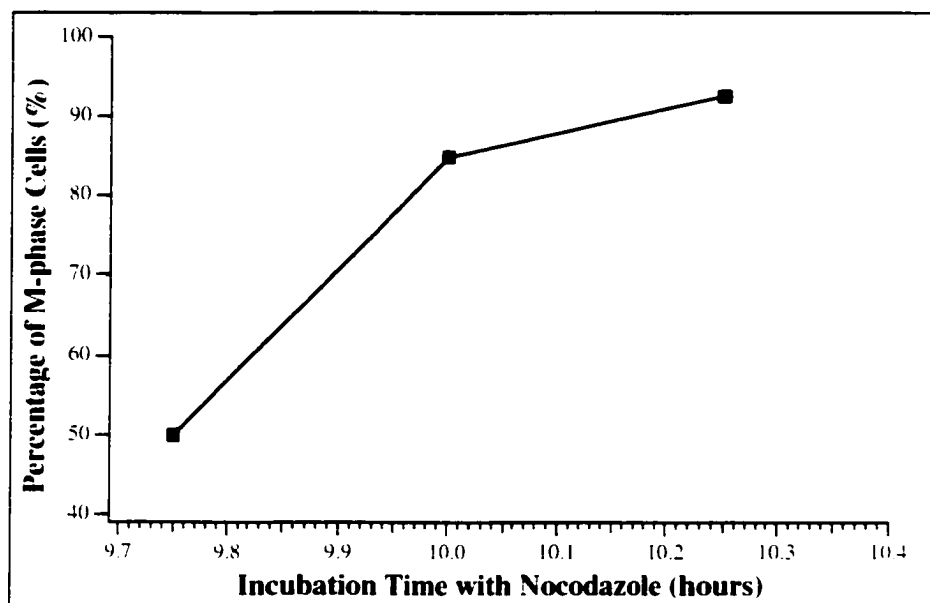
Figure 5.5 Characterization of synchronization efficiency to M phase. The cells were first blocked with thymidine. Five hours after release. nocodazole was added and incubated for different lengths of time before harvesting. MI readings were combined with FACS results to assess the synchrony.

143

5.3.3 HeLa cell synchronization and synchrony assessment

Synchronization of cells at the G_1/S phase border is generally achieved by inhibition of

DNA synthesis using chemical inhibitors, including aphidicolin, hydroxyurea, or excess

thymidine (23-25). We synchronized cells in 2.5 mM thymidine for 24 h. This

concentration of thymidine inhibits the enzyme ribonucleotide reductase, leading to a

dCydTP deficiency that prevents cells from completing DNA replication. Hence, they

become arrested at the G_1/S phase border. Synchronization of cells with excess thymidine

was the first reliable method to be widely used (26). This method enables very good

synchrony in S, G2 and G1 phases, demonstrated by the flow cytometric measurements

of DNA distribution shown in Figure 5.6 A, B and C.

Treatment of cells with the anti-microtubule drug nocodazole was employed to

accumulate cells in metaphase (Figure 5.6D). This compound works because nocodazole

chemically interferes with the formation of microtubules in cells and microtubule

formation is an important structural feature of cells as they enter mitosis.

Synchronization efficiencies could were assessed using FACS based on DNA content and

MI which is used to monitor the progression of cell through M phase, when chromatin

condensation occurs. The general synchronization results are shown in Table 5.3.

Chemicals that inhibit cell cycle progression are advantageous for synchronization

because they are effective in a large variety of cell types, require no special equipment,

and lend themselves to applications that require large numbers of cells.
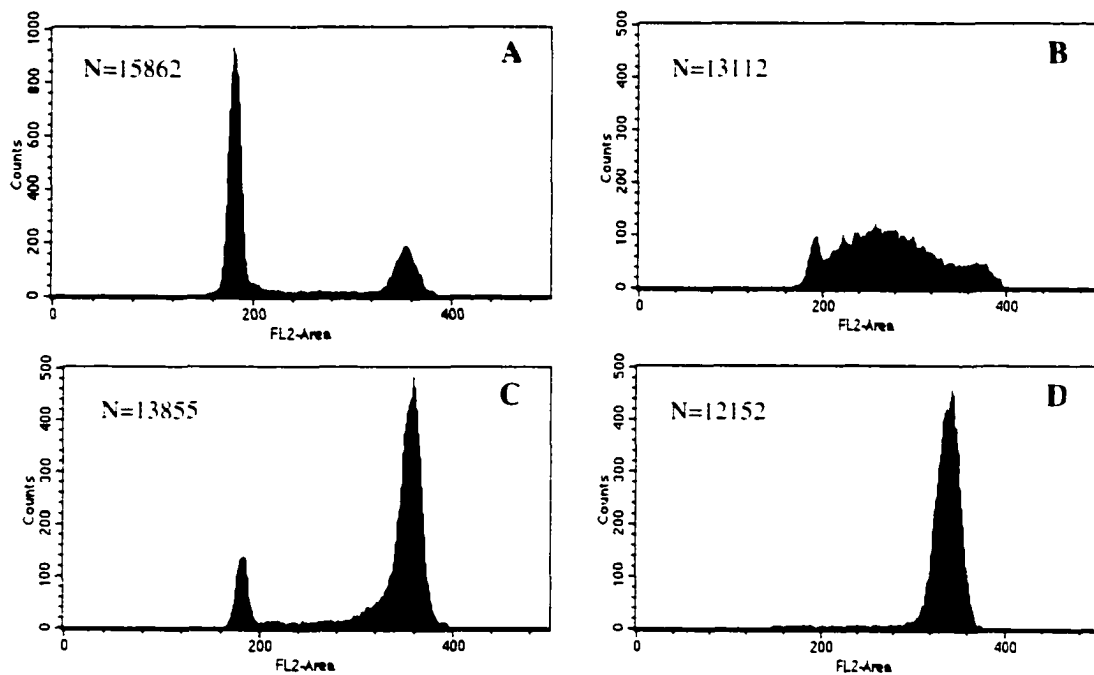
Figure 5.6 Flow cytometric analysis of HeLa cells in synchronized phases. N stands for

how many cells were scanned for the histogram.

(A) G₁-phase cells. 12 hours after release from thymidine blockage:

(B) S-phase cells. 1.5 hours after release from thymidine blockage:

(C) G₂-phase cells. 6.5 hours after release from thymidine blockage:

(D) M-phase cells. Incubated with nocodazole for 10 hour 20 minutes. beginning five

hours after release from thymidine blockage.

145

Table 5.3 Percentage of HeLa cells in desired phases in synchronized samples.

Phase Sample	Approximate Percentage
G_1	65%
S	80%
G_2	55%
M	90%

146

5.3.4 hENT1 quantification on asynchronous and synchronous HeLa cells

Once synchronized cells were obtained, the hENT1-CE-LIF quantification assay discussed previously (Chapter 3) was applied to obtain the hENT1 expression levels at each cell-cycle phase. As clearly shown in Figure 5.7, hENT1 protein amount changes through the cell cycle. When the cells are dividing or doing DNA synthesis, i.e. during M and S phases, more hENT1 protein is expressed. On the other hand, during the G_1 and G_2 phases, less hENT1 was expressed. Proliferating leukemic blast cells have been reported to have a higher density of H^3-NBMPR binding sites than their mature non-proliferating end-cells of differentiation (27, 28). Also a close correlation has been shown between proliferation rate and the number of nucleoside transporters in lymphomas and myeloid leukemias (29). There are also literature reporting that nucleoside transport is not correlated with S-phase expression in certain cell types (30). The results obtained here are in agreement with a hypothesis that proliferation rate and hENT1 are correlated.

The same experiment was repeated three times for cells at each of the phases (See Table 5.4). It was noticed that the quantification results here were higher than those obtained in Chapter 3. The author is not sure why this has happened. However, the hENT1 amounts on S and G_1 phase cells are extremely close to reference paper (11), which reported 9.0×10^5 and 4.5×10^5 NBMPR binding sites on S and G_1 cells respectively.

RT-PCR analysis was also carried out on the synchronous HeLa cells to quantify mRNA for hENT1. However, no difference could be detected. This may suggest that the hENT1 protein expression is not regulated at the mRNA level.

147
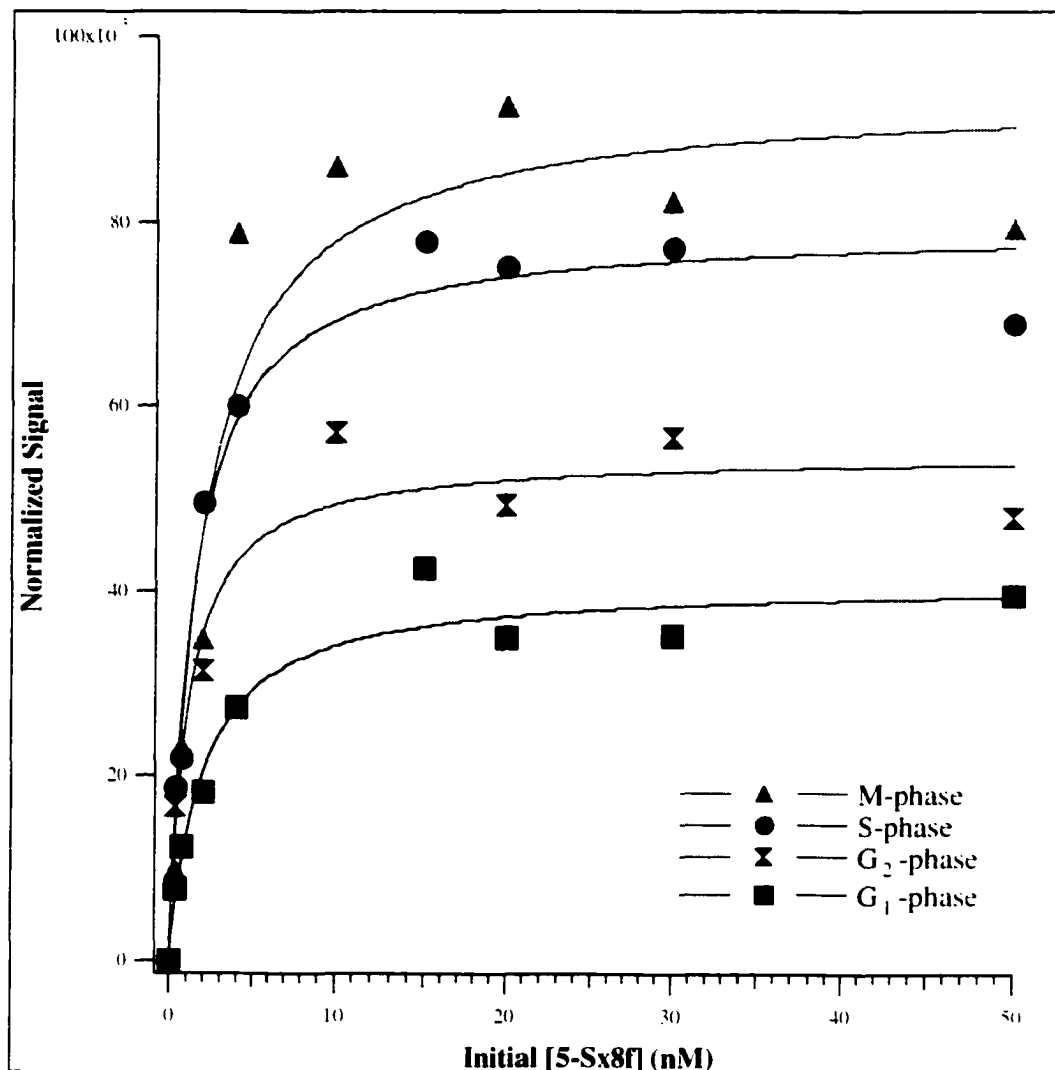
Figure 5.7 Equilibrium binding analysis of 5-Sx8f as a surrogate marker for the presence

of the hENT1 protein on cells at different phases. All the data points have been

normalized to the signal of 1×10^5 cells.

148

Table 5.4 Quantification results on the four phases of HeLa cells studied.

Experiment	hENT1 Abundance at Specific Phases $(\times 10^5/\text{cell})$			
	G_1	S	G_2	M
1	3.7	7.5	5.6	8.0
2	3.4	7.6	4.7	9.5
3	4.9	9.4	6.9	9.1
Average	4.0	8.2	5.7	8.9

The nonsynchronized HeLa cells gave a number of 6.4×10^5 hENT1 sites/cell.

149

Chemical treatment has been linked to the possible disruption of normal cell cycle regulatory processes and unbalanced cell growth induces an apoptotic phenotype in some cell types. However, as shown in Section 5.3.2, our cells continued progressing through the rest of the cell cycle normally after released from the thymidine blockage. In addition, it has been reported that hENT1 expression did not change with the addition of thymidine using a procedure to stain cells simultaneously for hENT1 protein and DNA (31). It is not known whether nocodazole might affect the expression of hENT1.

5.4 Conclusion

This is the first successful application of CE-LIF (See Chapter 3) to probe the hENT1 protein abundance differences on the plasma membranes of cells of different cell-cycle phases. The study further confirms the reliability of the developed hENT1-CE-LIF assay (See Chapter 3). Different expression levels of hENT1 at different phases suggest its expression is correlated with the cell proliferation rate.

The use of conventional cell synchronization techniques was essential in obtaining cells at specific phases. They enabled the study of cell cycle-regulated biological events, which are usually hidden with standard cell culture. However, the protocols for synchronizing cells are very tedious and time-consuming. The synchronized cells are only relatively more homogenous than nonsynchronized cell population. Extremely high synchrony is very hard to achieve. Chemical treatment has also been linked to the possible disruption of normal cell cycle regulatory processes in some cases (32, 33). Therefore, single cell methods would be more desirable. Our lab has developed a method of correlating cell cycle with oligosaccharide metabolic activity in single cells (34). Each single cell, before

150

entering a capillary for further study, was stained with a fluorescent dye, Hoechst 33342, to allow measurement of its the DNA content and to determine the specific phase this cell is in. This technique is much faster than conventional cell synchronization techniques. And since the analysis is based on single cells, the results are truly representative of that specific phase.

5.5 References

1.   Howard, A.: Pelc, S. R.. *Heridity* **1953**, 6, 261-273.

2.   Unit 8.1 of *Current Protocols in Cell Biology* John Wiley & Sons, Inc. **1998**.

3.   Mitchison, J. M. *The Biology of the Cell Cycle* CambridGuoe University Press. Chapter 2 **1971**.

4.   Campisi, J.: Morreo, G.: Pardee, A. B. *Expt. Cell Res.* **1997**, 152, 459-462.

5.   Bonapace, I. M.: Addeo, R.: Altuui, L.: Cicatielles, L.: Bifullo, M.: Laezza, C.: Salzano, S.: Sica, V.: Bresciani, F.: Weisz, A. *Oncogene* **1996**, 12, 753-763.

6.   Lalande, M. *Exp. Cell Res.* **1990**, 186, 332-339.

7.   Peterson, E. O.: Bakke, O.: Lindmo, T.: Oftebro, R. *Cell Tissue Kinet.* **1977**, 10, 511-522.

8.   Rice, G. C.: Dean, P. N.: Gray, J. W.: Dewey, W. C. *Cytometry* **1984**, 5, 289-298.

9.   Young, J. D.: Jarvis, S. M. *Biosci. Rep.* **1983**, 3, 309-322.

10.   Cass, C. E.: Belt, J. A.: Paterson, A. R. P. *Prog. Clin. Biol. Res.* **1987**, 230, 13-40

11.   Cass, C. E.: DAhlig, E.: Lau, E. Y.: Paterson, A. R. P. *Cancer Res.* **1979**, 39, 1245-1252.

12.   Stambrook, P. J.: Sisken, J. E. *J. Cell Biol.* **1972**, 52, 514-525.

151

13. Plagemann. P. G. W.: Richey. D. P.. Zylka. J. M.: Erbe. J. *Exp. Cell Res.* **1974**. 83. 303-310.

14. Johnson. R. T.: Downes. C. S.: Meyn. R. E. *in The Cell Cycle: A Practical Approach*. Oxford University Press. **1994**. 1-24.

15. Rao. P. N.: Johnson. R. T. *Nature* **1970**. 225. 159-164.

16. Vindeløv. L. L.: Christensen. I. J.: Nissen. N. I. *Cytometry* **1983**. 3. 323-327.

17. Unit 8.3 in *Current Protocols in Cell Biology*. John Wiley & Sons. Inc. **1998**.

18. Swerdlow. H. P.: Wu. S. L.: Harke. H. R.: Dovichi. N. J. *J. Chromatogr.* **1990**. 516. 61-67.

19. Tan. W. G.: Tyrrell. D. L. J.: Dovichi. N. J. *J. Chromatogr. A* **1999**. 853. 309-319.

20. Cao. G.: Liu. L. M.: Cleary. S. F. *Exp. Cell Res.* **1991**. 193. 405-410.

21. Knehr. M.: Poppe. M.: Enulescu. M.: Eickelbaum. W.: Schroeter. D.: Paweletz. N. *Exp. Cell Res.* **1995**. 217. 546-553.

22. Xeros. N. *Nature* **1962**. 194. 682-685.

23. Grdina. D. J.: Meistrich. M. L.: Meyn. R. E.: Johnson. T. S.: White. R. A.: *in Techniques in Cell Cycle Analysis*. Humana Press **1987**. 367-402.

24. Sinclair. W. K. *Science* **1965**. 150. 1729-1731.

25. Heintz. N.: Sive. H. L.: Roeder. R. G. *Mol. Cell Biol.* **1983**. 3. 539-550.

26. Bootsman. D.: Budke. L.: Vos. O. *Exp. Cell Res.* **1964**. 33. 301-304.

27. Wiley. J. S.: Jones. S. P.: Sawyer. W. H.: Paterson. A. R. P. *J. Clin. Invest.* **1982**. 69. 479-489.

28. White. J. C.: Rathmell. J. P.: Capizzi. R. L. *J. Clin. Invest.* **1987**. 79. 380-387.

29. Wiley. J. S.: Snooke. M. B.: Jamieson. G. P. *Br. J. Haematol.* **1989**. 71. 203-

30. Powell. B. L.: White. J. C.: Gregory. B. W.: Brockschmidt. R. C. A.: Lyerly. E. S.: Choriey. H. M.: Capizzi. R. L. *Leukemia* **1991**. 5. 598-601.

152

31.   Pressacco. J.: Wiley. J. S.: Jamieson. G. P.: Erlichman C.: Hedley. D. W. *Br. J. Cancer* **1995**. 72. 939-942

32.   Gong. J.: Traganos. F.: DArzynkiewicz. Z. *Cell Growth Differ.* **1995**. 6. 1485-1493.

33.   Urbani. L.: Sherwood. S. W.: Schimke. R. T. *Exp. Cell Res* **1995**. 219. 159-168.

34.   Krylov. S. N.: Zhang. Z.: Chan. N. W. C.: Arriaga. E.: Palcic. M. M.: Dovichi. N. J. *Cytometry* **1999**. 37. 15-20.

CHAPTER 6

Study of Cell Cycle Phase Dependent Biological Events Using Cell Synchronization Techniques: (II) Probing HeLa Cell Protein Expression Differences during the Cell Cycle

154

6.1 Introduction

The genome revolution has changed the paradigm for the comprehensive analysis of biological processes and systems. It is hypothesized that biological processes and systems can be described based on the comparison of global quantitative gene expression patterns from cells or tissues representing different states. However, there are many possibilities regarding the fate of an organism's DNA that can not be predicted by simply knowing the genetic code. For example, genes may be present, but mutated or not transcribed, some genes may be transcribed into mRNA but not translated into protein, the mRNA expression may not be correlated with protein expression, or post-translational modifications may occur to proteins (1, 2). As a result, direct measurement of protein expression is essential for biological processes and systems. There has been an increasing interest in undertaking a protein-based effort aimed at identifying the protein constituents of cells and determining their patterns of expression and post-translational modifications (3-5). Global analysis of gene expression at the protein level is termed proteomics (6).

The field of proteomics represents a huge undertaking for scientists. The standard method for proteomic analysis involves protein extraction from cells, protein separation by sodium dodecylsulfate polyacrylamide gel electrophoresis (SDS-PAGE) or 2-D gel electrophoresis, in-gel enzymatic digestion, and mass spectrometry (MS) or tandem MS identification of proteins of interest. This approach has been applied successfully to many areas of proteomics, but unfortunately it also has shortcomings. For example, many biologically important proteins are only expressed or post-translationally modified at certain phases during the cell cycle, or the expression or modification levels are regulated in a cell cycle-dependent manner (7-10). Therefore, protein expression based on

155

asynchronous cell populations does not reveal accurate quantitative information. Also, several drawbacks are inherent to slab gel electrophoresis. Firstly, large amounts of proteins must be loaded onto the gels for separation and detection, which requires large numbers of cell. Secondly, only highly abundant proteins are seen on gels even with sensitive silver staining techniques. Furthermore, processes for slab gel electrophoresis, especially 2-D gel electrophoresis, are very tedious, manually intensive, and time-consuming. These are all obstacles for detecting and quantifying low-abundance proteins in a complex sample. (5). Hence, it would be useful to develop techniques that allow for the tracking of changes in protein expression during the cell cycle and the analysis of proteins with better sensitivity.

In this chapter, protein expression changes during the cell cycle process have been followed by SDS-PAGE and 2-D gel electrophoresis. A synchronization step before the protein extraction and separation has allowed more detailed information on the protein expression at the level of specific cell cycle phase. In addition, high-speed separation of SDS-protein with capillary gel electrophoresis (CGE) was developed to separate the proteins by size and is based on the utilization of a replaceable polyethylene oxide (PEO) solution (11-13). This SDS-CGE-LIF assay was also applied to profile protein expression during the cell cycle. With a much better sensitivity than slab gel electrophoresis, this assay was able to detect low-abundance proteins and thus offers additional and useful information to SDS-PAGE and 2-D gel electrophoresis. Although this chapter's study is at a very preliminary stage, it may one day contribute to proteomic studies.

156

6.2 Experimental

6.2.1 Reagents and chemicals

β-Mercaptoethanol. bromophenol blue. iodoacetamide and polyethylene oxide (PEO)

(MW=100 000) were obtained from Aldrich (Milwaukee. WI). Bio-Rad (Hercules. CA)

supplied the ammonium persulfate (APS). N,N,N',N'-tetramethylethylenediamine

(TEMED). 10X TGS buffer. γ-methacryloxy-propyltrimethoxysilane (MAPS) and the

Silver Stain Plus Kit. Dithiothreitol (DTT) was purchased from ICN Biomedicals

(Aurora. OH). The Microcon YM-10 centrifugal device filters were obtained from

Millipore (Bedford. MA). From Pharmacia (Quebec. Canada) the following was

obtained: 2% (w/v) methylene bisacrylamide. 40% (w/v) acrylamide. immobilized pH

gradient (IPG) buffer. Immobiline™ DryStrip. pH 3-10. 7 cm strips and the Low

Molecular Weight Calibration Kit. Tris(hydroxymethyl) aminomethane (Tris). 2-

(cyclohexylamino)-ethanesulphonic acid (CHES). t-octylphenoxypolyethoxyethanol

(Triton X-100). mineral oil and standard proteins for capillary gel electrophoresis

including β-lactoglobulin. trypsin inhibitor. carbonic anhydrase. ovalbumin. bovine

serum albumin. conalbumin and β-galactosidase were purchased from Sigma (St. Louis.

MO). SDS was purchased from BDH (Toronto. ON. Canada). 3-(2-furoyl)quinoline-2-

carboxaldehyde (FQ) and potassium cyanide (KCN) were obtained from Molecular

Probes (Eugene. OR). The Coomassie® Protein Plus Assay and bovine gamma globulin

were from Pierce (Rockford. IL).

157

6.2.2 Cell culture and cell synchronization

See Sections 5.2.1 and 5.2.2.

6.2.3 Cell extract preparation and protein quantification

The water-soluble proteins from synchronous and asynchronous HeLa cells were extracted by means of sonication (14). After washing three times with phosphate-buffered saline (PBS), 10^8 cells were resuspended in approximately 100 μL of distilled deionized water. The suspension was sonicated for 30 minutes at 4°C. After spinning the sonicated product at 9,000 g for 10 minutes, the supernatants were removed and protein content was quantified utilizing the Coomassie® Plus Protein Assay kit. Serial dilutions of bovine gamma globulin at concentrations of 30 μg/mL, 25 μg/mL, 20 μg/mL, 15 μg/mL, and 10 μg/mL along with a blank solution containing 0.5 M NaCl were used to construct the calibration curve for protein quantification. Soluble cell extracts from different cell phase samples were diluted in 0.5 M NaCl (dilutions were based on the extract concentrations, usually 1/100, 1/200, 1/300 and 1/500). Then 150 μL of each sample was pipetted into the well of a 96-well microtiter plate (Costar, Acton, MA). The sample, blank and the calibration standards were then mixed with 150 μL of Coomassie® Plus Protein Assay. Absorbance at 590 nm was measured in a Thermomax microplate reader (Molecular Devices, Sunnyvale, CA). Extracts were stored with proper concentrations (2 μg/μL for SDS-PAGE analysis and 5 μg/μL for 2-D gel electrophoresis) at –80 °C until used. All tubes used were siliconized (Fisher, Fair Lawn, NJ) to minimize protein loss.

158

6.2.4 SDS-PAGE sample preparation

Twelve μg of each sample was loaded into individual lane of the mini-gels. The samples were diluted 1:1 with SDS reducing buffer (composition: 0.0625 M TrisHCl. pH 6.8. 2.3% (w/v) SDS. 5% (v/v) β-mercaptoethanol. 10% (w/v) glycerol. 0.00125% (w/v) bromophenol blue). Standards employed were 1 μL of the Low Molecular Weight Calibration Kit diluted in 9 μL of SDS reducing buffer. The samples and standards were denatured at 95°C for at least 5 minutes, pulsed in the centrifuge to spin down condensation, and then loaded onto the gels.

6.2.5 SDS-PAGE

The Bio-Rad Mini-PROTEAN and the Gibco BRL Vertical Gel Electrophoresis systems were used for SDS-PAGE separations. Mini-gels (1 mm × 7cm × 10 cm) consisted of a 12% polyacrylamide (12% T. 2.7% C) separating gel and a 4% polyacrylamide (4% T. 2.7% C) stacking gel for separating proteins with molecular weights ranging from approximately 15 kDa to 100 kDa. The electrophoresis buffer consisted of 25 mM Tris. 192 mM glycine. and 0.1% (w/v) SDS. pH 8.3. Samples were run at 200 V for 45-50 minutes. The gels were visualized using the Bio-Rad Silver Stain Plus Kit.

6.2.6 Two-dimensional (2-D) electrophoresis sample preparation

For each 2-D gel analysis. 200 μg of protein sample was used. First. the protein sample was diluted with distilled deionized water to a total volume of 100 μL. The protein solution was transferred to the top portion of a Microcon YM-10 centrifugation filter. The device was spun at 12.200 rpm for 5 minutes. The filter was then removed from the device. inverted into a new tube and the retentate spun out of the filter at 3.200 rpm for 3

159

minutes. The liquid was then transferred to a new filter unit and spun for 11 minutes at 12.200 rpm. The filter was again inverted into a new tube and the retentate was spun into the tube for 30 seconds at 3.200 rpm. To the filter. ~90 µL rehydration buffer (8 M urea. 2% (w/v) Triton X-100. 0.5% (v/v) IPG Buffer. 0.28% (w/v) DTT. trace bromophenol blue) was added. vortexed lightly. and spun into the sample tube at 3.200 rpm for 3 minutes. The final sample volume was 125 µL.

6.2.7 2D-gel electrophoresis

The 7 cm Immobiline™ DryStrips (pH 3-10 linear gradient) and corresponding strip holders were utilized for the first dimension of isoelectric focusing (IEF). The sample from Section 6.2.6 was applied evenly to the bottom of the strip holder. The Immobiline™ DryStrip's plastic backing was removed and the strip was applied gel-side towards the sample. taking care not to introduce bubbles into the sample. The strip was then covered with about 400 µL of mineral oil to prevent sample dehydration. and the strip holder cover was placed on top of the strip holder. The strip was then rehydrated overnight (between 12-17 hours) at 20°C on the IPGphor unit (Pharmacia. Quebec.

Canada). The following morning. electrode wicks (in-house-made from filter paper) were added to the strip holder. The small pieces of filter paper were dampened with water and then blotted of excess water on another piece of filter paper. The wicks were then applied over top of each electrode of the strip holder. Caution was used to prevent the introduction of any bubbles into the sample solution. If required. more mineral oil was added to the strip holder to prevent sample dehydration during IEF.

Table 6.1 shows the IEF program utilized for the protein samples. After completion of the IEF dimension. each strip was equilibrated in two different solutions to ensure complete

160

Table 6.1 IEF program utilized for 2-D electrophoresis of HeLa cell extracts.

Note that the current is limited to 50-75 µA per strip. The protocol is also programmed based on the attainment of volthours.

Step	Volts	Volthours	Gradient
1	500	250	step and hold
2	1000	500	step and hold
3	8000	8000	step and hold

denaturation of the proteins before the second dimension. Each strip was placed in a 15 mL Fisher tube which contained 3 mL of DTT-containing equilibration solution (composition: 50 mM TrisHCl. pH 8.8, 6 M urea, 30% (v/v) glycerol, 2% (w/v) SDS, 1% (w/v) DTT, and trace bromophenol blue). The Fisher tube was rocked for 15 minutes. The IEF strip was then removed from the Fisher tube and rinsed gently with deionized distilled water. The IEF strip was then placed in a 15 mL Fisher tube containing 3 mL of iodoacetamide-containing SDS equilibration solution (same composition as the DTT-containing equilibration solution, except it contained 2.5% (w/v) iodoacetamide instead of DTT). The tube was rocked again for 15 minutes. The IEF strip was removed from the Fisher tube, rinsed gently with water, and then placed on top of the SDS-PAGE gel. Molecular weight size standards were loaded onto the gel and electrophoresis was at 200 V. The Bio-Rad Silver Stain Plus Kit was utilized to visualize the gels.

6.2.8 CGE sample preparation

Protein samples were pre-labeled with FQ before CE analysis. Typically, 5 μL of 2 μg/μL protein mixture solution was mixed with 5 μL of 2.0% (w/v) SDS solution and then heated at 90°C for 5 minutes to denature the proteins. The denatured protein solution was derivatized by adding 5 μL of this solution with 5 μL of 2.0 mM KCN in a 500 μL microcentrifuge tube containing 100 nmol of previously dried FQ. The mixture was incubated for 5 minutes at 65°C and then diluted with the running buffer for analysis.

162

6.2.9 Capillary coating

Fused-silica capillaries with 140 µm O.D., 50 µm I.D. and 40 cm in length (Polymicro Technologies, Phoenix, AZ) were used in this work. The capillaries were coated using the method introduced by Hjérten (15). First, the capillary was treated with 0.5 M sodium hydroxide and washed with water for 1 hour. Then after reacting with MAPS at room temperature for 1 hour, the capillary was washed with water and then filled with a 4% acrylamide solution containing 0.1% (w/v) APS and 0.1% (v/v) TEMED. After polymerization for 1 hour, the capillary was rinsed with water to push excess polyacrylamide out of the capillary.

6.2.10 CE-LIF instrument

The CE instrument with a sheath flow cuvette LIF detector was built in-house as described previously (16). The high voltage was provided by a 0-30 kV dCyd power supply (CZE 1000, Spellman, Plainview, NY, USA). The excitation source was an argon ion laser (Model 2211-15SL, Uniphase, San Jose, CA) operated at 12 mW. The 488 nm laser line was focused ~30 µm from the tip of the capillary using a 6.3× objective (Melles Griot, Nepean, ON, Canada). Fluorescence was filtered with a 630DF30 bandpass filter (Omega Optical, Brattleboro, VT), collected with a 60×, 0.7 NA microscope objective (MO 0060LWD, Universe Kokagu, Oyster Bay, NY) and then detected with a photomultiplier tube (R1477, Hamamatsu, Middlesex, NJ). Data sampling was accomplished with a 16-bit data acquisition board (NB-MIO 16XH-18, National Instruments, Austin, TX) connected to a Macintosh computer.

163

6.2.11 Capillary electrophoretic conditions

2% (w/v) PEO sieving buffer was prepared by dissolving polymer in the running buffer of 0.1 M Tris, 0.1 M CHES and 0.1% (w/v) SDS (pH 8.6). Before use, the polymer solution was degassed for 30 minutes by sonication. The sieving polymer solution was pumped through the capillary by helium gas. Protein samples, after 5 seconds injection at (-) 100 V/cm, were separated with (-) 300 V/cm.

6.3 Results and Discussion

SDS-PAGE has been used for more than 30 years as an extremely popular method for size-based separations of proteins (17, 18). Without surprise, the results obtained using this approach (shown in Figure 6.1) demonstrated that protein expressions did change during the HeLa cell cycling process. Qualitative changes, i.e. on-and-off expression of certain protein(s) are difficult to determine because of the limited separation efficiency of SDS-PAGE and the high background introduced by silver staining. However, close investigation revealed many quantitative protein expression level changes. The rectangular highlighted regions of Figure 6.1 indicate areas of observed protein expression changes with cell cycle phases. Specifically examining the rectangular highlighted area starting at 30 kDa, bands A and B show significant expression level variation with cell cycle phase. During G_1 phase, band A is of higher intensity than that of band B. In S phase, the intensity of band A decreases and is similar to that of band B. A's intensity continues decrease in G_2 and when reaching M phase, band A almost disappears in the background. The relative intensities of these two bands in the asynchronous cell lysate appear to be an average of all four phases.
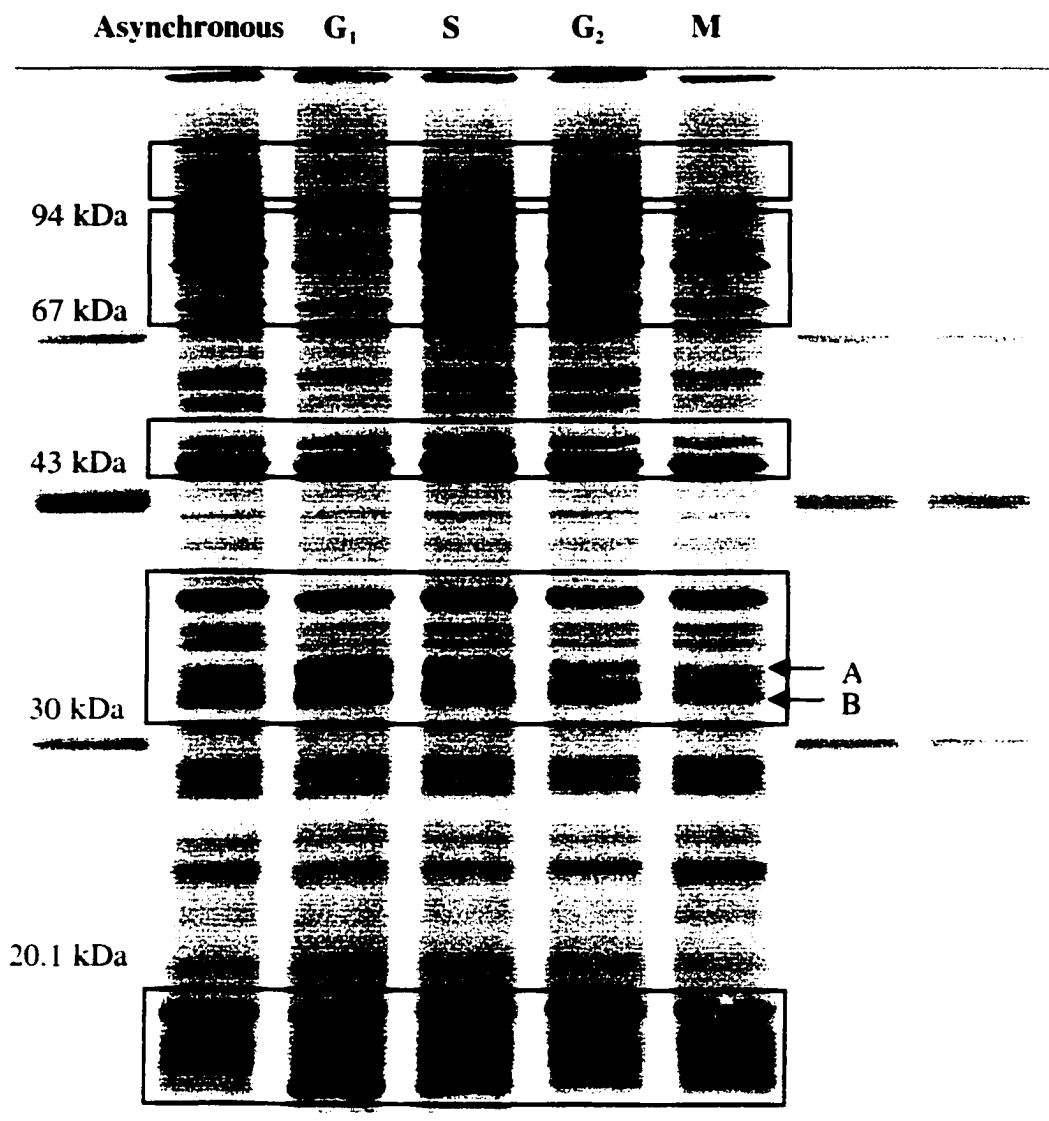
164

Figure 6.1 SDS-PAGE of extracts from asynchronous and synchronized HeLa cells. Water-soluble proteins with molecular weights ranging form 15 kDa to 100 kDa were separated and detected. Many quantitative changes in the protein expressions were observed as shown by the highlighted areas. Separation details: gel: 12% separating gel. 4% stacking gel. sample: 12 μg/lane. electrophoresis voltage: 200 V. stain: silver stain.

In order to probe more detailed differences in expression level, 2-D gel electrophoresis was applied to three of the samples shown in Figure 6.1, extracts from asynchronous, G_1, and M phase HeLa cells (shown in Figures 6.2, 6.3, and 6.4 respectively). As one of the most powerful separation techniques currently available to separate complex protein mixtures (19-21), 2-D gel electrophoresis was able to resolve more proteins of the mixtures and thus reveal more differences between these complex samples. In addition to many up-and-down regulations of proteins, some on-and-off protein expression could also be probed which was not achievable by the use of SDS-PAGE only. The arrow-pointed circle in Figures 6.3 and 6.4 is an example. This protein, with molecular weight ~ 45 kDa and pI ~ 6, is expressed in M phase but not in G_1 phase. This protein may be important in the regulation process for cells to be activated and undergo mitosis. However, if only asynchronous HeLa cell population was extracted for protein profiling and analysis, this protein's specific biological function and expression characteristics would be hidden since the protein would be detected as depicted in Figure 6.2. Although further investigation and confirmation of these changes are not possible with only 2-D gel separation, it is safe to say that the cell synchronization tool is useful and necessary.

Up to this stage, the goal of probing the expression difference from one cell cycle phase to another has been fulfilled successfully with conventional slab-gel electrophoresis techniques. Gel profiles are very reproducible, thanks to the modern SDS-PAGE and IPG technologies (22, 23), thus making it very easy to compare the profiles obtained from different samples and different days. pI and molecular weight information of those proteins of interest with different expression levels could be extracted from the 2-D maps. These information is a great help to more detailed and accurate understanding of certain proteins and cell cycle regulation.
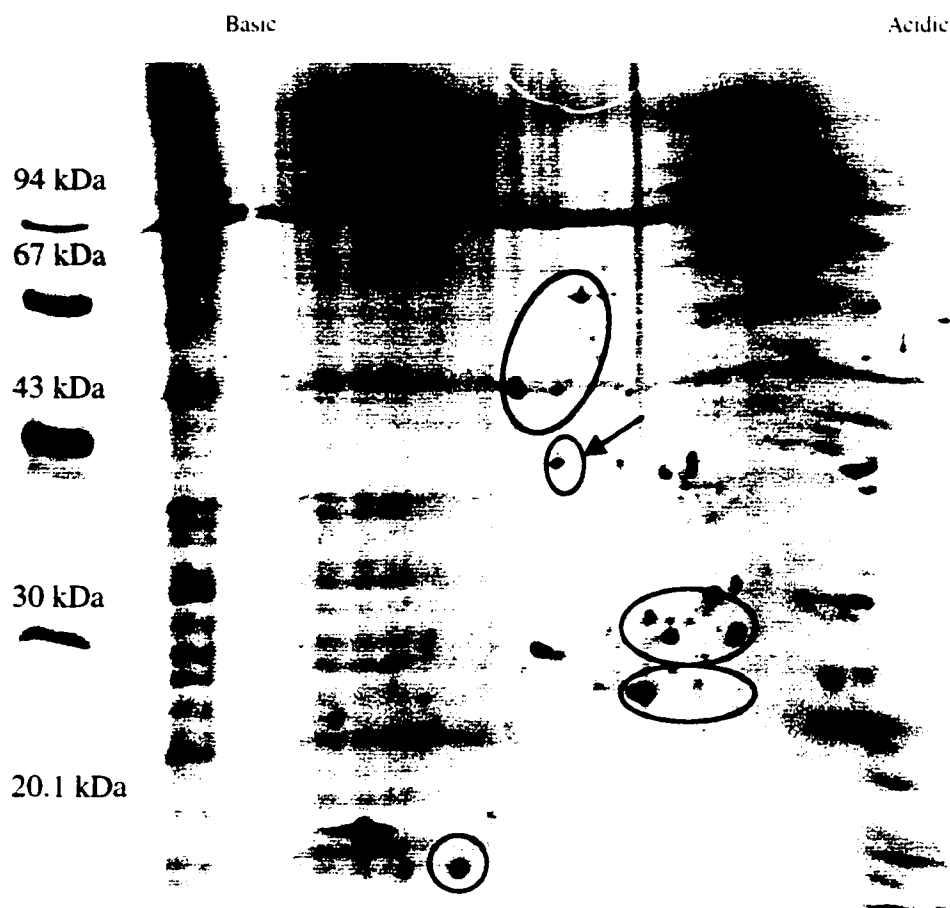
166

Figure 6.2 2-D electrophoresis of asynchronous HeLa water-soluble cell extract. Circled areas show the difference in protein expressions in comparison with Figures 6.3 and 6.4. Separation details: IEF: Immobiline™ DryStrip pH 3-10 linear gradient. 7 cm long. IEF program is shown in Table 6.1. SDS-PAGE: gel: 12% separating gel, 4% stacking gel. electrophoresis voltage: 200 V. stain: silver stain.

94 kDa

67 kDa

43 kDa

30 kDa

Figure 6.3 2-D electrophoresis of G_1-phase HeLa water-soluble cell extract. Circled areas show the difference in protein expressions in comparison with Figures 6.2 and 6.4. Separation details: IEF: Immobiline™ DryStrip pH 3-10 linear gradient. 7 cm long. IEF program is shown in Table 6.1. SDS-PAGE: gel: 12% separating gel. 4% stacking gel. electrophoresis voltage: 200 V. stain: silver stain.
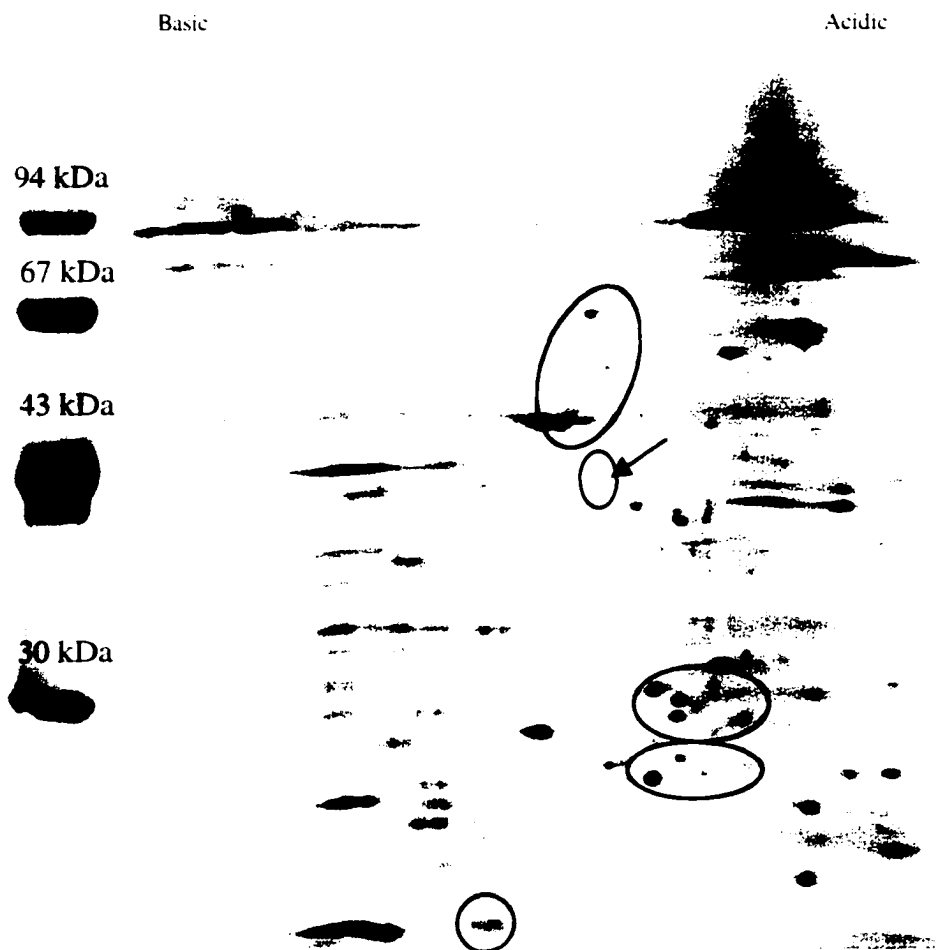
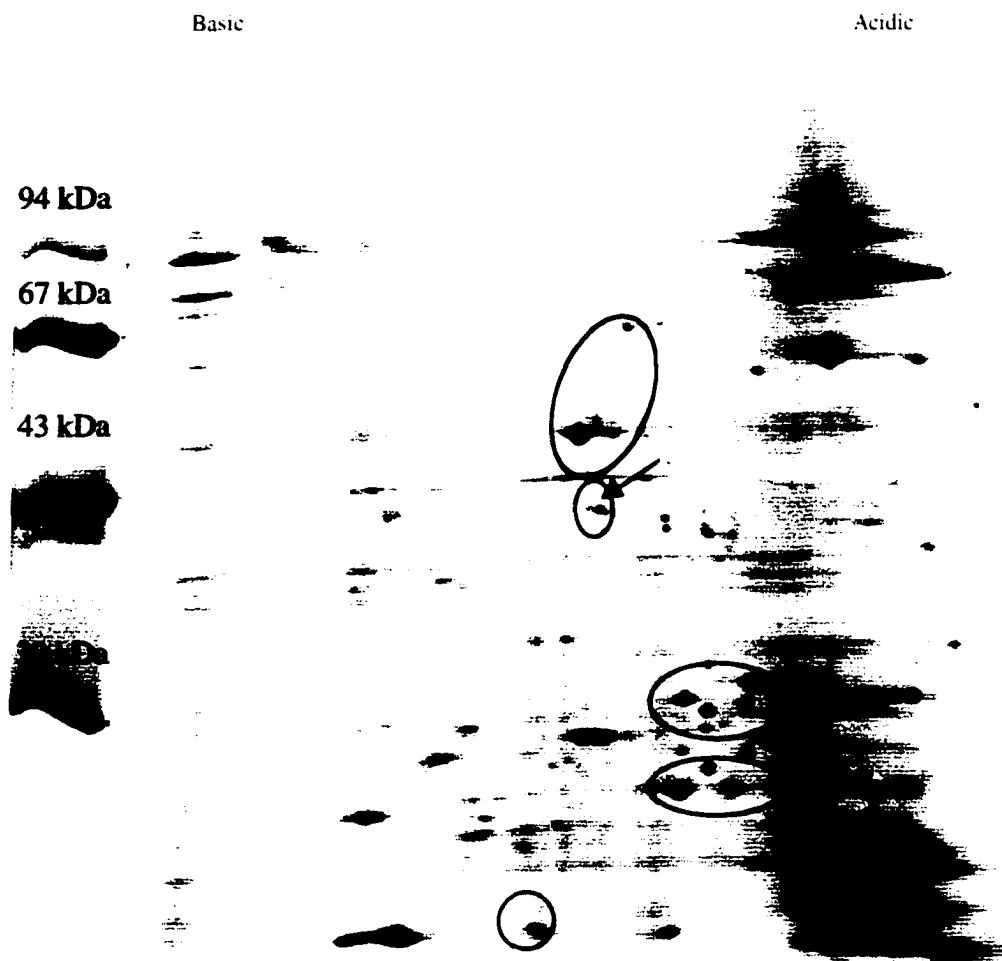Figure 6.4 2-D electrophoresis of M-phase HeLa water-soluble cell extract. Circled areas show the difference in protein expressions in comparison with Figures 6.2 and 6.3. Separation details: IEF: Immobiline™ DryStrip pH 3-10 linear gradient. 7 cm long. IEF program is shown in Table 6.1. SDS-PAGE: gel: 12% separating gel. 4% stacking gel. electrophoresis voltage: 200 V. stain: silver stain.

169

However, as discussed in Section 6.1, there are drawbacks inherent to the slab gel electrophoresis techniques for protein separation and detection: poor sensitivity is the major disadvantage. As for this project specifically, protein samples were extracted from synchronized cell population. Since cell synchronization efficiency will decrease with the increased requirement of cell numbers, the resulting protein mixture concentration will be even lower. Therefore, seeking high sensitivity protein separation and detection techniques are more important in this study. CGE separation and LIF detection of SDS-proteins is a likely solution to this problem.

In this study, poly(ethylene oxide) (PEO) was utilized as a replaceable sieving matrix. Proteins were first labeled with FQ and then separated by CGE and finally detected by LIF. Figure 6.5 shows the PEO-based CGE separation of five standard proteins. FQ is a fluorogenic dye that creates a fluorescent product when reacted with ε-amine groups of lysine residues in proteins. As a result, FQ can be used at a highly excessive concentration without causing a high background signal. This feature enables the labeling of proteins at low concentrations and thus improves the detection sensitivity (16). The limits of detection (LOD) for the five protein standards in this study are in the order of 10^{-10} M for concentration and low attomoles for mass.

With greatly improved sensitivity, SDS-CGE-LIF separations and detection of protein samples extracted from different cell phases gave additional useful information to those obtained with traditional SDS-PAGE or even 2-D analysis. Shown in Figure 6.6, separations carried out in a capillary format are approximately 10 minutes faster than those of SDS-PAGE. In addition, the process of protein pre-labeling with FQ for SDS-CGE-LIF takes much less time than silver staining procedures in SDS-PAGE analysis.
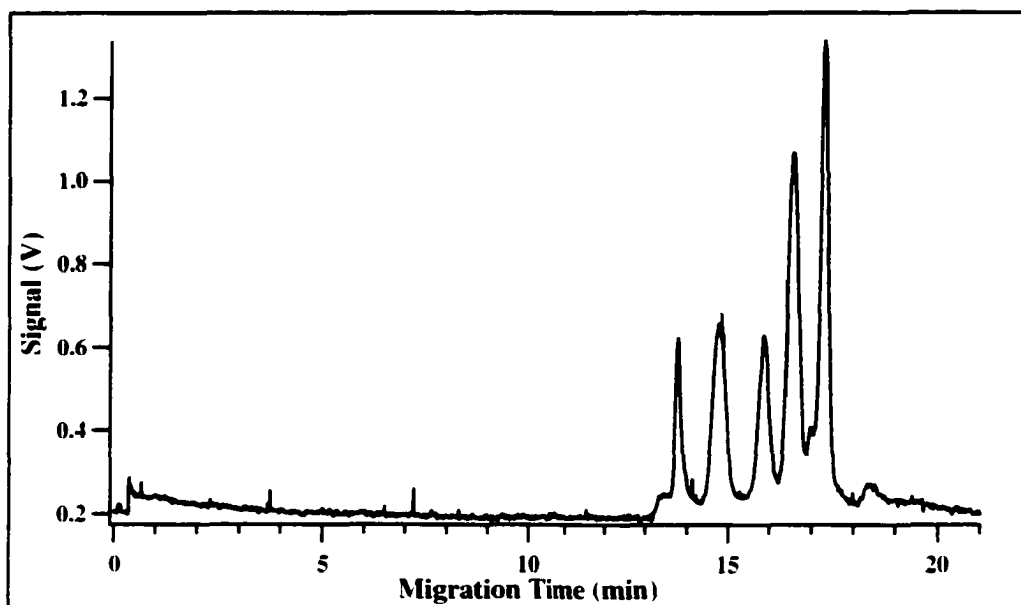
Figure 6.5 PEO-CGE-LIF separation and detection of five standard proteins. The peaks

from left to right are: β-lactoglubin, 18.4 kDa: carbonic anhydrase. 30 kDa: ovalbumin.

43 kDa: bovine serum albumin. 67 kDa: conalbumin. 78 kDa. Each of the standards is 0.2

μM. Experimental conditions: capillary. L = 40 cm. I.D/O.D. = 50/140 μm: injection. (-)

100 V/cm for 5 seconds: separation. (-) 300 V/cm: sieving buffer. 0.1 M Tris-0.1 M

CHES with 2% (w/v) PEO and 0.1% (w/v) SDS.

171

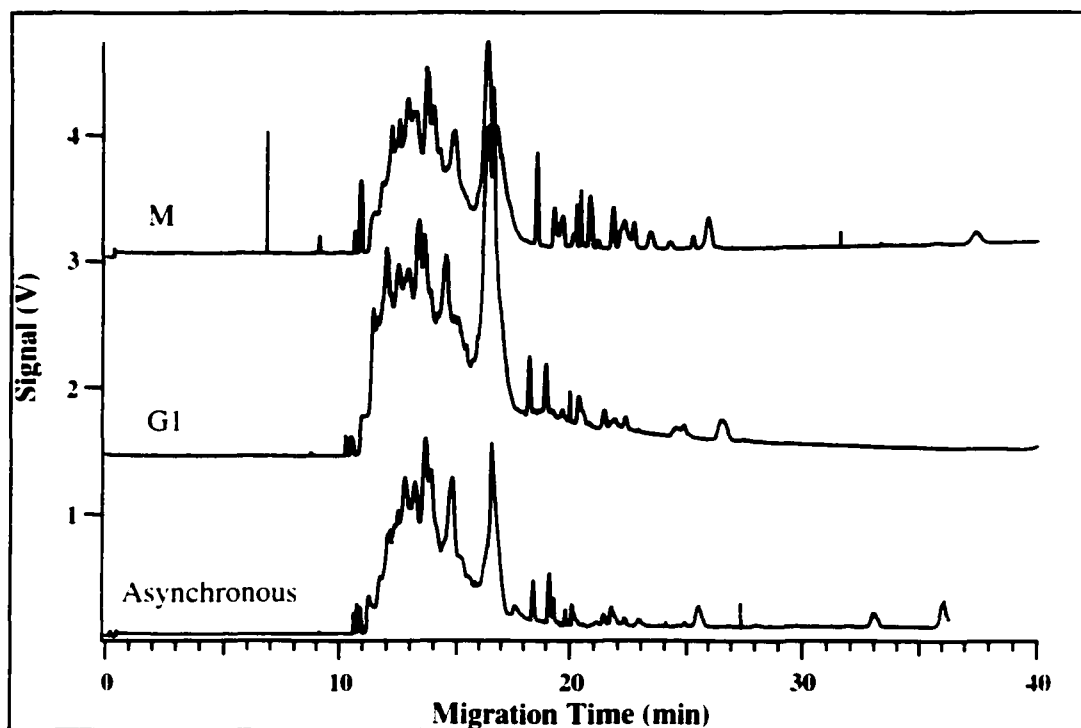Figure 6.6 PEO-CGE-LIF separation and detection of water-soluble proteins extracted from asynchronous. G_1-phase and M-phase HeLa cells. Experimental conditions: capillary. L = 40 cm. I.D/O.D. = 50/140 μm: injection. (-) 100 V/cm for 5 seconds: separation. (-) 300 V/cm: sieving buffer. 0.1 M Tris-0.1 M CHES with 2% (w/v) PEO and 0.1% (w/v) SDS.

172

Depicted in Figure 6.7, many expression changes were observed using this SDS-CGE-LIF technique. for example. the qualitative change shown in Frames 1 and 2. and the quantitative regulation shown in Frames 3-5. More importantly. along with highly expressed proteins (Figure 6.7A). proteins with very low concentrations could also be detected to allow for greater comparison between cell cycle phases (Figure 6.7B).

For further comparison. separation profiles of protein extract from asynchronous HeLa cells with both SDS-PAGE and SDS-CGE-LIF are shown in Figure 6.8. Protein molecular weight ranges for both techniques are similar with the gel concentration used in this study (size range: 15-100 kDa. 12% separation gel for SDS-PAGE and 2% w/v PEO for SDS-CGE). Although sensitive and able to detect low concentration proteins. SDS-CGE did not resolve as many proteins as SDS-PAGE did. Approximately 30 protein peaks were observed in the CGE separation while SDS-PAGE resolved ~100 protein bands. Due to different resolving power and detection methods. separation profiles for the same protein mixture are not similar both qualitatively and quantitatively. For example. bands between 20 kDa to 30 kDa in the SDS-PAGE run were of low intensity while proteins in this size range produced the most intensive signal in SDS-CGE run. This might imply that proteins in this molecular weight range contain more lysine groups. which react with FQ to give fluorescence signals. Alternatively. this observation implies that lower molecular weight proteins denature more completely than higher molecular weight proteins. so more lysine groups are exposed to FQ and thus the labeling potential is much higher. In addition. although separation speed for SDS-CGE seems faster for one single run than that of SDS-PAGE. parallel analysis by SDS-PAGE makes it actually faster to analyze large numbers of samples. At this stage. SDS-PAGE is still superior to SDS-CGE in terms of separation ability. Further developments are required to improve
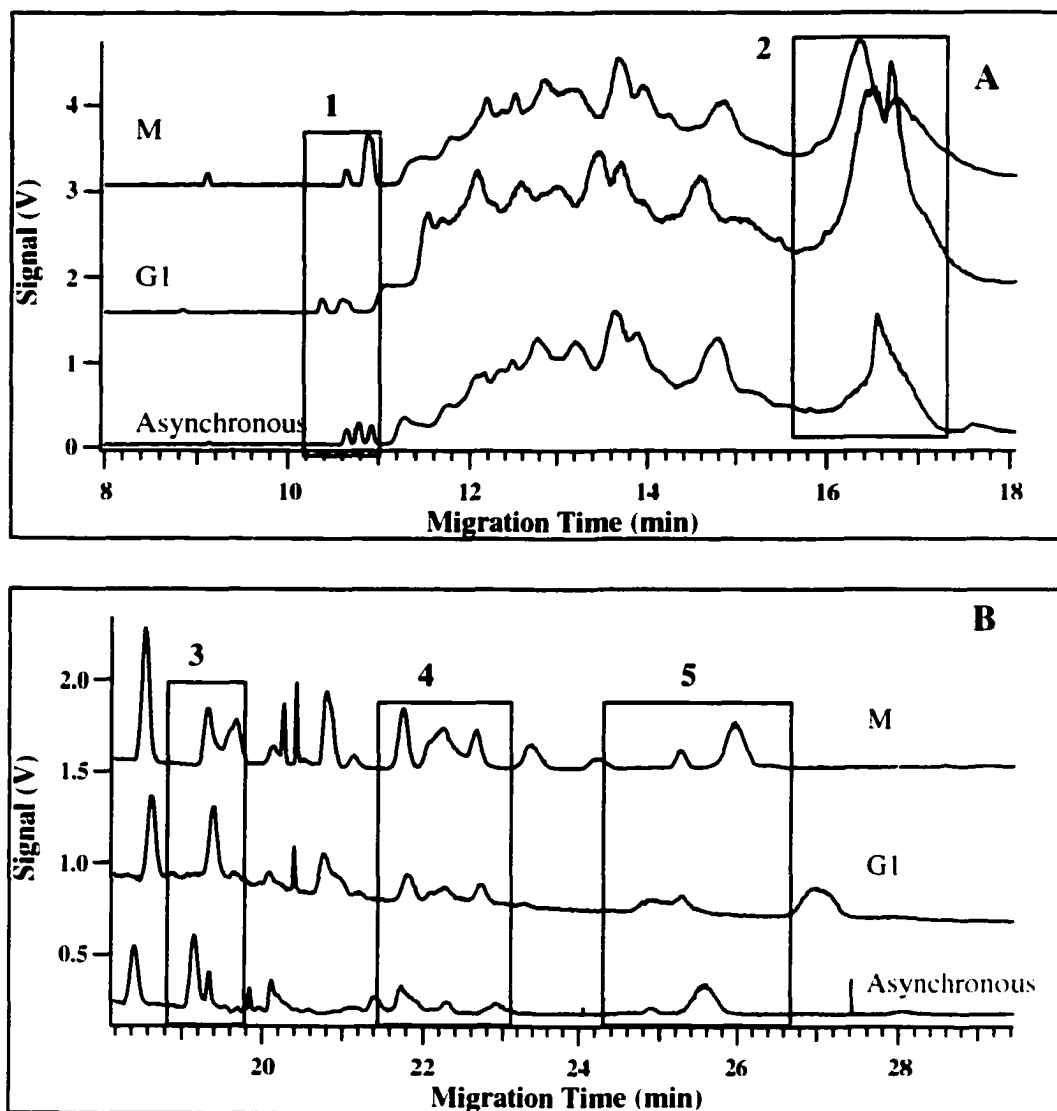
173

Figure 6.7 Expanded electropherograms of Figure 6.6. Areas highlighted by rectangular frames are some of the examples showing the expression differences.

Experimental conditions: capillary. L = 40 cm. I.D/O.D. = 50/140 µm: injection. (-) 100 V/cm for 5 seconds: separation. (-) 300 V/cm: sieving buffer. 0.1 M Tris-0.1 M CHES with 2% (w/v) PEO and 0.1% (w/v) SDS.

174

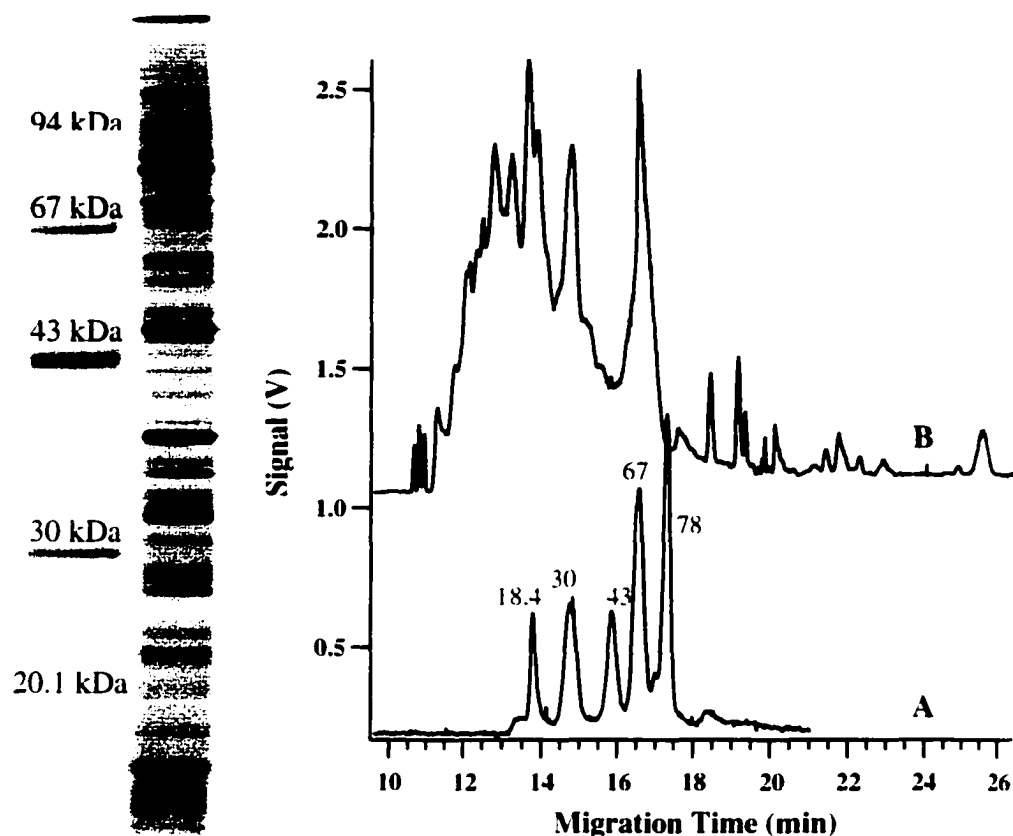Figure 6.8 Comparison of SDS-PAGE gel and SDS-CGE separations of the asynchronous HeLa cell water-solution extracts. The experimental conditions were the same as described in Figures 6.1 and 6.6. Electropherogram A is the separation profile of the five protein standards. Numbers on top of each peak indicate the protein molecular weights in kDa. Electropherogram B shows the protein expression of asynchronous HeLa cell lysate.

175

the separation efficiency of SDS-CGE and to design instrumentation that enables high throughput protein analysis.

6.4 Conclusion

Both slab gel electrophoresis and capillary gel electrophoresis have been successfully applied to synchronized HeLa cells to probe the general protein expression differences during the cell cycling process. Qualitatively, on-and-off protein expressions were observed. Quantitative up-and-down protein regulations were also detected. SDS-PAGE, 2-D gel electrophoresis and SDS-CGE all have different advantages and drawbacks and may be used to solve different problems. Thus results obtained from different methodologies should be considered together to make more accurate and reliable judgements.

In this study, only protein separation techniques were applied. Useful information about the proteins was revealed such as approximate molecular weight and pI, possible modifications, and relative abundance, etc. However, proteins of interest were not identified. Future work should involve the use of MS to identify these proteins.

SDS-CGE separations have many advantages over conventional slab gel techniques and may one day replace them. SDS-CGE-LIF was used successfully in this study and demonstrated to be a useful to understanding the protein expression variations during the cell cycle process. However, SDS-CGE separations of proteins must be improved in terms of resolving power and also throughput.

176

Moreover. as discussed in Chapter 5. cell synchronization is tedious. relative. and protocols are tailored to specific cell lines. Ultimately. protein profiling at a single cell basis would be ideal after staining the cellular DNA content to judge the cell phases (14. 24). Future work should be performed at the single cell level of analysis.

6.5 References

1. Celis. J. E.; Østergaard. M.; Jensen. N. A.; Gromova. I.; Rasmussen. H.; Gromov. P. *FEBS Letters* **1998**. 430. 64-72.

2. Voloulescu. V. E.; Zhang. L.; Vogelstein. B; Kinzler. K. W. *Science* **1995**. 270. 484-487.

3. Hanash. S. M.; Teichroew. D. *Electrophoresis* **1998**. 19. 2004-2009.

4. Arnott. D.; O'Connell. K. L.; King. K. L.; Stults. J. T. *Anal. Biochem.* **1998**. 258. 1-18.

5. Gygi. S. P.; Corthals. G. L.; Zhang. Y.; Rochon. Y.; Aebersold. R. *PNAS* **2000**. 97(17). 9390-9395.

6. Wilkins. J. *Biotechnology and Genetic Engineering Reviews* **1996**. 13. 19-50.

7. Ajiro. K.; Yoda. K.; Utsumi. K.; Nishikawa. Y. *J. Biol. Chem.* **1996**. 271(22). 13197-13201.

8. Sunkara. P. S.; Chang. C. C.; Lachman. P. J. *J. Biochem. Biophys. Res. Commun.* **1985**. 127(2). 546-551.

9. Chang. Z-F.; Huang. D-Y.; Hsue. N-C. *J. Biol. Chem.* **1994**. 269(33). 21249-21254.

10. Nilsson. A.; Sirzen. F.; Lewensohn. R.; Wang. N.; Skog. S. *Cell Prolif.* **1999**. 32. 239-248.

177

11. Ganzler, K.; Greve, K. S.; Cohen, A. S.; Karger, B. L.; Guttman, A.; Cooke, N. *Anal. Chem.* **1992**, 64, 2665-2671.

12. Guttman, A.; Horvath, J.; Cooke, N. *Anal. Chem.* **1993**, 65, 199-203.

13. Benedek, K.; Guttman, A. *J. Chromatogr.* **1994**, 680, 375-381.

14. Zhang, Z.; Krylov, S.; Arriaga, E. A.; Polakowski, R.; Dovichi, N. J. *Anal. Chem.* **2000**, 72, 318-322.

15. Hjérten, S. *J. Chromatogr.* **1985**, 347, 191-196.

16. Pinto, D. M.; Arriaga, E. A.; Craig, D. B.; Angelova, J.; Sharma, N.; Ahmadzadeh, H.; Dovichi, N. J. *Anal. Chem.* **1997**, 69, 3015-3021.

17. Shapiro, A.; Vinuela, E.; Maizel, J. *J. Biochem. Biophys. Res. Commun.* **1967**, 28, 815-820.

18. Weber, K.; Osborn, M. *J. Biol. Chem.* **1969**, 244, 4406-4412.

19. O'Farrell, P. H. *J. Biol. Chem.* **1975**, 250, 4007-4021.

20. Norbeck, J.I Blomberg, A. *FEMS Microbiology Letters* **1996**, 137, 1-8.

21. Ethell, D. W.; Steeves, J. D. *Developmental Brain Research* **1993**, 76, 163-169.

22. Righetti, D. G. *Immobolized pH Gradients: Theory and Methodology*, Elsevier: Amsterdam, **1990**.

23. James, P. *Biochem. Biophys. Res. Commun.* **1997**, 132, 1-6.

24. Krylov, S. N.; Zhang, Z.; Chan, N. W. C.; Arriaga, E.; Palcic, M. M.; Dovichi, N. J. *Cytometry* **1999**, 37, 15-20.

CHAPTER 7

Conclusions and Future Work

179

7.1 Thesis summary and future directions

The role of high sensitivity and high efficiency analysis of biomolecules has become increasingly important in biological and clinical research. In this thesis, development and application of techniques such as CE-LIF, PCR, cell synchronization and slab gel electrophoresis were presented in an effort to address a few of the challenging goals of biological and clinical research. The future direction of this work will be in the area of high-throughput CE and analysis by CE at the single-cell level.

CE is a powerful micro-scale separation technique well suited to the analysis of a wide range of molecules, thanks to the availability of several separation modes. In Chapter 1, a brief overview of CE and CE separations of biologically important molecules was presented. Applications of CE to clinical research were also reviewed in this chapter.

Quantification of PCR amplification product is key in determining virus concentrations in clinics. Chapter 2 discussed the development of a CGE-LIF based method for accurate and reliable PCR quantification. Duck hepatitis B virus (DHBV) was used as the model in this study. The developed technique was validated by evaluating its linearity, sensitivity, accuracy and precision. Since no specific competitor or probe design is required, this method is more convenient and applicable to a wider variety of PCR amplifications than the TaqMan and conventional QC-PCR assays. Future work will include the detection and quantification of a large number of targets from a single set of PCR amplifications and also the integration of the assay into automated capillary array electrophoresis instruments. These improvements will to a great extent increase the throughput and speed of the analysis.

180

Chapters 3 and 4 are two parts of a nucleoside anti-cancer drug resistance mechanism study. hENT1 is the major mediator of several major anti-cancer nucleoside drugs and dCK is the key enzyme in nucleoside anti-cancer drug activation and toxicity. Both hENT1 and dCK deficiency will result in nucleoside drug resistance. Therefore. it would be extremely helpful to measure hENT1 levels and dCK activities before prescribing nucleoside anti-cancer drugs to the patient. In clinics. however. technical difficulties of separating malignant clones from normal cells as needed by other methods make it almost impossible to achieve this goal. For this reason. new approaches to hENT1 and dCK assays that have the potential of extension to single-cell analysis are required.

Chapter 3 presents the first use of CE-LIF in quantification of 5-Sx8f binding as an indication of hENT1 abundance in the plasma membrane. This CE-LIF based method provides high precision and reliability in both qualitative and quantitative aspects and was successfully applied to study five cultured human cell lines. Results from this novel assay are compatible with those obtained from conventional flow cytometry analysis. At this stage. the hENT1-CE-LIF assay was still based on a large number of cells. In the future. single-cell analysis of hENT1 will be conducted. which was proved to be possible by the theoretical sensitivity of this method and the success of single-cell proteomic analysis reported by this group.

Chapter 4 presents the study of use of a fluorescent dye labeled deoxycytidine ([TAMRA]dCyd) as a substrate for measuring dCK activity. A series of studies were successfully carried out. including the separation condition. substrate preparation. enzyme kinetics and substrate uptake and distribution. However. the result of the kinetic study demonstrates that [TAMRA]dCyd is not an ideal substrate for dCK due to a low

181

V_{max} value. This low V_{max} complicated the enzyme assay in cell extracts where conventional inhibitor working conditions may not yet be optimized. In addition, cellular uptake of [TAMRA]dCyd was not efficient and the intracellular distribution of [TAMRA]dCyd requires further studies. In the future, seeking a suitable fluorescent substrate for dCK will be the most crucial aspect in this study. In parallel to this, studies on matters such as assisting the fluorescent substrate uptake, optimizing the enzyme assay conditions and localizing the substrate in the cytoplasm are also required in the future.

Chapters 5 and 6 illustrated the importance of cell synchronization techniques in understanding some cell cycle-dependent biological events. HeLa cells were successfully synchronized with thymidine and nocodazole blockages and used as models in the studies of both chapters.

Chapter 5 presents the first successful application of CE-LIF to probe hENT1 protein abundance differences in the plasma membranes of HeLa cells with different cell-cycle phases. This study, in turn, confirms the usability of the developed hENT1-CE-LIF assay (Chapter 3). Different expression levels of hENT1 at different cell-cycle phases suggest its expression may be correlated with cell proliferation. Although successful, the protocols for synchronizing cells are very tedious, time-consuming and varied from one cell line to another. Chemical treatment has also been linked to the possible disruption of normal cell cycle regulatory processes in some cases. Therefore, in the future, single cell analysis for studying cell-cycle dependent events would be much more desirable as previously demonstrated by this group. Each cell, before entering a capillary for further study, was stained with a fluorescent dye to allow its DNA content to be measured and to

182

determine the specific cell cycle phase of this cell. In addition, results based on single cells are truly representative of that specific phase.

In Chapter 6, slab gel electrophoresis, including SDS-PAGE and 2-D gel electrophoresis, and CGE have been applied to synchronized HeLa cells to probe the general protein expression differences during the cell cycle. Both qualitative on-and-off protein expressions and quantitative up-and-down protein regulations were detected. It was demonstrated that different separation methods have different advantages and drawbacks. judgements have to be based on an overall consideration of the results obtained from different methodologies. SDS-CGE separations have many promising advantages over conventional slab gel techniques. However. SDS-CGE separations of proteins must be improved in resolving power and throughput to replace slab gel electrophoresis. which still plays an important role in understanding proteomics especially when it is combined with MS. For the study presented in this chapter. future work should involve the use of MS to identify the proteins regulated by the cell cycle. Moreover. similar to the discussion in the paragraph on Chapter 5. drawbacks associated with conventional cell synchronization techniques might be overcome by developing single-cell-based assays.

183